

Complete spectral energy distribution of the hot, helium-rich white dwarf RX J0503.9–2854^{★,★★,★★★}

D. Hoyer¹, T. Rauch¹, K. Werner¹, J. W. Kruk², and P. Quinet^{3,4}

¹ Institute for Astronomy and Astrophysics, Kepler Center for Astro and Particle Physics, Eberhard Karls University, Sand 1, 72076 Tübingen, Germany

e-mail: rauch@astro.uni-tuebingen.de

² NASA Goddard Space Flight Center, Greenbelt, MD 20771, USA

³ Physique Atomique et Astrophysique, Université de Mons – UMONS, 7000 Mons, Belgium

⁴ IPNAS, Université de Liège, Sart Tilman, 4000 Liège, Belgium

Received 10 October 2016 / Accepted 17 October 2016

ABSTRACT

Context. In the line-of-sight toward the DO-type white dwarf RX J0503.9–2854, the density of the interstellar medium (ISM) is very low, and thus the contamination of the stellar spectrum almost negligible. This allows to identify many metal lines in a wide wavelength range from the extreme ultraviolet to the near infrared.

Aims. In previous spectral analyses, many metal lines in the ultraviolet spectrum of RX J0503.9–2854 have been identified. A complete line list of observed and identified lines is presented here.

Methods. We compared synthetic spectra that had been calculated from model atmospheres in non-local thermodynamical equilibrium, with observations.

Results. In total, we identified 1272 lines (279 of them were newly assigned) in the wavelength range from the extreme ultraviolet to the near infrared. 287 lines remain unidentified. A close inspection of the EUV shows that still no good fit to the observed shape of the stellar continuum flux can be achieved although He, C, N, O, Al, Si, P, S, Ca, Sc, Ti, V, Cr, Mn, Fe, Cr, Ni, Zn, Ga, Ge, As, Kr, Zr, Mo, Sn, Xe, and Ba are included in the stellar atmosphere models.

Conclusions. There are two possible reasons for the deviation between observed and synthetic flux in the EUV may have two reasons. Opacities from hitherto unconsidered elements in the model-atmosphere calculation may be missing, and/or the effective temperature is slightly lower than previously determined.

Key words. atomic data – line: identification – stars: abundances – stars: individual: RX J0503.9–2854 – virtual observatory tools

1. Introduction

The white dwarf (WD) RX J0503.9–2854 (henceforth RE 0503–289, WD 0501–289 McCook & Sion 1999a,b) was discovered in the ROSAT (ROentgen SATellite) wide field camera all-sky survey of extreme-ultraviolet (EUV) sources (Pounds et al. 1993). Barstow et al. (1993) reported its discovery by the Extreme Ultraviolet Explorer (EUVE), and identified it with a peculiar He-rich DO-type WD, namely MCT 0501–2858 in the Montreal-Cambridge-Tololo survey of southern hemisphere blue stars (Demers et al. 1986). They found that RE 0503–289 is located in a direction with very low density of the interstellar medium (ISM). In the line of sight (LOS) toward RE 0503–289, Vennes et al. (1994) measured a column density of $\log(N_{\text{H I}}/\text{cm}^{-2}) = 17.75 - 18.00$ using EUVE photometry data. Rauch et al. (2016c) resolved at least two ISM components in the LOS toward RE 0503–289

based on high-resolution and high signal-to-noise ultraviolet (UV) spectroscopy performed by Far Ultraviolet Spectroscopic Explorer (FUSE) and HST/STIS (Hubble Space Telescope / Space Telescope Imaging Spectrograph) and measured a very low ($E_{B-V} = 0.015 \pm 0.002$) interstellar reddening.

The almost negligible contamination by ISM line absorption allows us to identify even weak lines of many species from so far He up to trans-iron elements as heavy as Ba (Table 2). For reliable abundance analyses of these elements, a precise T_{eff} and $\log g$ determination is a prerequisite to keep error propagation as small as possible. An initial constraint of $T_{\text{eff}} = 60\,000 - 70\,000$ K was given by Vennes et al. (1994) from EUV photometry. The first spectral analysis by means of non-local thermodynamic equilibrium (NLTE) stellar atmosphere models considering opacities of H, He, and C was published by Barstow et al. (1994). They found $T_{\text{eff}} = 60\,000 - 80\,000$ K and $\log(g/\text{cm/s}^2) = 7.5 - 8.0$. Dreizler & Werner (1996) used ultraviolet (UV) spectra in addition and NLTE model atmospheres and determined $T_{\text{eff}} = 70\,000 \pm 5\,000$ K and $\log g = 7.5 \pm 0.5$. Recently, Rauch et al. (2016c) analyzed optical and ultraviolet (FUSE and HST/STIS) spectra and significantly reduced the error limits to $\pm 2\,000$ K and ± 0.1 , respectively. Table 1 summarizes previous analyses.

* Based on observations with the NASA/ESA Hubble Space Telescope, obtained at the Space Telescope Science Institute, which is operated by the Association of Universities for Research in Astronomy, Inc., under NASA contract NAS5-26666.

** Based on observations made with the NASA-CNES-CSA Far Ultraviolet Spectroscopic Explorer.

*** Based on observations made with ESO Telescopes at the La Silla Paranal Observatory under program IDs 072.D-0362, 165.H-0588, and 167.D-0407.

Table 1. History of T_{eff} and $\log g$ determinations (cf., Müller-Ringat 2013). PM denotes photometry.

T_{eff} / kK	$\log g$	Model atmosphere	Method	Comment	Reference
60–90			EUV, PM	very low N_{H_1}	Barstow et al. (1993)
60–80			EUV, OPT	very low N_{H_1}	Barstow et al. (1993)
60–80	7.5–8.0	He, HHeC	NLTE, OPT, UV, EUV	EUV problem ^a	Barstow et al. (1994)
60–70			EUV, PM	very low N_{H_1}	Vennes et al. (1994)
70 ^b	7.0	HeCNOSiFeNi	LTE, EUV, UV		Polomski et al. (1995)
65 ^c	7.5 ^d	HHeC	NLTE, OPT	no H detectable, upper limit 5 % (mass fraction)	Werner (1996)
70	7.5	HHeCNOSi	NLTE, OPT, UV	$M = 0.49 M_{\odot}$	Dreizler & Werner (1996)
66.6–70.4	7.13–7.27	HHe	LTE, UV	$M = 0.40 M_{\odot}$	Vennes et al. (1998)
70 ^e	7.5 ^e		NLTE, diffusion	no good fit achieved	Dreizler (1999)
69–75	7.26–7.63	HHeC	NLTE, OPT, UV, EUV	EUV problem ^a	Barstow et al. (2000)
		HHeCNOSiFeNi			
65–70	7.5 ^e	HeCNi, HeONi	NLTE, EUV	EUV problem ^a	Werner et al. (2001)
70 ^e	7.5 ^e	HHeCNOSiFeNi+PS	NLTE, UV	EUV problem ^a	Barstow et al. (2007)
			LTE		
68–72	7.4–7.6	HeCNOAlSiPS+CaScTiVCrMnFeCrNi+ZnGaGeAsKrZrMoSnXeBa	NLTE, OPT, UV	$M = 0.514^{+0.15}_{-0.05} M_{\odot}$	Rauch et al. (2016c)

Notes. ^(a) Sect. 7, ^(b) adopted upper limit of Vennes et al. (1994), ^(c) adopted value close to lower limit of Barstow et al. (1994), ^(d) adopted from Barstow et al. (1994), ^(e) adopted from Dreizler & Werner (1996)

Table 2. Photospheric abundances (mass fraction) of RE 0503–289. The reference for the 1st line identifications is given in the final column.

Element	Abundance	1 st Line identifications
He	9.73×10^{-1}	Barstow et al. (1994)
C	2.22×10^{-2}	Barstow et al. (1994)
N	5.49×10^{-5}	Dreizler & Werner (1996)
O	2.94×10^{-3}	Polomski et al. (1995), Dreizler & Werner (1996)
Al	5.01×10^{-5}	Rauch et al. (2016a)
Si	1.60×10^{-4}	Polomski et al. (1995), Dreizler & Werner (1996)
P	1.06×10^{-6}	Vennes et al. (1998); Barstow et al. (2007)
S	3.96×10^{-5}	Barstow et al. (2007)
Ni	7.25×10^{-5}	Barstow et al. (2000)
Zn	1.13×10^{-4}	Rauch et al. (2014a)
Ga	3.44×10^{-5}	Werner et al. (2012b), Rauch et al. (2015b)
Ge	1.58×10^{-4}	Werner et al. (2012b), Rauch et al. (2012)
As	1.60×10^{-5}	Werner et al. (2012b)
Se		Werner et al. (2012b)
Kr	5.04×10^{-4}	Werner et al. (2012b), Rauch et al. (2016c)
Zr	3.00×10^{-4}	Rauch et al. (2016a)
Mo	1.88×10^{-4}	Rauch et al. (2016b)
Sn	2.06×10^{-4}	Werner et al. (2012b)
Te		Werner et al. (2012b)
I		Werner et al. (2012b)
Xe	1.26×10^{-4}	Werner et al. (2012b), Rauch et al. (2015a), Rauch et al. (2016a)
Ba	3.57×10^{-4}	Rauch et al. (2014b)

2. Observations

In this paper, we used the observed spectra that are briefly described in the following. If they are compared to synthetic spectra, the latter are convolved with Gaussians to model the respective instrument’s resolution.

Extreme ultraviolet observations by the EUVE observatory were performed using the short-wavelength ($70 \text{ \AA} < \lambda < 190 \text{ \AA}$), the medium-wavelength ($140 \text{ \AA} < \lambda < 380 \text{ \AA}$), and the long-wavelength ($280 \text{ \AA} < \lambda < 760 \text{ \AA}$) spectrometers with a resolving power of $R \approx 300$. Details of the data reduction are given by Dupuis et al. (1995).

Far ultraviolet spectra ($910 \text{ \AA} < \lambda < 1190 \text{ \AA}$, $R \approx 20\,000$) were obtained with FUSE. Their data IDs are M1123601 (2000-12-04), M1124201 (2001-02-02), and P2041601 (2000-12-05). The spectra were shifted to rest wavelengths and co-added. For details see Werner et al. (2012b).

Ultraviolet spectroscopy was performed with HST/STIS on 2014-08-14. Two observations with grating E140M ($1144 \text{ \AA} < \lambda < 1709 \text{ \AA}$, $R \approx 45\,800$) and two observations with grating E230M ($1690 \text{ \AA} < \lambda < 2366 \text{ \AA}$, $2277 \text{ \AA} < \lambda < 3073 \text{ \AA}$, $R \approx 30\,000$) were co-added. These observations are retrievable from the Barbara A. Mikulski Archive for Space Telescopes (MAST).

Optical spectra ($3290 \text{ \AA} < \lambda < 4524 \text{ \AA}$, $4604 \text{ \AA} < \lambda < 5609 \text{ \AA}$, $5673 \text{ \AA} < \lambda < 6641 \text{ \AA}$) were obtained on 2000-09-09 and 2001-04-08 in the framework of the Supernova Ia Progenitor Survey project (SPY, Napiwotzki et al. 2001, 2003). The Ultraviolet and Visual Echelle Spectrograph (UVES) attached to the Very Large Telescope (VLT) located at the European Southern Observatory (ESO) on Cerro Paranal in Chile was employed to achieve a resolution of about 0.2 \AA . In addition, we use a spectrum taken with the Echelle Multi Mode Instrument (EMMI) attached to the New

Table 3. Newly calculated transition probabilities.

Element	Ions	Reference
Zn	IV - V	Rauch et al. (2014a)
Ga	IV - VI	Rauch et al. (2015b)
Ge	V - VI	Rauch et al. (2012)
Kr	IV - VII	Rauch et al. (2016c)
Zr	IV - VII	Rauch et al. (2016a)
Tc	II - VI	Werner et al. (2015)
Mo	IV - VII	Rauch et al. (2016b)
Xe	IV - VII	Rauch et al. (2015a, 2016a)
Ba	V - VII	Rauch et al. (2014b)

Technology Telescope (NTT) (1992-01, $4094 \text{ \AA} < \lambda < 4994 \text{ \AA}$, resolution of about 3.0 \AA).

Near infrared spectroscopy ($9500 \text{ \AA} < \lambda < 13420 \text{ \AA}$, $R \approx 950$) was performed on 2003-12-10 using the Son-of-Isaac (SofI) instrument at the NTT. The spectrum used here was digitized with Dexter¹ from Fig. 1 in Dobbie et al. (2005).

3. Model atmospheres and atomic data

The stellar model atmospheres used for this paper were calculated with our Tübingen NLTE Model Atmosphere Package (TMAP², Werner et al. 2003, 2012a). They assume plane-parallel geometry, are chemically homogeneous, and in hydrostatic and radiative equilibrium. An adaptation is the New Generation Radiative Transport (NGRT) code (Dreizler & Wolff 1999; Schuh et al. 2002) that can consider diffusion in addition to calculate stratified stellar atmospheres.

The Tübingen Model Atom Database (TMAD³) provides ready-to-use model atoms in TMAP format for many species up to Ba. TMAD has been constructed as part of the Tübingen contribution to the German Astrophysical Virtual Observatory (GAVO⁴).

Werner et al. (2012b) discovered lines of trans-iron elements, namely Ga (atomic number $Z = 31$), Ge (32), As (33), Se (34), Kr (36), Mo (42), Sn (50), Te (52), I (53), and Xe (54), in the FUSE spectrum of RE 0503–289. For precise abundance determinations of these species, reliable atomic data is mandatory. For example, reliable transition probabilities are required, not only for lines that are identified in the observation but for the complete model atoms that are considered in the model-atmosphere calculations. Due to the lack of such data, Werner et al. (2012b) were restricted to abundance determinations of Kr and Xe only.

We initiated the calculation of new transition probabilities that were then used to determine the abundance of the respective element. Table 3 gives an overview of the so far calculated data. To provide easy access to this data, the registered Tübingen Oscillator Strengths Service (TOSS) has been created within the GAVO project.

To construct model atoms for the use within TMAP, the elements given in Table 3 require the calculation of so-called super levels and super lines with our Iron Opacity and Interface (IrOnIc, Rauch & Deetjen 2003) due to the very high number

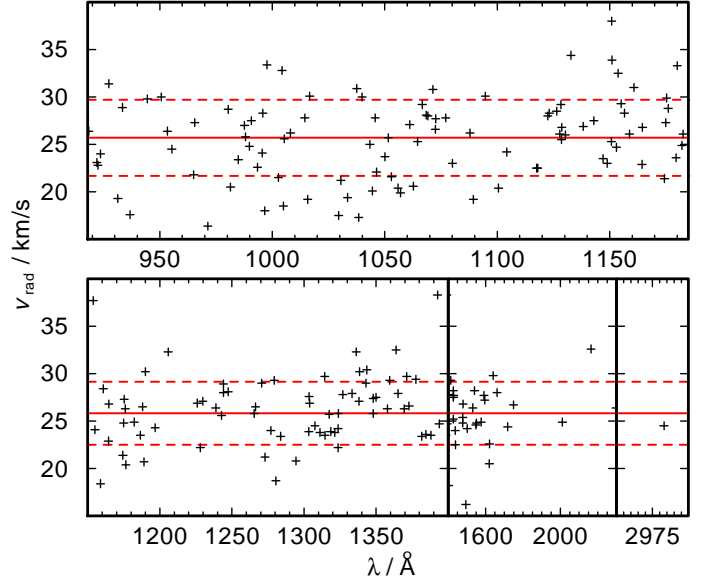


Fig. 1. Determination of v_{rad} from individual lines in the FUSE (top panel) and HST/STIS observations (bottom). The full horizontal lines indicate the average v_{rad} for FUSE and HST/STIS, respectively. The dashed lines show the 1σ error.

of atomic levels and lines. We transferred the TOSS data into Kurucz’s data format⁵ that can be read by IrOnIc.

4. Radial velocity and gravitational redshift

To shift the observation to rest wavelength, we determined the radial velocity v_{rad} of RE 0503–289 from FUSE and HST/STIS spectra. To measure the wavelengths of the line centers, we used IRAF⁶ to fit Gaussians to the line profiles. In total, we evaluated 100 lines in the FUSE wavelength range and 103 lines in the STIS wavelength range (Fig. 1). The averages are $v_{\text{rad}}^{\text{FUSE}} = 25.7 \pm 4.2 \text{ km/s}$ and $v_{\text{rad}}^{\text{STIS}} = 25.8 \pm 3.7 \text{ km/s}$. We adopted the mean value of $v_{\text{rad}} = 25.7^{+3.6}_{-4.0} \text{ km/s}$. From this value, the gravitational redshift z has to be subtracted. To calculate z and the respective radial velocity, we created the GAVO tool Tübingen Gravitational REDshift calculator (TGRED, Fig. C.2). For RE 0503–289, we derive $v_{\text{rad}}^{\text{gred}} = 15.5^{+6.7}_{-4.6} \text{ km/s}$. The true radial velocity is then $v_{\text{rad}}^{\text{RE 0503-289}} = 10.2^{+8.2}_{-8.6} \text{ km/s}$.

5. Line identification

To unambiguously identify lines in our observed spectra (Sect. 2), we used the best synthetic model of Rauch et al. (2016a) and calculated additional spectra with oscillator strengths set to zero for individual elements. This allows to find weak lines, even if they are blended by stronger lines. The detection limit is an equivalent width of $W_{\lambda} = 2 \text{ m\AA}$. Table 4 shows the total numbers of lines identified in the four wavelength ranges and the numbers of lines that were suited to determine W_{λ} and v_{rad} . The current line lists are presented in Tables A.1 – A.5, a regularly updated version is available at <http://astro.uni-tuebingen.de/~hoyer/objects/RE0503-289>.

⁵ <http://kurucz.harvard.edu/atoms.html>

⁶ IRAF is distributed by the National Optical Astronomy Observatory, which is operated by the Associated Universities for Research in Astronomy, Inc., under cooperative agreement with the National Science Foundation.

¹ <http://dc.zah.uni-heidelberg.de/sdexter>

² <http://astro.uni-tuebingen.de/~TMAP>

³ <http://astro.uni-tuebingen.de/~TMAD>

⁴ <http://www.g-vo.org>

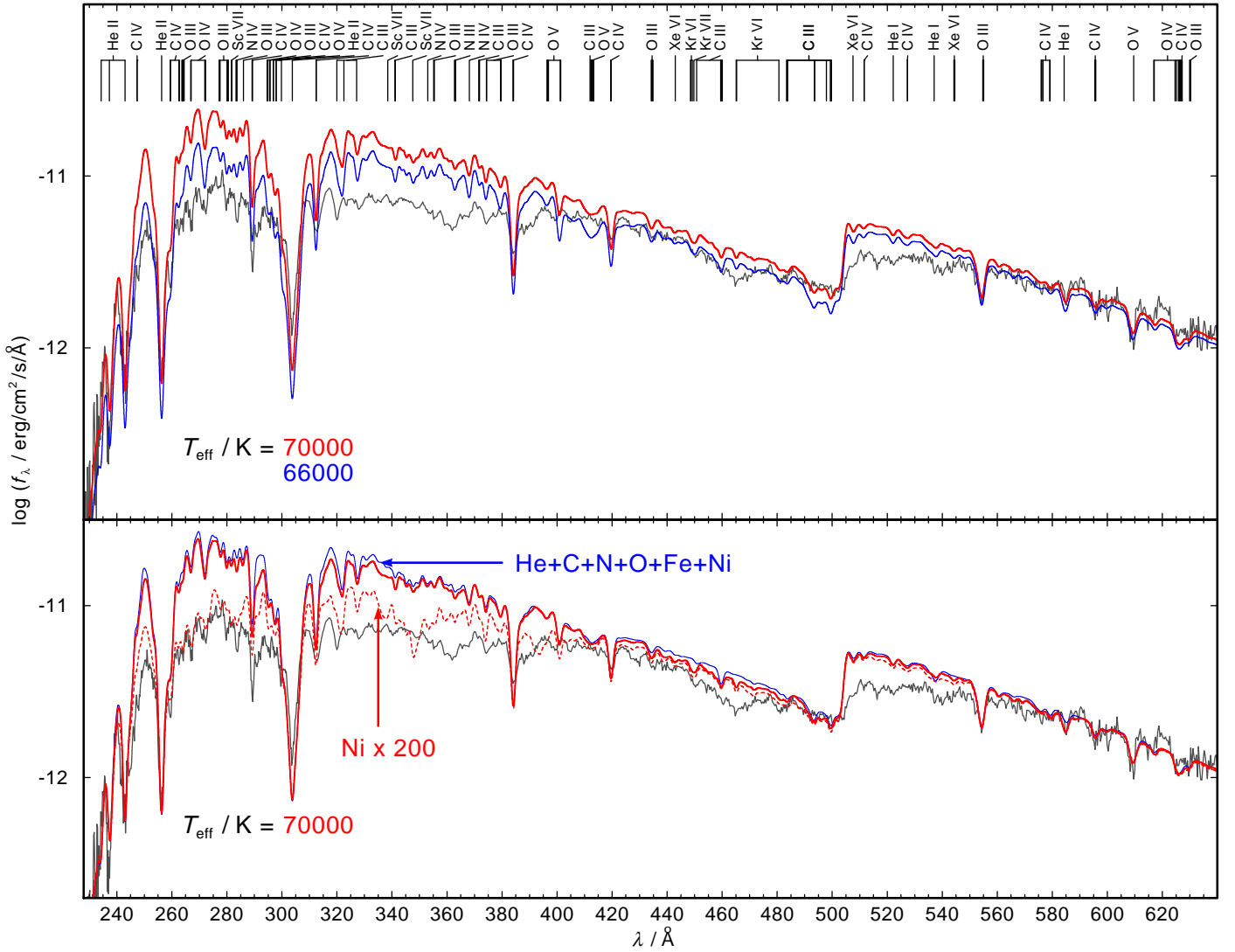


Fig. 3. Comparison of the EUVE observation (gray line in both panels) with our models. Top panel: Two models with $T_{\text{eff}} = 70\,000$ K (red) and $T_{\text{eff}} = 66\,000$ K (blue). Identified photospheric lines are marked at the top. Bottom panel: Three models with $T_{\text{eff}} = 70\,000$ K. Red, thick line: model from the top panel, red, dashed line: model with 200 times increased Ni abundance, blue, thin line: model that considered only opacities of He, C, N, O, Fe, and Ni.

sity of interstellar H I of $1.5 \pm 0.2 \times 10^{18} \text{ cm}^{-2}$ (measured from $L\beta$, Rauch et al. 2016c), we can calculate $E_{B-V} = 0.00039^{+0.00017}_{-0.00012}$ which is within error limits well in agreement with our result.

A close look at the EUV wavelength range shows still a significant difference between model and observation (Fig. 3, top panel), most prominent between 250 \AA and 400 \AA and between 504 \AA and 550 \AA . Our present models reduced the deviation by about a factor of two compared the models of Werner et al. (2001). The EUV problem cannot be solved by using a cooler model, even at $T_{\text{eff}} = 66\,000$ K, which is already outside the error range of $T_{\text{eff}} = 70\,000 \pm 2000$ K given by Rauch et al. (2016c), no sufficient improvement is achieved. The impact of metal opacities is demonstrated in Fig. 3 by a model that considered only opacities from He, C, N, O, Fe, and Ni with same abundance ratios like our best model. To test the impact of additional opacity, we artificially increased the Ni abundance by factor of 200 to match the model’s flux to the observed between 250 \AA and 280 \AA . This reduced the flux discrepancy between 300 \AA and 400 \AA as well while the wavelength region above the He I ground-state threshold is unaffected. However, we conclude that

even in our advanced models opacity is missing from elements that are hitherto not considered. To include, for example, other trans-iron elements requires detailed laboratory measurements of their spectra and the extensive calculation of transition probabilities.

8. What is the nature of RE 0503–289?

RE 0503–289 was first classified to be a DO-type WD (Barstow et al. 1993). Its optical spectrum exhibits an absorption trough around C IV $\lambda\lambda 4646.62 - 4687.95 \text{ \AA}$ and He II $\lambda 4685.80 \text{ \AA}$. This trough is the spectroscopic criterion for the H-deficient PG 1159-type stars (e.g., Werner & Herwig 2006). Figure 4 shows the comparison of the wavelength region around this trough for the PG 1159 prototype PG 1159–035 (V★ GW Vir, WD 1159–035, $T_{\text{eff}} = 140\,000 \pm 5\,000$ K, $\log g = 7.0 \pm 0.5$, Jahn et al. 2007) and the O(He)-type WD KPD 0005+5106 (WD 0005+511, $T_{\text{eff}} = 195\,000 \pm 15\,000$ K, $\log g = 6.7 \pm 0.2$, Werner & Rauch 2015). Both objects are at an earlier state of stellar evolution than RE 0503–289. The

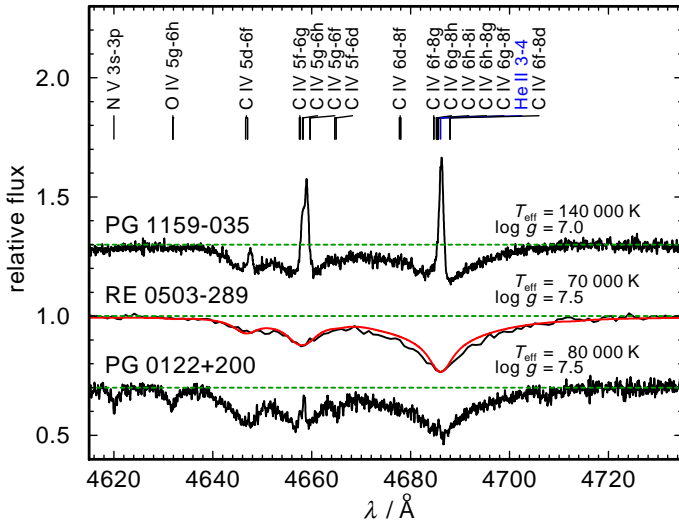


Fig. 4. Section of the optical spectra of PG 1159–035 (from SPY, shifted by 0.3 in flux units), RE 0503–289 (EMMI), and PG 0122+200 (KECK, shifted by –0.3) (from top to bottom) around the PG 1159 absorption trough. For RE 0503–289, the synthetic spectrum of Rauch et al. (2016a) is overplotted (red line). The green, dashed lines indicate the continuum level.

strengths of the PG 1159 absorption troughs are almost the same for the much hotter PG 1159–035 and RE 0503–289, although their photospheric C abundances are significantly different, $\approx 48\%$ by mass (Jahn et al. 2007) and $\approx 2\%$, respectively. The cool PG 1159-type star PG 0122+200 has about 22 % of C in its photosphere (Werner & Rauch 2014).

In a $\log T_{\text{eff}} - \log g$ diagram (Fig. 5), RE 0503–289 is located at the so-called PG 1159 wind limit (Unglaub & Bues 2000, their Fig. 13, digitized with Dexter) that was predicted for a ten-times-reduced mass-loss rate (line A, calculated with $\dot{M} = 1.29 \times 10^{-15} L^{1.86}$ from Bloeker 1995; Pauldrach et al. 1988). This line approximately separates the regions that are populated by PG 1159-type stars and DO-type WDs. Lines B and C in Fig. 5 show where the photospheric C content is reduced by factors of 0.5 and 0.1, respectively, when using the mass-loss rate given above. To the right of line D, no PG 1159 star is located.

Werner et al. (2014) suggested a mass ratio $C/He = 0.02$ to conserve previously assigned spectroscopic classes. However, PG 1159 stars span a wide range of C/He (0.03 – 0.33, Werner et al. 2014).

RE 0503–289 is located close to line B of Unglaub & Bues (2000) in Fig. 5, that is, its C abundance should be already reduced by a factor of 0.5. Thus, it is likely that RE 0503–289 had a $C/He \approx 0.05$ in its antecedent PG 1159-star phase. Even now, its C/He lies a bit higher than 0.02 and RE 0503–289 may be classified as a PG 1159 star as well. This is corroborated by the still high efficiency of radiative levitation that is responsible for the extremely high overabundances of trans-iron elements (Rauch et al. 2016b). However, the transition from a PG 1159-type star to a DO-type star is smooth and RE 0503–289 is an ideal object to study this in detail. Unfortunately, the strong radiative levitation of trans-iron elements wipes out all information about their asymptotic giant branch (AGB) abundances and RE 0503–289 is not suited to constrain AGB nucleosynthesis models.

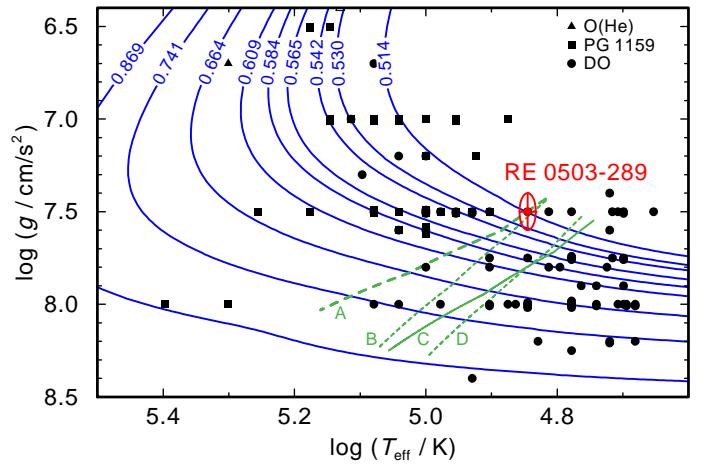


Fig. 5. Location of RE 0503–289 and related objects (Hügelmeier et al. 2006; Kepler et al. 2016; Reindl et al. 2014b,a; Werner & Herwig 2006) in the $\log T_{\text{eff}} - \log g$ plane (cf., <http://www.star.le.ac.uk/~nr152/He.html> for stellar parameters). Evolutionary tracks for H-deficient WDs (Althaus et al. 2009) labeled with their respective masses in M_{\odot} are plotted for comparison. Transition limits predicted by Unglaub & Bues (2000) are indicated (see text for details).

9. Results

RE 0503–289 fulfills criteria of PG 1159 star and of DO-type WD classifications. The presence of the strong PG 1159 absorption trough around $\text{He II } \lambda 4685.80 \text{ \AA}$ (Fig. 4) shows that RE 0503–289 could be classified as a PG 1159 star, although its C abundance would then be the lowest of this group. It is located close to the so-called PG 1159 wind limit (Fig. 5), meaning that it is close to the regime in which gravitation will dominate and pull metals down, out of the atmosphere. The strongly increased abundances of trans-iron elements, however, indicate that radiative levitation is still efficiently counteracting this process. Thus, RE 0503–289 has not arrived in its final stage of evolution. Formally, due to its $\log g > 7$, the DO-type WD classification is right.

In the observed spectra, we identified 1272 lines in the wavelength range from the extreme ultraviolet to the near infrared. 287 lines remain unidentified. The best model of Rauch et al. (2016a) reproduces well most of the identified lines.

The EUV problem (Sect. 7) – the difference between observed and synthetic flux in the EUV is still present. Our advanced model atmospheres include opacities of 27 metals but their flux in the EUV is still partly about a factor of approximately two too high compared with the observation. We expect that missing metal opacities are the reason for this discrepancy.

Acknowledgements. DH and TR are supported by the German Aerospace Center (DLR, grants 50 OR 1501 and 05 OR 1507, respectively). The German Astrophysical Virtual Observatory (GAVO) project at Tübingen had been supported by the Federal Ministry of Education and Research (BMBF, 05 AC 6 VTB, 05 AC 11 VTB). Financial support from the Belgian FRS-FNRS is also acknowledged. PQ is research director of this organization. Some of the data presented in this paper were obtained from the Mikulski Archive for Space Telescopes (MAST). STScI is operated by the Association of Universities for Research in Astronomy, Inc., under NASA contract NAS5-26555. Support for MAST for non-HST data is provided by the NASA Office of Space Science via grant NNX09AF08G and by other grants and contracts. We thank Ralf Napiwotzki for putting the reduced ESO/VLT spectra at our disposal. The TEUV tool (<http://astro-uni-tuebingen.de/~TEUV>), the TGRED tool (<http://astro-uni-tuebingen.de/~TGRED>), the TIRO service (<http://astro-uni-tuebingen.de/~TIRO>), the TMAD service (<http://astro-uni-tuebingen.de/~TMAD>), the TOSS service (<http://astro-uni-tuebingen.de/~TOSS>), and the TVIS tool (<http://astro-uni-tuebingen.de/~TVIS>).

astro-uni-tuebingen.de/~TVIS) used for this paper were constructed as part of the activities of the German Astrophysical Virtual Observatory. This work used the profile-fitting procedure OWENS developed by M. Lemoine and the FUSE French Team. This research has made use of NASA's Astrophysics Data System and of the SIMBAD database operated at CDS, Strasbourg, France.

References

- Althaus, L. G., Panei, J. A., Miller Bertolami, M. M., et al. 2009, *ApJ*, 704, 1605
- Barstow, M. A., Dobbie, P. D., Forbes, A. E., & Boyce, D. D. 2007, in *Astronomical Society of the Pacific Conference Series*, Vol. 372, 15th European Workshop on White Dwarfs, ed. R. Napiwotzki & M. R. Burleigh, 243
- Barstow, M. A., Dreizler, S., Holberg, J. B., et al. 2000, *Monthly Notices of the Royal Astronomical Society*, 314, 109
- Barstow, M. A., Holberg, J. B., Koester, D., Nousek, J. A., & Werner, K. 1995, in *Lecture Notes in Physics*, Berlin Springer Verlag, Vol. 443, *White Dwarfs*, ed. D. Koester & K. Werner, 302
- Barstow, M. A., Holberg, J. B., Werner, K., Buckley, D. A. H., & Stobie, R. S. 1994, *MNRAS*, 267, 653
- Barstow, M. A., Wesemael, F., Holberg, J. B., et al. 1993, *Advances in Space Research*, 13, 281
- Bloecker, T. 1995, *A&A*, 299, 755
- Cutri, R. M., Skrutskie, M. F., van Dyk, S., et al. 2003a, *2MASS All Sky Catalog of point sources*.
- Cutri, R. M., Skrutskie, M. F., van Dyk, S., et al. 2003b, *VizieR Online Data Catalog*, 2246
- Demers, S., Beland, S., Kibblewhite, E. J., Irwin, M. J., & Nithakorn, D. S. 1986, *AJ*, 92, 878
- Dobbie, P. D., Burleigh, M. R., Levan, A. J., et al. 2005, *A&A*, 439, 1159
- Dreizler, S. 1999, *Astronomy and Astrophysics*, 352, 632
- Dreizler, S. & Werner, K. 1996, *A&A*, 314, 217
- Dreizler, S. & Wolff, B. 1999, *A&A*, 348, 189
- Dupuis, J., Vennes, S., Bowyer, S., Pradhan, A. K., & Thejll, P. 1995, *ApJ*, 455, 574
- Fitzpatrick, E. L. 1999, *PASP*, 111, 63
- Groenewegen, M. A. T. & Lamers, H. J. G. L. M. 1989, *A&AS*, 79, 359
- Hügelmeier, S. D., Dreizler, S., Homeier, D., et al. 2006, *A&A*, 454, 617
- Jahn, D., Rauch, T., Reiff, E., et al. 2007, *A&A*, 462, 281
- Kepler, S. O., Pelisoli, I., Koester, D., et al. 2016, *MNRAS*, 455, 3413
- Kurucz, R. L. 1991, in *NATO ASIC Proc. 341: Stellar Atmospheres - Beyond Classical Models*, ed. L. Crivellari, I. Hubeny, & D. G. Hummer, 441
- Kurucz, R. L. 2009, in *American Institute of Physics Conference Series*, Vol. 1171, *American Institute of Physics Conference Series*, ed. I. Hubeny, J. M. Stone, K. MacGregor, & K. Werner, 43–51
- Kurucz, R. L. 2011, *Canadian Journal of Physics*, 89, 417
- McCook, G. P. & Sion, E. M. 1999a, *ApJS*, 121, 1
- McCook, G. P. & Sion, E. M. 1999b, *VizieR Online Data Catalog*, 3210, 0
- Morrison, R. & McCammon, D. 1983, *ApJ*, 270, 119
- Müller-Ringat, E. 2013, *Dissertation*, University of Tübingen, Germany, <http://nbn-resolving.de/urn:nbn:de:bsz:21-opus-67747>
- Napiwotzki, R., Christlieb, N., Drechsel, H., et al. 2001, *Astronomische Nachrichten*, 322, 411
- Napiwotzki, R., Christlieb, N., Drechsel, H., et al. 2003, *The Messenger*, 112, 25
- Pauldrach, A., Puls, J., Kudritzki, R. P., Mendez, R. H., & Heap, S. R. 1988, *A&A*, 207, 123
- Polomski, E. F., Vennes, S., & Chayer, P. 1995, in *Bulletin of the American Astronomical Society*, Vol. 27, *American Astronomical Society Meeting Abstracts*, 1311
- Pounds, K. A., Allan, D. J., Barber, C., et al. 1993, *MNRAS*, 260, 77
- Rauch, T. & Deetjen, J. L. 2003, in *Astronomical Society of the Pacific Conference Series*, Vol. 288, *Stellar Atmosphere Modeling*, ed. I. Hubeny, D. Mihalas, & K. Werner, 103
- Rauch, T., Gamrath, S., Quinet, P., et al. 2016a, *A&A* in prep.
- Rauch, T., Hoyer, D., Quinet, P., Gallardo, M., & Raineri, M. 2015a, *A&A*, 577, A88
- Rauch, T., Quinet, P., Hoyer, D., et al. 2016b, *A&A*, 587, A39
- Rauch, T., Quinet, P., Hoyer, D., et al. 2016c, *A&A*, 590, A128
- Rauch, T., Werner, K., Biéumont, É., Quinet, P., & Kruk, J. W. 2012, *A&A*, 546, A55
- Rauch, T., Werner, K., Quinet, P., & Kruk, J. W. 2014a, *A&A*, 564, A41
- Rauch, T., Werner, K., Quinet, P., & Kruk, J. W. 2014b, *A&A*, 566, A10
- Rauch, T., Werner, K., Quinet, P., & Kruk, J. W. 2015b, *A&A*, 577, A6
- Reindl, N., Rauch, T., Werner, K., et al. 2014a, *A&A*, 572, A117
- Reindl, N., Rauch, T., Werner, K., Kruk, J. W., & Todt, H. 2014b, *A&A*, 566, A116
- Schuh, S. L., Dreizler, S., & Wolff, B. 2002, *A&A*, 382, 164
- Seaton, M. J., Yan, Y., Mihalas, D., & Pradhan, A. K. 1994, *MNRAS*, 266, 805
- Unglaub, K. & Bues, I. 2000, *A&A*, 359, 1042
- Vennes, S., Dupuis, J., Bowyer, S., et al. 1994, *ApJ*, 421, L35
- Vennes, S., Dupuis, J., Chayer, P., et al. 1998, *The Astrophysical Journal*, 500, L41
- Werner, K. 1996, *Astronomy and Astrophysics*, 309, 861
- Werner, K., Deetjen, J. L., Dreizler, S., et al. 2003, in *Astronomical Society of the Pacific Conference Series*, Vol. 288, *Stellar Atmosphere Modeling*, ed. I. Hubeny, D. Mihalas, & K. Werner, 31
- Werner, K., Deetjen, J. L., Rauch, T., & Wolff, B. 2001, in *Astronomical Society of the Pacific Conference Series*, Vol. 226, *12th European Workshop on White Dwarfs*, ed. J. L. Provencal, H. L. Shipman, J. MacDonald, & S. Goodchild, 55
- Werner, K., Dreizler, S., & Rauch, T. 2012a, *TMAP: Tübingen NLTE Model-Atmosphere Package*, *Astrophysics Source Code Library* [record ascl:1212.015]
- Werner, K. & Herwig, F. 2006, *PASP*, 118, 183
- Werner, K. & Rauch, T. 2014, *A&A*, 569, A99
- Werner, K. & Rauch, T. 2015, *A&A*, 583, A131
- Werner, K., Rauch, T., & Kepler, S. O. 2014, *A&A*, 564, A53
- Werner, K., Rauch, T., Kučas, S., & Kruk, J. W. 2015, *A&A*, 574, A29
- Werner, K., Rauch, T., Ringat, E., & Kruk, J. W. 2012b, *ApJ*, 753, L7

Appendix A: Identified and unidentified lines in the spectrum of RE 0503–289

Table A.1. Identified lines in the EUVE observations of RE0503–289. Lower and upper levels are the configuration or the energy (cm^{-1} , for elements with an atomic number $Z \geq 20$). f is the oscillator strength, W_λ the observed equivalent width, and v_{rad} the measured radial velocity. “unid.” denotes observed but as yet unidentified lines. The theoretical wavelengths correspond to those given by NIST for He, C, N, O, Si, P, S, As, and Sn, by Kurucz (1991, 2009, 2011) for Fe, and Ni, and by Rauch et al. (2014a, 2015b, 2012, 2016c,a,b, 2015a, 2014b) for Zn, Ga, Ge, Kr, Zr, Mo, Xe, and Ba, respectively.

Ion	Levels		f	$W_\lambda / \text{m}\text{\AA}$	Wavelength / \AA		$v_{\text{rad}} / \text{km/s}$	Comment
	Lower	Upper			Theoretical	Observed		
He II	1	6	7.80×10^{-3}		234.347			newly identified
He II	1	5	1.39×10^{-2}		237.331			Vennes et al. (1998)
He II	1	4	2.90×10^{-2}		243.026			Vennes et al. (1998)
C IV	2p $^2\text{P}_{1/2}$	6s $^2\text{S}_{1/2}$	1.32×10^{-3}		247.341			newly identified
C IV	2p $^2\text{P}_{3/2}$	6s $^2\text{S}_{1/2}$	1.32×10^{-3}		247.407			newly identified
He II	1	3	7.91×10^{-2}		256.316			Vennes et al. (1998)
C IV	2p $^2\text{P}_{1/2}^o$	5d $^2\text{D}_{3/2}$	4.57×10^{-2}		259.468			
C IV	2p $^2\text{P}_{3/2}^o$	5d $^2\text{D}_{5/2}$	4.11×10^{-2}		259.539			
C IV	2p $^2\text{P}_{3/2}^o$	5d $^2\text{D}_{3/2}$	4.56×10^{-3}		259.540			
C IV	2p $^2\text{P}_{1/2}$	5s $^2\text{S}_{1/2}$	2.64×10^{-3}		262.547			
C IV	2p $^2\text{P}_{3/2}$	5s $^2\text{S}_{1/2}$	2.64×10^{-3}		262.621			
O IV	2p ² $^2\text{D}_{5/2}$	3d $^2\text{D}_{5/2}^o$	1.48×10^{-1}		266.931			
O IV	2p ² $^2\text{D}_{3/2}$	3d $^2\text{D}_{5/2}^o$	1.60×10^{-2}		266.941			
O IV	2p ² $^2\text{D}_{5/2}$	3d $^2\text{D}_{3/2}^o$	1.07×10^{-2}		266.971			
O IV	2p ² $^4\text{P}_{3/2}$	3s $^4\text{P}_{5/2}^o$	5.18×10^{-2}		271.990			
O IV	2p ² $^4\text{P}_{1/2}$	3s $^4\text{P}_{3/2}^o$	9.58×10^{-2}		272.076			
O IV	2p ² $^4\text{P}_{5/2}$	3s $^4\text{P}_{5/2}^o$	8.05×10^{-2}		272.127			
O IV	2p ² $^4\text{P}_{3/2}$	3s $^4\text{P}_{3/2}^o$	1.53×10^{-2}		272.173			
O IV	2p ² $^4\text{P}_{1/2}$	3s $^4\text{P}_{1/2}^o$	1.91×10^{-2}		272.176			
O III	2p ² $^3\text{P}_1$	4s $^3\text{P}_2^o$	4.61×10^{-3}		280.109			
O III	2p ² $^3\text{P}_0$	4s $^3\text{P}_1^o$	1.11×10^{-2}		280.234			
O III	2p ² $^3\text{P}_2$	4s $^3\text{P}_2^o$	8.30×10^{-3}		280.261			
O III	2p ² $^3\text{P}_1$	4s $^3\text{P}_1^o$	2.77×10^{-3}		280.323			
O III	2p ² $^3\text{P}_1$	4s $^3\text{P}_0^o$	3.69×10^{-3}		280.408			
O III	2p ² $^3\text{P}_2$	4s $^3\text{P}_1^o$	2.76×10^{-3}		280.474			
N IV	2p $^3\text{P}_0^o$	3d $^3\text{D}_1$	6.21×10^{-1}		283.417			newly identified
N IV	2p $^3\text{P}_1^o$	3d $^3\text{D}_2$	4.59×10^{-1}		283.465			newly identified
N IV	2p $^3\text{P}_1^o$	3d $^3\text{D}_1$	1.53×10^{-1}		283.468			newly identified
N IV	2p $^3\text{P}_2^o$	3d $^3\text{D}_3$	4.14×10^{-1}		283.574			newly identified
N IV	2p $^3\text{P}_2^o$	3d $^3\text{D}_2$	9.20×10^{-2}		283.581			newly identified
N IV	2p $^3\text{P}_2^o$	3d $^3\text{D}_1$	6.17×10^{-3}		283.584			newly identified
C IV	2p $^2\text{P}_{1/2}^o$	4d $^2\text{D}_{3/2}$	1.22×10^{-1}		289.141			
C IV	2p $^2\text{P}_{3/2}^o$	4d $^2\text{D}_{5/2}$	1.01×10^{-1}		289.292			
C IV	2p $^2\text{P}_{3/2}^o$	4d $^2\text{D}_{3/2}$	1.22×10^{-2}		289.231			
O IV	2p ² $^2\text{P}_{3/2}$	3d $^2\text{P}_{3/2}^o$	7.07×10^{-2}		299.853			newly identified

Table A.1. Continued.

Ion	Levels		f	$W_\lambda /$ mÅ	Wavelength/ Å		$v_{\text{rad}} /$ km/s	Comment
	Lower	Upper			Theoretical	Observed		
He II	1	2	4.16×10^{-1}		303.783			newly identified
C IV	2s $^2S_{1/2}$	3p $^2P_{3/2}^o$	1.36×10^{-1}		312.420			
C IV	2s $^2S_{1/2}$	3p $^2P_{1/2}^o$	6.78×10^{-2}		312.451			
C III	2s 2 1S_0	3s' $^1P_1^o$	4.51×10^{-2}		322.574			newly identified
C III	2p $^3P_2^o$	6d 3D_1	2.71×10^{-4}		327.171			newly identified
C III	2p $^3P_2^o$	6d 3D_1	4.04×10^{-3}		327.171			newly identified
C III	2p $^3P_2^o$	6d 3D_1	2.56×10^{-2}		327.171			newly identified
O III	2p 2 3P_1	3s $^3P_0^o$	2.78×10^{-2}		374.328			
O III	2p 2 3P_2	3s $^3P_1^o$	2.08×10^{-2}		374.432			
C IV	2s $^2P_{1/2}^o$	3d $^2D_{3/2}$	6.44×10^{-1}		384.031			
C IV	2s $^2P_{3/2}^o$	3d $^2D_{5/2}$	5.80×10^{-1}		384.174			
C IV	2s $^2P_{3/2}^o$	3d $^2D_{3/2}$	6.43×10^{-2}		384.190			
C IV	2p $^2P_{1/2}^o$	3s $^2S_{1/2}$	3.76×10^{-2}		419.525			
C IV	2p $^2P_{3/2}^o$	3s $^2S_{1/2}$	3.76×10^{-2}		419.714			
O III	2p 3 $^3D_2^o$	3s 3P_2	6.86×10^{-3}		434.320			
O III	2p 3 $^3D_1^o$	3s 3P_2	2.88×10^{-2}		434.329			
O III	2p 3 $^3D_2^o$	3s 3P_1	6.44×10^{-4}		434.648			
O III	2p 3 $^3D_1^o$	3s 3P_1	1.60×10^{-2}		434.657			
O III	2p 3 $^3D_1^o$	3s 3P_0	2.13×10^{-2}		434.846			
Kr VI	115479	338447	5.78×10^{-1}		448.495			newly identified
Kr VI	115479	338364	1.71×10^{-1}		448.662			newly identified
Kr VI	115479	338119	1.13		449.156			newly identified
He I	1s 1S	4p $^1P^o$	2.99×10^{-2}		522.213			newly identified
He I	1s 1S	3p $^1P^o$	7.35×10^{-2}		537.030			newly identified
O III	2p 3 $^3D_2^o$	3p 3P_1	6.20×10^{-5}		554.759			newly identified
O III	2p 3 $^3D_1^o$	3p 3P_1	1.52×10^{-3}		554.773			newly identified
O III	2p 3 $^3D_1^o$	3p 3P_0	2.05×10^{-3}		555.026			newly identified
He I	1s 1S	2p $^1P^o$	2.76×10^{-1}		584.334			newly identified
O V	2p' 3D_1	4d' $^3D_2^o$	1.38×10^{-2}		609.591			newly identified
O IV	2p 2 $^4P_{1/2}$	2p 3 $^4S_{3/2}^o$	1.26×10^{-1}		624.619			newly identified
O IV	2p 2 $^4P_{3/2}$	2p 3 $^4S_{3/2}^o$	1.26×10^{-1}		625.127			newly identified
O IV	2p 2 $^4P_{5/2}$	2p 3 $^4S_{3/2}^o$	1.26×10^{-1}		625.853			newly identified
O IV	3p $^2P_{1/2}^o$	3p' $^2P_{3/2}$	6.22×10^{-2}		626.198			newly identified
O IV	3p $^2P_{1/2}^o$	3p' $^2P_{1/2}$	1.24×10^{-1}		626.446			newly identified
O IV	3p $^2P_{3/2}^o$	3p' $^2P_{3/2}$	1.56×10^{-1}		626.539			newly identified
O IV	3p $^2P_{3/2}^o$	3p' $^2P_{1/2}$	3.11×10^{-2}		626.786			newly identified
C IV	3d $^2D_{3/2}$	7f $^2F_{5/2}^o$	2.58×10^{-2}		627.102			newly identified
C IV	3d $^2D_{5/2}$	7f $^2F_{5/2}^o$	1.23×10^{-3}		627.143			newly identified

Table A.1. Continued.

Ion	Levels		f	$W_\lambda /$ mÅ	Wavelength/Å		$v_{\text{rad}} /$ km/s	Comment
	Lower	Upper			Theoretical	Observed		
C iv	3D $^2\text{D}_{5/2}$	7f $^2\text{F}_{7/2}^o$	2.45×10^{-2}		627.144			newly identified

Table A.2. Like Table A.1, for the FUSE observations.

Ion	Levels		f	$W_\lambda /$ mÅ	Wavelength/Å		$v_{\text{rad}} /$ km/s	Comment
	Lower	Upper			Theoretical	Observed		
H i	1	25			913.215			ISM multi-component
H i	1	24			913.339			ISM multi-component
H i	1	23			913.480			ISM multi-component
H i	1	22			913.641			ISM multi-component
H i	1	21			913.826			ISM multi-component
H i	1	20			914.039			ISM multi-component
H i	1	19			914.286			ISM multi-component
H i	1	18			914.576			ISM multi-component
H i	1	17			914.919			ISM multi-component
H i	1	16			915.329			ISM multi-component
N ii					915.613			ISM multi-component
H i	1	15			915.834			ISM multi-component
H i	1	14			916.429			ISM multi-component
H i	1	13			917.181			ISM multi-component
H i	1	12			918.129			ISM multi-component
Ge vi	306243	415143	2.34×10^{-4}		918.278			
Kr vii	170835	279714.8	1.39×10^{-1}	12.2	918.444	918.53	26.4	
H i	1	11			919.351			ISM multi-component
Kr vi	170084	278787	3.01×10^{-3}		919.938			
H i	1	10			920.963			ISM multi-component
O iv	2s2p ² $^2\text{P}_{1/2}$	2p ³ $^2\text{P}_{3/2}^o$	5.62×10^{-2}		921.296			
O iv	2s2p ² $^2\text{P}_{1/2}$	2p ³ $^2\text{P}_{1/2}^o$	1.12×10^{-1}		921.365			
N iv	2s2p $^3\text{P}_1^o$	2p ² $^3\text{P}_2$	9.38×10^{-2}	75.7	921.994	922.07	23.1	
N iv	2s2p $^3\text{P}_0^o$	2p ² $^3\text{P}_1$	2.25×10^{-1}	91.6	922.519	922.59	22.8	
N iv	2s2p $^3\text{P}_1^o$	2p ² $^3\text{P}_1$	5.62×10^{-2}		923.056			
H i	1	9			923.150			ISM multi-component
N iv	2s2p $^3\text{P}_2^o$	2p ² $^3\text{P}_2$	1.69×10^{-1}		923.220			
O iv	2s2p ² $^2\text{P}_{3/2}$	2p ³ $^2\text{P}_{3/2}^o$	1.41×10^{-1}		923.367			
O iv	2s2p ² $^2\text{P}_{3/2}$	2p ³ $^2\text{P}_{1/2}^o$	2.81×10^{-2}		923.436			
N iv	2s2p $^3\text{P}_1^o$	2p ² $^3\text{P}_0$	7.49×10^{-2}	69.5	923.676	923.75	24.0	
S v	3s3p $^1\text{P}_1^o$	3p ² $^1\text{S}_0$	1.71×10^{-1}		924.220			blend with N iv
N iv	2s2p $^3\text{P}_2^o$	2p ² $^3\text{P}_1$	5.61×10^{-2}		924.284			blend with S v
Ge vi	303696	411886	2.34×10^{-4}		924.302			blend with N iv

Table A.2. Continued.

Ion	Levels		f	$W_\lambda /$ mÅ	Wavelength/ Å		$v_{\text{rad}} /$ km/s	Comment
	Lower	Upper			Theoretical	Observed		
Ba VII	226198	334319	1.27×10^{-3}		924.892			newly identified
Ba VII	42514	150634	1.74×10^{-3}		924.898			newly identified
H I	1	8			926.226			ISM multi-component
Ge VI	303696	411592	3.63×10^{-1}		926.824			
Kr VI	0	107836	1.58×10^{-3}	16.5	927.334	927.43	31.4	
Xe VI	$5p^2 \ ^2D_{3/2}$	$5p^3 \ ^2D_{3/2}^o$	3.53×10^{-2}		928.371			
Xe VI	$5p^2 \ ^2P_{3/2}$	$5p^3 \ ^2P_{3/2}^o$	4.87×10^{-2}		929.141			
O I					929.517			ISM multi-component
Ge VI	313025	420542	2.44×10^{-1}		930.082			
Ge VI	306243	413728	8.07×10^{-4}		930.366			
H I	1	7			930.748			ISM multi-component
Kr VI	8110	115479	2.23×10^{-3}	19.1	931.368	931.43	19.3	
				15.3		931.98		unid.
S VI	$3s \ ^2S_{1/2}$	$3p \ ^2P_{3/2}^o$	4.36×10^{-1}	57.9	933.378	933.47	28.9	
O I					936.630			ISM multi-component
Ge IV	190852.5	84102.3	8.91×10^{-1}		936.765	936.82	17.6	
Ba VI	36156	142852	7.40×10^{-3}		937.241			
Ba VII	15507	122163	1.08×10^{-2}		937.595			newly identified
H I	1	6			927.803			ISM multi-component
Ge IV	190601.5	84102.3	9.89×10^{-2}		938.973			
Ge V	234219	340296	8.22×10^{-3}		942.717			
Ba VII	42514	148547	3.40×10^{-3}		943.102			
Kr VI	170084	276011	3.88×10^{-2}		944.046			
S VI	2S	$^2P^o$	2.20×10^{-1}	59.8	944.523	944.62	29.8	
				14.8		946.06		unid.
Ge VI	306243	411886	1.28×10^{-1}		946.589			
Ge VI	303696	409188	1.15×10^{-1}		947.937			blend with C IV
C IV	$3s \ ^2S_{1/2}$	$4p \ ^2P_{3/2}^o$	1.36×10^{-1}		948.090			
C IV	$3s \ ^2S_{1/2}$	$4p \ ^2P_{1/2}^o$	6.78×10^{-2}		948.208			
O I					948.686			ISM multi-component
H I	1	5			949.743			ISM multi-component
P IV	$3s^2 \ ^1S_0$	$3p \ ^1P_1^o$	1.60	33.1	950.655	950.75	30.0	
O I					950.887			ISM multi-component
N I					951.079			ISM multi-component
Ge VI	308657	413728	1.03×10^{-1}		951.739			
				40.9		952.90		unid.
Ba VI	23547	128436	6.95×10^{-3}	11.0	953.388	953.47	26.4	
N I					953.415			ISM multi-component
N I					953.655			ISM multi-component
N I					953.970			ISM multi-component

Table A.2. Continued.

Ion	Levels		f	$W_\lambda /$ mÅ	Wavelength/ Å		$v_{\text{rad}} /$ km/s	Comment
	Lower	Upper			Theoretical	Observed		
N IV	2s2p $^1P^o_1$	2p 2 1S_0	1.33×10^{-1}	13.6		954.45		unid.
Kr VI	222122	326657	2.68×10^{-2}	71.8	955.334	955.41	24.5	
Ge V	235967	340296	3.17×10^{-2}		956.617			
He II	2	9	5.43×10^{-3}		958.509			
P I					958.698			
N I					963.800			ISM multi-component
N I					963.990			ISM multi-component
N I					964.626			ISM multi-component
Kr VI	223040	326657	1.59×10^{-1}	25.6	965.093	965.16	21.8	
Ge V	235967	339540	3.56×10^{-2}	24.3	965.501	965.59	27.3	
Ge VI	310199	413728	2.62×10^{-1}		965.914			
						966.78		unid.
						966.84		unid.
						966.88		unid.
Ge VI	308657	412038	1.67×10^{-1}		967.300			newly identified
Xe VI	5p 2 $^2D_{5/2}$	5p 3 $^2D^o_{3/2}$	1.06×10^{-2}		967.550			
						968.26		unid.
Ge VI	308657	411886	1.96×10^{-1}		968.723			
Kr VI	8110	111193	4.34×10^{-4}		970.092			
Ge V	234219	337168	1.22×10^{-1}	16.0	971.357	971.41	16.4	
Ge VI	306243	409188	1.81×10^{-1}		971.392			blend with Ge v
O I					971.737			ISM multi-component
O I					971.738			ISM multi-component
O I					971.738			ISM multi-component
He II	2	8	8.04×10^{-3}		972.111			
D I					972.272			ISM multi-component
H I	1	4			972.537			ISM multi-component
O I					976.448			ISM multi-component
C III					977.020			ISM multi-component
C III	2s3s 3S_1	2p($^2P^o$)3d $^3P^o_2$	8.93×10^{-3}		977.020			
Ge V			3.56×10^{-3}		977.798			
N III	2s2p 2 $^2D_{5/2}$	2p 3 $^2D^o_{3/2}$	9.79×10^{-3}		979.768			
N III	2p 2 $^2D_{3/2}$	2p 3 $^2D^o_{3/2}$	1.27×10^{-1}		979.832			
N III	2s2p 2 $^2D_{5/2}$	2p 3 $^2D^o_{5/2}$	1.33×10^{-1}		979.905			
N III	2s2p 2 $^2D_{3/2}$	2p 3 $^2D^o_{5/2}$	1.44×10^{-2}		979.969			
Kr VI	222122	324120	1.31×10^{-1}	22.7	980.411	980.51	28.7	
C III	3s 3S_1	3d' $^3P^o_2$	8.98×10^{-1}	24.9	981.462	981.53	20.5	
Ge V	238765	340296	1.08×10^{-1}	20.7	984.923	985.00	23.4	
Ge V			1.13×10^{-3}		987.064			
As V	4s $^2S_{1/2}$	4p $^2P^o_{3/2}$	5.28×10^{-1}	35.7	987.651	987.74	27.0	

Table A.2. Continued.

Ion	Levels		f	$W_\lambda /$ mÅ	Wavelength/ Å		$v_{\text{rad}} /$ km/s	Comment
	Lower	Upper			Theoretical	Observed		
Fe I					987.687			ISM multi-component
Ge V	235967	337168	1.00×10^{-1}	21.6	988.132	988.22	25.8	
O IV	3d $^4\text{F}_{3/2}^o$	4f $^4\text{G}_{5/2}$	7.72×10^{-1}		988.523			
O IV	3d $^4\text{F}_{5/2}^o$	4f $^4\text{G}_{7/2}$	6.89×10^{-1}		988.573			
O I					988.578			ISM multi-component
Fe V	357329.1	256177.9	5.88×10^{-1}		988.619			
O IV	3d $^4\text{F}_{7/2}^o$	4f $^4\text{G}_{9/2}$	6.87×10^{-1}		988.627			
O I					988.655			ISM multi-component
O IV	3d $^4\text{F}_{9/2}^o$	4f $^4\text{G}_{11/2}$	7.20×10^{-1}		988.708			
O I					988.773			ISM multi-component
N III	2p $^2\text{P}_{1/2}^o$	2s2p 2 $^2\text{D}_{3/2}$	1.23×10^{-1}	37.0	989.799	989.88	24.8	
Si II					989.873			ISM multi-component
Ge V	234219	335161	1.13×10^{-1}	10.8	990.668	990.76	27.5	
N III	2p $^2\text{P}_{3/2}^o$	2s2p 2 $^2\text{D}_{3/2}$	1.20×10^{-2}		991.511			
N III	2p $^2\text{P}_{3/2}^o$	2p 2 $^2\text{D}_{5/2}$	1.11×10^{-1}		991.577			
He II	2	7	1.27×10^{-2}		992.363			
Ba VII	21499	122163	5.38×10^{-3}	14.2	993.411	993.49	22.6	
Xe VII	5s 2 S $_0$	5p $^3\text{P}_1^o$	2.45×10^{-1}	26.2	995.511	995.59	24.1	
Mo VI	182404	282826	1.12	12.9	995.806	995.90	28.3	
Xe VII	5p $^2\text{P}_{1/2}^o$	5p 2 $^4\text{P}_{3/2}$	5.66×10^{-5}		996.233			
Se IV				21.7	996.710	996.77	18.0	
P V	3d $^2\text{D}_{5/2}$	4p $^2\text{P}_{3/2}^o$	1.50×10^{-1}	28.5	997.612	997.72	33.4	
				18.5		999.49		unid. uncertain, newly identified
Zn V	231122	331087	2.69×10^{-2}		1000.350			
S VI	4d $^2\text{D}_{3/2}$	5f $^2\text{F}_{5/2}^o$	6.72×10^{-1}		1000.372			
Zr V	437678	537502	1.27×10^{-1}		1001.765			uncertain unid.
				20.2		1001.99		
C III	3p $^1\text{P}_1^o$	6d $^1\text{D}_2$	4.12×10^{-2}		1001.988			
Zr V	277146	376898	1.11×10^{-2}		1002.484			
Kr VI	8110	107836	3.30×10^{-4}	16.3	1002.748	1002.82	21.5	
Ge V				33.6	1004.380	1004.49	32.8	
C III	3s $^1\text{S}_0$	3d' $^1\text{P}_1^o$	5.49×10^{-2}		1004.596			
Ge V	238765	338274	5.41×10^{-2}	14.0	1004.938	1005.00	18.5	newly identified
Ge V			5.41×10^{-2}	15.9	1005.304	1005.39	25.6	
				16.6		1007.15		unid.
Ge V	235967	335161	1.21×10^{-2}	11.5	1008.122	1008.21	26.2	
O III	3s $^3\text{P}_2^o$	4p $^3\text{D}_3$	5.04×10^{-2}		1008.384			
				19.6		1008.66		unid.
				20.4		1009.81		unid.

Table A.2. Continued.

Ion	Levels		f	$W_\lambda /$ mÅ	Wavelength/Å		$v_{\text{rad}} /$ km/s	Comment
	Lower	Upper			Theoretical	Observed		
Ga v	236072	335089	7.80×10^{-2}		1009.928			
Kr vi	275380	374279	7.23×10^{-3}		1011.133			
Mo v	157851	256676	1.52×10^{-1}		1011.889			
				8.5		1012.44 1013.80 1014.01		unid. unid. unid.
Ga v	246093	344668	2.82×10^{-1}	11.0	1014.456	1014.55	27.8	
Ga v	246133	344668	2.86×10^{-2}		1014.868			
				13.0		1015.33		unid.
Ga v	231711	330174	9.59×10^{-2}		1015.610			
Kr vi	180339	278787	7.40×10^{-3}	12.0	1015.765	1015.83	19.2	
C iii	3p $^3P_0^o$	6d 3D_1	4.74×10^{-2}		1016.340			
C iii	3p $^3P_1^o$	6d 3D_1	1.19×10^{-2}		1016.399			
C iii	3p $^3P_1^o$	6d 3D_2	3.56×10^{-2}		1016.399			
C iii	3p $^3P_2^o$	6d 3D_1	4.78×10^{-4}		1016.534			
C iii	3p $^3P_2^o$	6d 3D_2	7.13×10^{-3}		1016.534			
C iii	3p $^3P_2^o$	6d 3D_3	3.98×10^{-2}		1016.534			
Ge v	241935	340296	1.95×10^{-1}	27.9	1016.668	1016.77	30.1	
				10.0		1017.21		unid.
Xe vi	5p ² $^2P_{1/2}$	5p ³ $^4S_{3/2}$	1.88×10^{-3}		1017.265			
Zn v	231831	330069	3.36×10^{-2}		1017.935			newly identified
				32.7		1018.13		unid.
				20.3		1018.57		unid.
Ga v	246133	344200	3.07×10^{-1}		1019.711			
				9.1		1021.49		unid.
				19.0		1021.73		unid.
He ii	2	6	2.21×10^{-2}		1025.272			
D i					1025.440			ISM multi-component
H i	1	3			1025.722			ISM multi-component
				9.9		1027.13		unid.
As v	4s $^2S_{1/2}$	4p $^2P_{1/2}^o$	2.53×10^{-1}	36.1	1029.480	1029.54	17.5	
Zn v	231997	329085	4.38×10^{-2}		1029.992			
P iv	3p $^3P_1^o$	3p ² 3P_1	1.20×10^{-1}	21.8	1030.517	1030.59 1031.22 1031.42	21.2	unid. unid.
O vi	2s $^2S_{1/2}$	2p $^2P_{3/2}^o$	1.33×10^{-1}		1031.912			
O vi					1031.926			ISM multi-component
Zn v	221631	318436	9.66×10^{-3}		1033.009			blend with Ge v, newly identified
Ge v	238765	335560	6.96×10^{-2}		1033.107			blend with Zn v, newly identified
Ge v			6.96×10^{-2}		1033.428			blend with Ca iii

Table A.2. Continued.

Ion	Levels		f	$W_\lambda /$ mÅ	Wavelength/ Å		$v_{\text{rad}} /$ km/s	Comment
	Lower	Upper			Theoretical	Observed		
Ca III	277380.86	374143.84	1.03×10^{-5}	12.4 17.1 16.2	1033.453	1033.52 1034.18 1034.60	19.4	blend with Ge v unid. unid.
Ge v	234219	330791	1.01×10^{-3}		1035.504			
Zn v	231831	328369	1.25×10^{-2}		1035.859			
Zn v	285885	382420	5.02×10^{-2}		1035.887			
N IV	3d 3D_3	4f $^3F_4^o$	8.56×10^{-1}		1036.119			
N IV	3d 3D_2	4f $^3F_3^o$	8.28×10^{-1}		1036.149			
N IV	3d 3D_1	4f $^3F_2^o$	9.33×10^{-1}		1036.196			
N IV	3d 3D_2	4f $^3F_2^o$	1.05×10^{-1}		1036.237			
N IV	3d 3D_3	4f $^3F_3^o$	7.53×10^{-2}		1036.239			
C II					1036.337			ISM multi-component
C II					1037.018			ISM multi-component
O VI	2s $^2S_{1/2}$	2p $^2P_{1/2}^o$	6.60×10^{-2}	21.0		1037.24		unid.
O VI				35.3	1037.613	1037.72	30.9	ISM multi-component
Ge v	241935	338274	1.45×10^{-1}	42.3	1038.430	1038.49	17.3	
Mo VI	187331	283611	9.73×10^{-1}		1038.640			blend with Zn v
Ga v	214000	310267	4.38×10^{-2}		1038.778			blend with Mo VI, newly identified
O I					1039.230			unid.
Ge VI	313025	409188	3.69×10^{-2}		1039.892			ISM multi-component
S v	3s3d 1D_2	3p3d $^1F_3^o$	3.41×10^{-1}	21.0	1039.916	1040.02	30.0	blend with S v
O III	2p ³ $^1P_1^o$	3p 1D_2	2.42×10^{-2}		1040.320			blend with Ge VI
				35.4		1041.03		unid.
				16.2		1041.32		unid.
Zn v	286575	382420	2.54×10^{-1}	9.8 9.4	1043.353	1043.44 1043.80	25.0	unid.
Sn IV				19.2	1044.490	1044.56	20.1	
Kr VI	180339	276011	5.24×10^{-2}		1045.238			
O IV	3p $^2P_{1/2}^o$	4s $^2S_{1/2}$	9.21×10^{-2}		1045.364			
Ge v	234219	329848	3.93×10^{-1}	62.5	1045.713	1045.81	27.8	
O IV	3p $^3P_{3/2}^o$	4s $^2S_{1/2}$	9.19×10^{-2}	29.3	1046.313	1046.39	22.1	
						1047.02		unid.
Zn v	222940	318436	2.65×10^{-2}		1047.164			uncertain, blend with Mo VI, newly identified
Mo VI	187331	282826	1.07×10^{-1}		1047.182			blend with Zn v
Ga v	242026	337491	1.31×10^{-1}		1047.504			blend with O IV, newly identified
O IV	3s $^2S_{1/2}$	2s2p($^3P^o$)3s $^2P_{3/2}^o$	2.89×10^{-2}		1047.590			blend with Ga v
Ge v	464652	560097	1.18×10^{-1}		1047.730			newly identified

Table A.2. Continued.

Ion	Levels		f	$W_\lambda /$ mÅ	Wavelength/ Å		$v_{\text{rad}} /$ km/s	Comment
	Lower	Upper			Theoretical	Observed		
Ar I					1048.220			ISM multi-component
Ge V	464077	559463	2.43×10^{-1}		1048.371			blend with Zn V, newly identified
Zn V	285523	380902	1.01×10^{-1}		1048.448			blend with Ge V, newly identified
				16.9		1048.59		unid.
						1048.97		unid.
Ge V	241935	337168	1.55×10^{-1}	34.5	1050.057	1050.14	23.7	
Ga V	210052	305249	1.95×10^{-1}		1050.453			blend with O IV
O IV	3s $^2S_{1/2}$	2s2p($^3P^o$)3s $^2P^o_{1/2}$	1.44×10^{-2}		1050.505			blend with Ga V
				14.4		1051.18		unid.
As V				19.2	1051.600	1051.69	25.7	
Kr VI	183817	278787	4.76×10^{-3}	12.8	1052.964	1053.04	21.6	
						1053.24		unid.
Zr VI	427119	522036	2.20×10^{-1}		1053.548			
Ge V	235967	330791	8.93×10^{-2}		1054.590			
Zn V	221631	316339	5.31×10^{-2}	30.4	1055.878	1055.95	20.4	
Se VI				10.7	1056.980	1057.05	19.9	
Ga V	212121	306628	1.65×10^{-1}		1058.123			blend with Zn V
Zn V	198962	293463	6.01×10^{-3}		1058.185			blend with Ga V, newly identified
				7.9		1059.39		unid.
				28.8		1060.70		unid.
C IV	4p $^2P^o_{3/2}$	10d $^2D_{3/2}$	1.30×10^{-3}		1060.740			
C IV	4p $^2P^o_{3/2}$	10d $^2D_{5/2}$	1.17×10^{-2}		1060.740			
Kr VI	183817	278062	6.58×10^{-2}	25.6	1061.064	1061.16	27.1	
O IV	2s2p($^3P^o$)3d $^4D^o_{1/2}$	2s2p($^3P^o$)4f $^4F_{3/2}$	7.40×10^{-1}		1061.780			
Zn V	221631	315801	1.40×10^{-2}		1061.914			newly identified
O IV	2s2p($^3P^o$)3d $^4D^o_{5/2}$	2s2p($^3P^o$)4f $^4F_{7/2}$	6.02×10^{-1}		1062.133			
O IV	2s2p($^3P^o$)3d $^4D^o_{7/2}$	2s2p($^3P^o$)4f $^4F_{9/2}$	6.60×10^{-1}		1062.271			
Ga V	236072	330174	2.58×10^{-1}	13.9	1062.677	1062.75	20.6	
Ge V	464853	558877	8.57×10^{-1}		1063.554			
Ga V	231711	325713	3.82×10^{-2}		1063.807			newly identified
Zn V	222042	316029	8.15×10^{-2}		1063.979			
Se VI				25.3	1064.620	1064.71	25.3	
Zr VI	421258	515171	4.55×10^{-1}		1064.818			
				24.7		1065.43		unid.
				41.8		1065.69		unid.
Si IV	3d $^2D_{5/2}$	4f $^2F^o_{5/2}$	4.34×10^{-2}	64.5	1066.636	1066.74	29.2	
O IV	3d $^2D_{3/2}$	4f $^2F^o_{5/2}$	7.97×10^{-1}		1067.768			
O IV	3d $^2D_{5/2}$	4f $^2F^o_{7/2}$	7.59×10^{-1}		1067.832			
O IV	3d $^2D_{5/2}$	4f $^2F^o_{5/2}$	3.80×10^{-2}		1067.958			

Table A.2. Continued.

Ion	Levels		f	$W_\lambda /$ mÅ	Wavelength/ Å		$v_{\text{rad}} /$ km/s	Comment
	Lower	Upper			Theoretical	Observed		
Zn v	221631	315239	5.19×10^{-2}		1068.284			
Ge v	234219	327891	6.53×10^{-2}	25.4	1068.430	1068.53	28.1	
Zr v	378753	472338	1.68×10^{-1}		1068.551			blend with Ga v
Ga v	232968	326549	1.61×10^{-1}		1068.593			blend with Zr v
Ga v	242026	335605	1.65×10^{-2}		1068.616			
Ge v	241935	335560	8.73×10^{-2}	27.8	1069.130	1069.23	28.0	
Ge v	461829	555337	5.02×10^{-1}		1069.420			blend with Ga v
Ga v	235609	329103	2.87×10^{-1}		1069.587			blend with Ge v, newly identified
Zn v	235599	329085	7.85×10^{-2}		1069.674			blend with Ga v
Ge v	461815	555299	6.07×10^{-1}		1069.703			
Zn v	231997	325476	3.03×10^{-2}		1069.764			
Ge v	461829	555299	1.10×10^{-1}		1069.859			
				6.2		1070.81		unid.
				19.0		1071.04		unid.
Ga v	235752	329112	2.75×10^{-1}		1071.123			
Ga v	235752	329108	2.34×10^{-1}		1071.168			
Te vi				65.0	1071.400	1071.51	30.8	blend with Zn v
Zn v	221631	314958	3.27×10^{-2}		1071.501			blend with Te vi
Ge v	461418	554658	9.97×10^{-1}	17.1	1072.495	1072.59	26.6	
Ge v	241935	335161	2.52×10^{-1}	41.4	1072.661	1072.76	27.7	
Zn v	222042	315239	2.14×10^{-1}	24.8	1072.992	1073.04		
Ga v	212121	305249	1.22×10^{-1}		1073.791			
Zn v	222940	316029	6.35×10^{-2}		1074.241			
Ge v	461643	554690	9.68×10^{-1}		1074.719			
						1074.93		unid.
Zn v	240446	333455	3.01×10^{-1}		1075.171			
Zn v	222042	314958	1.95×10^{-2}		1076.239			
				21.3		1076.44		unid.
				20.9		1076.80		unid.
Zn v	222940	315801	1.56×10^{-1}		1076.878			
Xe vii	5p $^1\text{P}^o_1$	5p 2 ^1D	8.10×10^{-1}	26.1	1077.120	1077.22	27.8	
Ga v	231711	324407	2.96×10^{-1}		1078.795			newly identified
O iv	3p $^2\text{P}^o_{3/2}$	2s2p($^3\text{P}^o$)3p $^2\text{D}_{5/2}$	5.18×10^{-2}		1079.056			
Ga v	214000	306628	1.56×10^{-1}		1079.587			
Ga v	215237	307864	2.23×10^{-1}		1079.599			
Ga v	231711	324314	1.29×10^{-2}		1079.879			
Xe vi	5p $^2\text{P}^o_{1/2}$	5p 2 $^4\text{P}_1$	1.90×10^{-3}	20.0	1080.077	1080.16	23.0	
Zn v	232946	325476	6.65×10^{-2}		1080.735			newly identified
O iv	3d $^2\text{D}^o_{3/2}$	4f $^2\text{F}_{5/2}$	7.33×10^{-1}		1080.967			
O iv	3d $^2\text{D}^o_{5/2}$	4f $^2\text{F}_{7/2}$	6.98×10^{-1}		1080.969			

Table A.2. Continued.

Ion	Levels		f	$W_\lambda /$ mÅ	Wavelength/Å		$v_{\text{rad}} /$ km/s	Comment
	Lower	Upper			Theoretical	Observed		
O iv	3p $^2P^o_{1/2}$	4p $^2D_{3/2}$	5.77×10^{-2}		1081.024			
N ii					1083.994			ISM multi-component
He ii	2	5	4.47×10^{-2}		1084.942			
						1086.60		unid.
Ge v	238765	330791	3.18×10^{-1}		1086.653			
Ge v	235967	327891	3.03×10^{-1}	27.0	1087.855	1087.95	26.2	
Zn v	235730	327581	2.87×10^{-1}		1088.709			newly identified
Sn v					1089.350	1089.42	19.2	
Ge v	235967	327753	1.42×10^{-1}		1089.491			
Zn v	260880	352553	2.98×10^{-1}		1090.831			
Xe vi	5p $^2P^o_{3/2}$	5p ² 4P_5	2.47×10^{-3}		1091.632			blend with Ga v
Ga v	221488	313088	2.70×10^{-1}		1091.703			blend with Xe vi
Ge v	238765	330333	1.01×10^{-1}		1092.089			
O iv	3d $^2D_{5/2}$	2s2p($^3P^o$)3d $^2F^o_{7/2}$	3.78×10^{-2}		1093.774			
				22.6		1094.00		unid.
Zn v	236969	328369	2.86×10^{-1}		1094.088			
				33.6		1094.23		unid.
Ga v	218301	309679	1.73×10^{-1}		1094.355			
Ni vi	347278.5	438639.4	2.27×10^{-1}		1094.560			
Se v				36.4	1094.680	1094.79	30.1	
Ga v	232968	324314	6.28×10^{-2}		1094.739			
Ga v	218301	309616	1.81×10^{-1}		1095.110			newly identified
Ge v	464077	555337	1.53×10^{-2}		1095.769			
Zn v	285885	377144	4.69×10^{-2}		1095.774			blend with Ge v
Zn v	235730	326987	2.94×10^{-2}		1095.797			
Zn v	239843	331087	1.30×10^{-1}		1095.961			
						1096.28		unid.
O iv	3d $^2D_{3/2}$	2s2p($^3P^o$)3d $^2F^o_{5/2}$	3.95×10^{-2}		1096.359			
Ge v	464706	555852	7.69×10^{-1}		1097.134			
Zn v	235599	326664	3.51×10^{-2}		1098.108			newly identified
				15.8		1099.02		unid.
Zr vi	427119	518062	8.55×10^{-1}		1099.591			
				11.6		1099.85		unid.
Ga v	243053	333929	4.24×10^{-1}		1100.401			newly identified
Ge v	469686	560547	9.01×10^{-1}	20.2	1100.585	1100.66	20.4	
Mo v	146977	237760	2.05×10^{-1}		1101.530			
Ga v	246133	336909	2.07×10^{-1}		1101.613			
Mo v	151195	241965	2.02×10^{-2}		1101.690			
Xe vi	5p ² $^2P_{1/2}$	5p ³ $^2D^o_{3/2}$	1.88×10^{-3}		1101.940			
						1102.26		unid.

Table A.2. Continued.

Ion	Levels		f	$W_\lambda /$ mÅ	Wavelength/ Å		$v_{\text{rad}} /$ km/s	Comment
	Lower	Upper			Theoretical	Observed		
Ga v	242026	332707	2.39×10^{-1}		1102.767			
Ga v	210052	300730	1.12×10^{-1}		1102.803			
Ga v	212121	302779	1.34×10^{-1}		1103.047			
				7.5		1103.37		unid.
				6.4		1103.56		unid.
Zn v	236969	327581	2.67×10^{-2}		1103.598			newly identified
Zn v	291107	381670	2.70×10^{-1}	34.7	1104.199	1104.29	24.2	newly identified
Ga v	221488	311991	1.35×10^{-1}		1104.936			
Ga v	236072	326549	3.18×10^{-2}		1105.253			
Ni v	229413	319860.4	3.02×10^{-4}		1105.615			blend with Ga v
Ga v	242026	332473	3.45×10^{-1}		1105.620			blend with Ni v
C iv					1106.330			forbidden C iv component
C iv					1106.770			forbidden C iv component
C iv	3p $^2\text{P}_{1/2}^o$	4d $^2\text{D}_{3/2}$	5.41×10^{-1}		1107.591			
C iv	3p $^2\text{P}_{3/2}^o$	4d $^2\text{D}_{5/2}$	4.86×10^{-1}		1107.930			
C iv	3p $^2\text{P}_{3/2}^o$	4d $^2\text{D}_{3/2}$	5.41×10^{-2}		1107.979			
Zn v	221631	311796	1.53×10^{-1}		1109.078			
Zn v	230614	320772	5.16×10^{-2}		1109.166			
Zn v	232946	322969	2.06×10^{-2}		1110.821			weak
Zn v	256235	346201	1.14×10^{-1}		1111.530			
Zn v	255763	345723	2.37×10^{-1}		1111.603			
Zn v	255763	345624	1.46×10^{-1}		1112.829			
						1114.19		unid.
Zn v	221631	311359	2.16×10^{-1}		1114.482			
Zn v	255482	345146	1.29×10^{-1}		1115.266			
Ga v	236072	325713	1.91×10^{-1}		1115.561			
Zn v	237032	326664	2.83×10^{-3}		1115.668			
Zn v	227195	316827	1.34×10^{-1}		1115.680			newly identified
Zn v	256235	345791	3.51×10^{-1}		1116.630			
Zn v	198962	288500	3.70×10^{-1}		1116.842			blend with Ge v
Ge v	234219	323749	1.97×10^{-1}		1116.949			blend with Zn v
				11.3		1117.37		unid.
Zn v	256235	345723	4.53×10^{-2}	17.3	1117.466	1117.55	22.5	newly identified
S vi	4f $^2\text{F}_{5/2}^o$	5g $^2\text{G}_{7/2}$	1.34		1117.756			
S vi	4f $^2\text{F}_{7/2}^o$	5g $^2\text{G}_{7/2}$	3.78×10^{-2}		1117.756			
S vi	4f $^2\text{F}_{7/2}^o$	5g $^2\text{G}_{9/2}$	1.30		1117.756			
P v	3s $^2\text{S}_{1/2}$	3p $^2\text{P}_{3/2}^o$	4.50×10^{-1}	95.6	1117.976	1118.06	22.5	
P v					1117.977			ISM multi-component
Zr vi	440555	529945	9.37×10^{-1}		1118.689			

Table A.2. Continued.

Ion	Levels		f	$W_\lambda /$ mÅ	Wavelength/Å		$v_{\text{rad}} /$ km/s	Comment
	Lower	Upper			Theoretical	Observed		
Zr v	382985	472338	1.42×10^{-1}		1119.158	1119.31 1119.68		uncertain unid. unid.
Zn v	255482	344771	2.05×10^{-1}		1119.950			
Zn v	232946	322224	8.00×10^{-2}		1120.101			blend with Zn v
I vI					1120.300			blend with I vI
Zn v	226334	315594	2.23×10^{-1}		1120.325			blend with I vI
Zn v	239843	329085	4.82×10^{-2}		1120.545			newly identified
				24.2		1120.95		unid.
Zn v	230435	319632	1.26×10^{-1}		1121.109			
Zn v	235903	325068	8.18×10^{-2}		1121.524			weak
Ge v			9.44×10^{-2}		1122.001			blend with S v, very weak
S v	3s3d 3D_3	3p3d $^3F_4^0$	1.73×10^{-1}		1122.031			blend with Ge v
						1122.24		unid.
Si iv	3p $^2P_{1/2}^0$	3d $^2D_{3/2}$	8.07×10^{-1}	43.7	1122.485	1122.59	28.0	
Zn v	240446	329533	1.62×10^{-1}		1122.502			blend with Si iv
				13.2		1122.79		unid.
Zn v	230435	319472	3.03×10^{-2}		1123.127			blend with Ga v
Ga v	215237	304272	2.81×10^{-1}	16.8	1123.154	1123.26 1123.70	28.3	unid.
Ge v	238765	327753	3.83×10^{-2}		1123.746			
Zn v	221631	310519	1.36×10^{-1}		1125.019			
Zn v	228335	317220	1.72×10^{-1}		1125.048			
Zn v	231997	320871	6.18×10^{-3}		1125.182			newly identified
Ge v	241935	330791	1.29×10^{-2}		1125.424			
C III	3d 3D_1	6f $^3F_2^0$	8.13×10^{-2}		1125.629			
C III	3d 3D_2	6f $^3F_3^0$	7.22×10^{-2}		1125.639			
C III	3d 3D_2	6f $^3F_2^0$	9.19×10^{-3}		1125.643			
C III	3d 3D_3	6f $^3F_4^0$	7.46×10^{-2}		1125.670			
Mo v	240878	329714	5.57×10^{-1}		1125.672			
C III	3d 3D_3	6f $^3F_3^0$	6.57×10^{-3}		1125.675			
C III	3d 3D_3	6f $^3F_2^0$	1.49×10^{-4}		1125.679			
Mo v	148949	237760	5.53×10^{-1}		1125.988			
Ga v	214000	302779	2.05×10^{-1}	27.0	1126.393	1126.50	28.5	
Ga v	235609	324314	3.96×10^{-2}		1127.332			
Ga v	215237	303911	1.41×10^{-1}		1127.726			
Ga v	246093	334765	3.63×10^{-1}	10.8	1127.752	1127.85	26.1	
P v	3s $^2S_{1/2}$	3p $^2P_{1/2}^0$	2.21×10^{-1}		1128.006			blend with Ga v
P v					1128.008			ISM multi-component
Ga v	218301	306947	3.07×10^{-1}		1128.082			blend with P v

Table A.2. Continued.

Ion	Levels		f	$W_\lambda /$ mÅ	Wavelength/ Å		$v_{\text{rad}} /$ km/s	Comment
	Lower	Upper			Theoretical	Observed		
Si iv	3p $^2P^o_{3/2}$	3d $^2D_{5/2}$	7.25×10^{-1}	53.4	1128.340	1128.45	29.2	
Ga v	212121	300730	1.94×10^{-1}	9.6	1128.554	1128.65	25.5	
S v	3d 3D_2	3d $^3F^o_3$	1.74×10^{-1}	12.1	1128.699	1128.80	26.8	
S v	3d 3D_3	3d $^3F^o_3$	1.55×10^{-2}		1128.812			
Zn v	255482	344070	5.38×10^{-2}		1128.813			newly identified
				8.8		1129.07 1129.45		unid.
Zn v	226334	314838	4.16×10^{-2}		1129.898			blend with Ga v
Ga v	214000	302499	1.75×10^{-1}		1129.956			blend with Zn v
Zn v	228335	316827	9.66×10^{-2}		1130.051			
Zn v	222042	310519	1.55×10^{-1}	7.1	1130.242	1130.34	26.0	
Ni vi	330141	418553.6	3.12×10^{-1}		1131.061			
Zn v	227195	315594	6.70×10^{-2}		1131.242			
Ga v	231711	320093	2.30×10^{-1}		1131.452			newly identified
Zn v	222940	311296	1.33×10^{-1}		1131.788			
Zn v	231122	319472	1.29×10^{-1}		1131.863			
Zn v	208715	297033	1.40×10^{-1}		1132.271			
Zn v	235599	323886	3.93×10^{-1}		1132.659			
Sn v					1132.790	1132.92	34.4	
Zn v	200644	288903	3.36×10^{-1}		1133.031			
Zn v	228335	316586	2.11×10^{-1}		1133.128			
Zn v	241829	330069	3.40×10^{-1}		1133.278			
Zn v	222042	310265	1.66×10^{-1}		1133.498			
S v	3s3d 3D_1	3p3d $^3F^o_2$	1.84×10^{-1}		1133.901			
S v	3s3d 3D_2	3p3d $^3F^o_2$	2.19×10^{-2}		1133.973			
N ii					1134.165			ISM multi-component
N ii					1134.415			ISM multi-component
N ii					1134.980			ISM multi-component
Zn v	208715	296796	1.50×10^{-2}		1135.324			
Zn v	200644	288704	4.32×10^{-2}		1135.588			
Ga v	212121	300144	1.98×10^{-1}		1136.067			
Zn v	228335	316339	7.85×10^{-2}		1136.311			blend with Xe vi, newly identified
Xe vi	5d $^2D_{5/2}$	6p $^2P^o_{3/2}$	1.91×10^{-1}		1136.410			blend with Zn v
Zn v	198962	286943	4.06×10^{-2}		1136.603			
Zn v	201973	289925	4.03×10^{-2}		1136.986			
				18.9		1137.33		unid.
Zn v	235730	323632	5.74×10^{-2}		1137.625			
Mo v	151195	239069	2.98×10^{-1}		1137.995			
Mo v	151213	239069	2.30×10^{-1}		1138.229			blend with Zn v
Zn v	201973	289827	3.67×10^{-1}	36.1	1138.248	1138.35	26.9	blend with Mo v

Table A.2. Continued.

Ion	Levels		f	$W_\lambda /$ mÅ	Wavelength/ Å		$v_{\text{rad}} /$ km/s	Comment
	Lower	Upper			Theoretical	Observed		
Zn v	256235	344070	1.72×10^{-1}		1138.497			
Zn v	210973	298801	1.93×10^{-2}		1138.586			newly identified
Zn v	230614	318436	2.59×10^{-2}		1138.671			newly identified
Zn v	202929	290731	4.08×10^{-3}		1138.933			newly identified
Zn v	231831	319632	3.28×10^{-3}		1138.937			newly identified
Ge v	235967	323749	9.14×10^{-3}		1139.187			blend with Zn v
Zn v	202929	290704	6.62×10^{-2}		1139.278			blend with Ge v
Ni vi	347278.5	435011.5	2.59×10^{-1}		1139.822			blend with C iii
C iii	2s3p P_1^o	2s5d D_2	8.86×10^{-2}		1139.899			
Zn v	222940	310659	8.37×10^{-2}		1139.997			blend with C iii, newly identified
Zn v	286575	374241	3.85×10^{-1}		1140.703			
Zn v	227195	314838	9.68×10^{-2}		1141.003			
Zn v	231997	319632	9.35×10^{-2}		1141.095			
Zn v	222042	309658	7.60×10^{-2}		1141.344			
						1142.10		unid.
Zn v	228335	315840	3.27×10^{-2}		1142.792			
Zn v	202929	290424	3.99×10^{-1}	18.6	1142.925	1143.03	27.5	
Zn v	237032	324526	3.40×10^{-1}		1142.938			
Zn v	203548	291022	8.87×10^{-2}		1143.196			
Fe ii					1143.226			ISM multi-component
Ba vii	61083	148547	2.88×10^{-3}		1143.317			newly identified
Zn v	255763	343221	1.16×10^{-1}		1143.403			
						1143.58		unid.
Zn v	210973	298375	1.27×10^{-1}		1144.136			
Ni vi	298130.5	385520.9	3.52×10^{-1}		1144.290			
Fe i					1144.938			ISM multi-component
Zn v	222940	310265	7.64×10^{-2}		1145.151			
				9.4		1145.55		unid.
Zn v	241829	329085	6.47×10^{-2}		1146.057			
Zn v	234582	321830	3.55×10^{-1}		1146.149			
Zn v	203548	290731	4.50×10^{-1}	25.3	1147.020	1147.11	23.5	
Zn v	203548	290704	1.63×10^{-1}		1147.371			
Zn v	255482	342616	2.00×10^{-1}		1147.648			newly identified
Mo v	153040	240110	4.03×10^{-1}		1148.502			
Zn v	232946	319984	3.33×10^{-1}	10.7	1148.922	1149.01	23.0	
Zn v	227195	314197	1.89×10^{-1}		1149.398			
Zn v	202929	289925	2.05×10^{-1}		1149.486			
Zn v	256235	343221	1.34×10^{-1}		1149.608			
Zn v	226334	313300	3.62×10^{-1}		1149.873			
Ni vi	330580.5	417538.4	1.17×10^{-1}		1149.982			

Table A.2. Continued.

Ion	Levels		f	$W_\lambda /$ mÅ	Wavelength/Å		$v_{\text{rad}} /$ km/s	Comment
	Lower	Upper			Theoretical	Observed		
Ni VI	376343.7	463301.5	2.29×10^{-1}		1149.983			
Ga V	218301	305249	2.22×10^{-2}		1150.113			
Ga V	210052	296992	2.24×10^{-1}		1150.219			
				25.1		1150.64		unid.
Zn V	212471	299372	1.66×10^{-1}	11.4	1150.743	1150.84	25.3	
O III	2p ³ ³ S ₁ ^o	2p ⁴ ³ P ₁	8.43×10^{-2}		1150.884	1151.03	38.0	
Se V					1151.000	1151.13	33.9	
Ni V	212095.8	298972.3	2.34×10^{-2}		1151.059			
Zn V	255763	342616	1.16×10^{-1}		1151.368			
Zn V	230614	317466	4.50×10^{-2}		1151.393			newly identified
Zr VI	427649	514487	2.33×10^{-1}		1151.571			
Zn V	201973	288704	2.26×10^{-1}	19.6	1152.985	1153.08	24.7	
Zn V	222940	309658	4.82×10^{-2}		1153.160			
				18.4		1153.56		unid.
O III	2p ³ ³ S ₁ ^o	2p ⁴ ³ P ₂	1.41×10^{-1}	37.2	1153.775	1153.90	32.5	
Zn V	208715	295293	7.17×10^{-2}	3.6	1155.027	1155.14	29.3	
Zn V	232946	319472	1.27×10^{-1}		1155.725			
Zn V	285885	372360	3.17×10^{-1}		1156.394			newly identified
Ga V	246133	332600	3.44×10^{-1}	12.4	1156.511	1156.62	28.3	
Zn V	231997	318436	2.76×10^{-2}		1156.885			
Zn V	203548	289925	2.90×10^{-2}		1157.725			newly identified
Ni VI	337993.9	424363.7	1.04×10^{-1}		1157.812			
				15.7		1158.00		unid.
Zn V	239843	326189	7.13×10^{-2}		1158.122			
Zn V	235903	322224	1.83×10^{-1}		1158.475			
Zn V	200644	286943	2.38×10^{-1}	24.6	1158.759	1158.86	26.1	
				27.3		1159.88		unid.
Zn V	226334	312534	1.04×10^{-2}		1160.091			weak
Zn V	234582	320772	2.88×10^{-1}		1160.221			
Sn V				37.6	1160.740	1160.86	31.0	blend with Zn V
Zn V	255482	341627	7.26×10^{-2}		1160.827			blend with Sn V, newly identified
				40.1		1161.99		unid.
Zn V	210973	297033	5.56×10^{-2}		1161.971			
Zn V	291107	377144	3.72×10^{-1}		1162.281			
Zn V	230614	316643	9.18×10^{-2}		1162.401			
Ge V	241935	327891	1.29×10^{-2}		1163.389			
Zn V	230435	316339	7.96×10^{-2}		1164.082			
Zn V	212471	298375	6.62×10^{-2}		1164.100			newly identified
O IV	3d ² F _{5/2} ^o	4f ² G _{7/2}	8.50×10^{-1}	16.7	1164.321	1164.41	22.9	
O IV	3d ² F _{7/2} ^o	4f ² G _{9/2}	8.26×10^{-1}	19.9	1164.546	1164.65	26.8	

Table A.2. Continued.

Ion	Levels		f	$W_\lambda /$ mÅ	Wavelength/ Å		$v_{\text{rad}} /$ km/s	Comment
	Lower	Upper			Theoretical	Observed		
Zn v	255763	341627	5.07×10^{-2}		1164.632			
Zn v	228335	314197	1.72×10^{-2}		1164.656			newly identified
Zn v	210973	296796	4.52×10^{-2}		1165.186			blend with Ge v
Ge v	241935	327753	1.48×10^{-2}		1165.259			blend with Zn v
				27.0		1165.40		unid.
Zn v	286575	372360	4.41×10^{-2}		1165.706			
Zn v	210973	296757	5.56×10^{-2}		1165.716			
Zn v	234846	320618	3.60×10^{-1}		1165.880			
C iv	3d $^2D_{3/2}$	4f $^2F_{5/2}^o$	1.02		1168.849			
C iv	3d $^2D_{5/2}$	4f $^2F_{7/2}^o$	4.88×10^{-2}		1168.993			
C iv	3d $^2D_{5/2}$	4f $^2F_{5/2}^o$	9.97×10^{-1}		1168.993			
Zn v	226334	311796	1.02×10^{-1}		1170.105			
C iv					1170.130			forbidden C iv component
C iv					1170.330			forbidden C iv component
Zn v	231831	317220	7.01×10^{-2}		1171.106			
Zn v	239843	325068	3.11×10^{-1}		1173.366			
Zn v	198962	284116	3.01×10^{-1}	24.1	1174.346	1174.43	21.4	
				12.3		1174.75		unid.
C iii	2s2p $^3P_1^o$	2p ² 3P_2	1.17×10^{-1}	108.5	1174.933	1175.04	27.3	
Zn v	235599	320709	1.24×10^{-1}		1174.945			blend with C iii
C iii	2s2p $^3P_0^o$	2p ² 3P_1	2.72×10^{-1}	112.4	1175.263	1175.38	29.9	
C iii	2s2p $^3P_1^o$	2p ² 3P_1	7.03×10^{-2}		1175.590			
C iii	2s2p $^3P_2^o$	2p ² 3P_2	2.11×10^{-1}		1175.711			
C iii	2s2p $^3P_1^o$	2p ² 3P_0	9.07×10^{-2}	98.9	1175.987	1176.10	28.8	
Zn v	226334	311359	8.10×10^{-2}		1176.122			blend with C iii
C iii	2s2p $^3P_2^o$	2p ² 3P_1	7.02×10^{-2}		1176.370			
Zn v	231831	316827	7.34×10^{-2}		1176.527			blend with C iii, newly identified
Ge v	238765	323749	2.06×10^{-3}		1176.690			blend with C iii
Zn v	198962	283933	1.86×10^{-1}		1176.868			newly identified
Zn v	201973	286936	1.46×10^{-1}		1176.980			newly identified
Zn v	226334	311295	7.56×10^{-2}		1177.016			newly identified
Zn v	202929	287888	1.00×10^{-1}		1177.036			newly identified
Zn v	200644	285603	1.68×10^{-1}		1177.044			newly identified
Zn v	231831	316786	3.06×10^{-1}		1177.087			newly identified
Zn v	260880	345723	8.22×10^{-2}		1178.639			newly identified
Zn v	241829	326664	1.12×10^{-1}		1178.759			
Ni v	232655.6	317477.9	9.35×10^{-3}		1178.935			
Zn v	236969	321776	1.93×10^{-1}		1179.145			
Zn v	230435	315239	1.10×10^{-1}		1179.179			
Xe vi	5p $^2P_{3/2}^o$	5p ² 4P_3	4.65×10^{-4}	19.9	1179.537	1179.63	23.6	

Table A.2. Continued.

Ion	Levels		f	$W_\lambda /$ mÅ	Wavelength/ Å		$v_{\text{rad}} /$ km/s	Comment
	Lower	Upper			Theoretical	Observed		
Zn v	208715	293463	2.79×10^{-1}	17.3	1179.969	1180.10	33.3	
Zn v	260880	345624	4.73×10^{-2}		1180.018			
Xe VI	5d $^2D_{3/2}$	6p $^2P_{1/2}^o$	1.54×10^{-1}		1181.455			
Zn v	227195	311796	2.22×10^{-2}		1182.019			
Mo VI	283610.94	368203.16	7.44×10^{-1}	16.1	1182.142	1182.24	24.9	
Zn v	212471	297033	7.26×10^{-2}	23.5	1182.567	1182.67	26.1	
Zn v	235730	320257	1.94×10^{-2}		1183.041			
Zn v	230435	314958	3.17×10^{-2}		1183.100			
Zn v	232946	317466	2.31×10^{-2}		1183.158			
Zn v	231831	316339	2.99×10^{-2}		1183.314			
Zn v	230614	314958	8.97×10^{-2}		1185.619			
Zn v	231997	316339	5.02×10^{-2}		1185.645			
Zn v	203548	287888	1.30×10^{-1}		1185.676			
Zn v	212471	296796	3.24×10^{-1}		1185.898			
Zn v	210973	295293	1.84×10^{-1}		1185.948			
Mo v	159857	244170	7.85×10^{-1}		1186.050			blend with Zn v
Zn v	235730	320043	2.18×10^{-1}		1186.057			blend with Mo v
Mo v	151195	235496	4.73×10^{-1}		1186.227			
Mo v	245600	329898	4.77×10^{-1}		1186.277			
Zn v	212471	296757	2.05×10^{-1}		1186.447			
Mo v	148949	233190	3.57×10^{-1}		1187.061			
Zn v	228335	312534	2.72×10^{-1}		1187.664			
Zn v	210973	295168	3.51×10^{-1}		1187.706			

Table A.3. Like Table A.1, for the HST/STIS observations.

Ion	Levels		f	$W_\lambda /$ mÅ	Wavelength/ Å		$v_{\text{rad}} /$ km/s	Comment
	Lower	Upper			Theoretical	Observed		
						1150.35		unid.
						1151.10		unid.
Zn v	201973	288704	2.26×10^{-1}		1152.985			
O III	$2p^3 \ ^3S_1$	$2p^4 \ ^3P_2$	1.41×10^{-1}		1153.775	1153.92	37.7	
Zn v	208715	295293	7.17×10^{-2}	29.8	1155.027	1155.12	24.1	
Zn v	285885	372360	3.17×10^{-1}		1156.394			newly identified
Ga v	246133	332600	3.44×10^{-1}		1156.511			
Zn v	231997	318436	2.76×10^{-2}		1156.885			
						1158.00		unid.
Zn v	200644	286943	2.38×10^{-1}	19.0	1158.759	1158.83	18.4	
						1159.90		unid.

Table A.3. Continued.

Ion	Levels		f	$W_\lambda /$ mÅ	Wavelength / Å		$v_{\text{rad}} /$ km/s	Comment
	Lower	Upper			Theoretical	Observed		
Sn v				36.4 25.2	1160.740	1160.85 1161.97	28.4	uncertain unid.
Ge v	241935	327891	1.29×10^{-2}		1163.389			
O iv	3d $^2\text{F}_{5/2}^o$	4f $^2\text{G}_{7/2}$	8.50×10^{-1}	17.7	1164.321	1164.41	22.9	
O iv	3d $^2\text{F}_{7/2}^o$	4f $^2\text{G}_{9/2}$	8.26×10^{-1}	44.0	1164.546	1164.65	26.8	
Zn v	255763	341627	5.07×10^{-2}		1164.632			
Zn v	228335	314197	1.72×10^{-2}		1164.656			newly identified
Zn v	210973	296796	4.52×10^{-2}		1165.186			blend with Ge v
Ge v	241935	327753	1.48×10^{-2}		1165.259			blend with Zn v
				23.1		1165.40		unid.
Zn v	210973	296757	5.56×10^{-2}		1165.716			
Zn v	234846	320618	3.60×10^{-1}		1165.880			
C iv	3d $^2\text{D}_{3/2}$	4f $^2\text{F}_{5/2}^o$	1.02		1168.849			
C iv	3d $^2\text{D}_{5/2}$	4f $^2\text{F}_{7/2}^o$	9.97×10^{-1}		1168.993			
C iv	3d $^2\text{D}_{5/2}$	4f $^2\text{F}_{5/2}^o$	4.88×10^{-2}		1168.993			
				10.2		1169.26		unid.
C iv					1170.130			forbidden C iv component
C iv					1170.330			forbidden C iv component
Zn v	231831	317220	7.01×10^{-2}		1171.106			
				15.4		1172.35 1173.37		unid. unid.
Zn v	239843	325068	3.11×10^{-1}		1173.366			
Zn v	237032	322224	7.26×10^{-2}		1173.823			newly identified
Zn v	230614	315801	1.79×10^{-1}		1173.892			newly identified
Zn v	198962	284116	3.01×10^{-1}	23.6	1174.346	1174.43	21.4	
				14.1		1174.72		unid.
C iii	2s2p $^3\text{P}_1^o$	2p 2 $^3\text{P}_2$	1.17×10^{-1}	100.0	1174.933	1175.03	24.8	
C iii	2s2p $^3\text{P}_0^o$	2p 2 $^3\text{P}_1$	2.72×10^{-1}	100.0	1175.263	1175.37	27.3	
C iii	2s2p $^3\text{P}_1^o$	2p 2 $^3\text{P}_1$	7.03×10^{-2}		1175.590			
C iii	2s2p $^3\text{P}_2^o$	2p 2 $^3\text{P}_2$	2.11×10^{-1}		1175.711			
C iii	2s2p $^3\text{P}_1^o$	2p 2 $^3\text{P}_0$	9.07×10^{-2}	104.7	1175.987	1176.09	26.3	blend with Zn v
Zn v	226334	311359	8.10×10^{-2}		1176.122			blend with C iii
C iii	2s2p $^3\text{P}_2^o$	2p 2 $^3\text{P}_1$	7.02×10^{-2}	130.7	1176.370	1176.45	20.4	blend with Zn v
Zn v	231831	316827	7.34×10^{-2}		1176.527			blend with C iii, newly identified
Ge v	238765	323749	2.06×10^{-3}		1176.690			blend with C iii
Zn v	198962	283933	1.86×10^{-1}		1176.868			newly identified
Zn v	201973	286936	1.46×10^{-1}		1176.980			newly identified
Zn v	226334	311295	7.56×10^{-2}		1177.016			newly identified
Zn v	202929	287888	1.00×10^{-1}		1177.036			newly identified
Zn v	200644	285603	1.68×10^{-1}		1177.044			newly identified

Table A.3. Continued.

Ion	Levels		f	$W_\lambda /$ mÅ	Wavelength / Å		$v_{\text{rad}} /$ km/s	Comment
	Lower	Upper			Theoretical	Observed		
Zn v	231831	316786	3.06×10^{-1}	20.2	1177.087	1178.68		newly identified
Zn v	260880	345723	8.22×10^{-2}		1178.639			unid.
Zn v	241829	326664	1.12×10^{-1}		1178.759			newly identified
Ni v	232655.6	317477.9	9.35×10^{-3}		1178.935			
Zn v	236969	321776	1.93×10^{-1}		1179.145			
Zn v	230435	315239	1.10×10^{-1}		1179.179			
Xe VI	5p $^2P_{3/2}^o$	5p ² $^4P_{3/2}$	4.65×10^{-4}		1179.537			
Zn v	208715	293463	2.79×10^{-1}		1179.969			
Xe VI	5d $^2D_{3/2}$	6p $^2P_{1/2}^o$	1.54×10^{-1}		1181.455			
Xe VI	5d $^2D_{5/2}$	5d $^4F_{7/2}^o$	6.24×10^{-3}		1181.474			newly identified
Zn v	227195	311796	2.22×10^{-2}		1182.019			
Zn IV	151574	236175	5.65×10^{-2}		1182.022			newly identified
Mo VI	283611	368203	7.44×10^{-1}	15.0	1182.142	1182.24	24.9	
Zn v	212471	297033	7.26×10^{-2}		1182.567			
Zn v	235730	320257	1.94×10^{-2}		1183.041			
Zn v	230435	314958	3.17×10^{-2}		1183.100			
Zn v	232946	317466	2.31×10^{-2}		1183.158			
Zn v	230614	314958	8.97×10^{-2}		1185.619			
Zn v	231997	316339	5.02×10^{-2}		1185.645			
Zn v	203548	287888	1.30×10^{-1}		1185.676			
Zn v	212471	296796	3.24×10^{-1}		1185.898			
Zn v	210973	295293	1.84×10^{-1}		1185.948			
Zn v	285523	369843	1.03×10^{-1}		1185.961			
Zn v	235730	320043	2.18×10^{-1}		1186.057			
Zn v	212471	296757	2.05×10^{-1}	18.0	1186.447	1186.54	23.5	
				8.9		1187.05		unid.
Zn v	228335	312534	2.72×10^{-1}		1187.664			
Zn v	210973	295168	3.51×10^{-1}		1187.706			
N IV	2s3s 1S_0	2p($^2P_{3/2}^o$)3s $^1P_1^o$	6.02×10^{-1}	24.8	1188.005	1188.11	26.5	
Ge IV	84102.3	0	5.52×10^{-1}	51.7	1189.028	1189.11	20.7	
Zn v	227195	311295	2.43×10^{-1}		1189.072			newly identified
Zn v	234846	318927	2.55×10^{-2}		1189.331			newly identified
Zn v	235903	319984	7.13×10^{-2}		1189.332			newly identified
Sn v				23.3	1189.920	1190.04	30.2	
Zn v	235599	319632	1.40×10^{-1}		1190.003			newly identified
Zn v	208715	292722	3.13×10^{-1}		1190.376			newly identified
Zn v	202929	286936	8.34×10^{-2}		1190.380			newly identified
				83.2		1190.48		unid.
Ga v	235609	319570	2.23×10^{-2}		1191.029			newly identified

Table A.3. Continued.

Ion	Levels		f	$W_\lambda /$ mÅ	Wavelength / Å		$v_{\text{rad}} /$ km/s	Comment
	Lower	Upper			Theoretical	Observed		
Zn v	260880	344771	6.24×10^{-2}	4.9	1192.014			newly identified
						1192.35		unid.
Ga iv	153086	236907	1.87×10^{-1}	60.1	1193.024			newly identified
Ga v	235752	319570	1.20×10^{-1}		1193.061			newly identified
						1193.34		unid.
Zn v	231997	315801	1.66×10^{-2}	3.1	1193.260			newly identified
C i					1193.264			ISM multi-component
						1193.45		unid.
Ba vii	157675	241412	3.06×10^{-3}	11.0	1194.221			newly identified
						1194.65		unid.
				20.2		1194.99		unid.
Zn v	201973	285603	7.16×10^{-2}	9.5	1195.745			newly identified
O iii	3p 3D_2	4d $^3F_3^o$	8.82×10^{-2}		1196.753	1196.85	24.3	
O iii	3p 3D_3	4d $^3F_4^o$	9.11×10^{-2}		1197.239			
O iii	3p 3D_1	4d $^3F_2^o$	9.93×10^{-2}		1197.331			
						1197.81		unid.
C iv	3d $^2D_{3/2}$	4p $^2P_{3/2}^o$	2.76×10^{-3}		1198.403			
C iv	3d $^2D_{5/2}$	4p $^2P_{3/2}^o$	1.65×10^{-2}		1198.554			
C iv	3d $^2D_{3/2}$	4p $^2P_{1/2}^o$	1.38×10^{-2}		1198.591			
Ni v	241773.6	325148.4	1.18×10^{-1}		1199.403			
N i					1199.550			ISM multi-component
				27.0		1199.61		unid.
				22.9		1199.75		unid.
				13.6		1199.99		unid.
				18.0		1200.28		unid.
N i					1200.223			ISM multi-component
Zn v	200644	283933	6.25×10^{-2}		1200.639			newly identified
Zn v	236969	320257	3.36×10^{-1}		1200.643			newly identified
N i					1200.710			ISM multi-component
Zr v	453681	536961	8.10×10^{-1}		1200.760			blend with Mo vi
Mo vi	151213	234490	5.26×10^{-1}		1200.808			blend with Zr v, newly identified
				19.5		1201.37		unid.
						1201.60		unid.
Zn v	234846	317978	2.38×10^{-1}		1202.906			newly identified
Zn v	239843	322969	4.20×10^{-2}		1202.983			newly identified
						1204.72		unid.
Zn v	231831	314838	9.24×10^{-2}		1204.722			newly identified
						1205.01		unid.
						1205.36		unid.
Sn v				14.1	1205.720	1205.85	32.3	
Si iii					1206.500			ISM multi-component

Table A.3. Continued.

Ion	Levels		f	$W_\lambda /$ mÅ	Wavelength / Å		$v_{\text{rad}} /$ km/s	Comment
	Lower	Upper			Theoretical	Observed		
C III	3d 1D_2	6f $^1F_3^o$	1.01×10^{-1}		1210.081	1209.56		unid.
						1213.15		unid.
						1214.31		unid.
He II	2	4	1.19×10^{-1}		1215.133			
				6.7		1219.94		unid.
				7.5		1220.07		unid.
				11.2		1220.23		unid.
Ge V	241935	323749	4.91×10^{-3}		1222.289	1221.46		unid.
						1222.80		unid.
Zn IV	160886	242640	2.88×10^{-1}		1223.182			newly identified
N IV	2s3p $^3P_2^o$	2s4s 3S_1	2.03×10^{-2}		1225.722			
Sb V				9.0	1226.000	1226.11	26.9	
Zn V	235903	317466	2.59×10^{-2}		1226.057			newly identified
Se V				43.7	1227.600	1227.64	9.8	
				6.9		1227.91		unid.
Ga IV	156025	237458	1.95×10^{-1}	17.3	1227.999	1228.090	22.2	newly identified
Xe VI	5p 2 $^2P_{3/2}^o$	5p 3 $^2D_{5/2}^o$	3.96×10^{-2}		1228.426			blend with Zn V, newly identified
Zn IV	160919	242320	3.07×10^{-1}		1228.486			blend with Xe VI, newly identified
				8.4		1228.93		unid.
				2.6		1229.04		unid.
Ni V	274695.4	356036.3	1.89×10^{-1}		1229.394			blend with Mo V
Mo V	157851	239189	1.52×10^{-1}		1229.447			blend with Ni V, newly identified
				3.7		1229.66		unid.
Ge IV	81311.4	0	2.66×10^{-1}	27.7	1229.839	1229.95	27.1	
C IV	3p $^2P_{1/2}^o$	4s $^2S_{1/2}$	8.14×10^{-2}		1230.043			
C IV	3p $^2P_{3/2}^o$	4s $^2S_{1/2}$	8.15×10^{-2}		1230.521			
Ni V	225200.7	306377.8	1.26×10^{-1}		1231.875			
				12.3		1232.01		unid.
Ni V	208163.7	289298	7.34×10^{-2}		1232.524			
						1232.73		unid.
Ni V	246240.9	327356.6	1.68×10^{-1}		1232.807			
Ni V	263805.8	344911.2	3.57×10^{-1}		1232.964			
Ni V	234082.1	315168.2	1.59×10^{-1}		1233.257			
Ni V	208164.6	289247.1	9.35×10^{-2}		1233.312			
Ni V	274695.4	355765.2	2.33×10^{-3}		1233.505			
Ni V	263735.7	344805.3	3.16×10^{-1}		1233.508			
Ni V	234125.4	315168.2	1.10×10^{-1}		1233.916			
						1234.41		unid.

Table A.3. Continued.

Ion	Levels		f	$W_\lambda /$ mÅ	Wavelength / Å		$v_{\text{rad}} /$ km/s	Comment
	Lower	Upper			Theoretical	Observed		
Ni v	208151.5	289163	1.33×10^{-1}		1234.393			
Ni v	233839.2	314756.4	2.15×10^{-1}		1235.831			
Ni v	240193.8	321081.9	3.86×10^{-2}		1236.276			
Ni v	234412.7	315300.7	1.12×10^{-1}		1236.277			
Zn v	230435	311296	4.58×10^{-2}		1236.689			newly identified
Zn v	234846	315594	3.44×10^{-5}		1238.425			newly identified
Zn v	260880	341627	1.01×10^{-1}		1238.430			newly identified
N v	2s $^2S_{1/2}$	2p $^2P_{3/2}^o$	1.56×10^{-1}	141.3	1238.821	1238.93	26.4	
Zn v	231831	312534	2.67×10^{-2}		1239.108			newly identified
				9.2		1239.82		unid.
Kr v	278928	359544	2.25×10^{-1}		1240.449			newly identified
Ni v	243331.5	323908.6	3.93×10^{-2}		1241.047			
Ni v	234125.4	314702.2	3.71×10^{-2}		1241.052			
Ni v	234275.2	314834.7	1.28×10^{-1}		1241.319			
Ni v	233839.2	314392	6.46×10^{-2}		1241.422			
						1241.86		unid.
						1241.99		unid.
Ni v	234082.1	314599.2	1.24×10^{-1}		1241.972			
Ni v	229408.8	309919.5	1.85×10^{-1}		1242.071			
O iv	3d $^2D_{3/2}$	4p $^2P_{3/2}^o$	8.21×10^{-3}		1242.176			
O iv	3d $^2D_{5/2}$	4p $^2P_{3/2}^o$	4.93×10^{-2}		1242.434			
N v	2s $^2S_{1/2}$	2p $^2P_{1/2}^o$	7.80×10^{-2}	132.4	1242.804	1242.91	25.6	blend with O iv
O iv	3d $^2D_{3/2}$	4p $^2P_{1/2}^o$	4.11×10^{-2}		1242.838			blend with N v
Ni v	234125.4	314562.8	1.46×10^{-1}		1243.203			
Ni vi	337993.9	418368.8	3.60×10^{-2}	21.2	1244.170	1244.29	28.9	
Ni v	164525.9	244900.5	3.97×10^{-1}	21.2	1244.174	1244.29	28.0	
Ni v	229408.8	309743.6	1.68×10^{-2}		1244.791			
Ni v	234275.2	314599.2	9.70×10^{-2}		1244.958			
Ni v	216596	296919.3	3.91×10^{-2}		1244.969			
Ni v	240193.8	320513.8	1.23×10^{-1}		1245.020			
Ni v	234082.1	314392	2.55×10^{-1}		1245.176			
Ni v	274695.4	354989.6	3.46×10^{-1}		1245.420			
Ga iv	156025	236312	1.38×10^{-1}		1245.529			newly identified
				9.5		1245.74		unid.
				10.1		1245.87		unid.
Zr v	491116	571376	8.57×10^{-3}		1245.951			
Zr v	457547	537807	7.85×10^{-1}		1245.951			
Ni v	263700.9	343905.7	3.56×10^{-1}		1246.808			
Zn v	208715	288903	3.85×10^{-2}		1247.074			newly identified
C iii	2s2p $^1P_1^o$	2p ² 1S_0	1.62×10^{-1}	93.2	1247.383	1247.50	28.1	

Table A.3. Continued.

Ion	Levels		f	$W_\lambda /$ mÅ	Wavelength / Å		$v_{\text{rad}} /$ km/s	Comment
	Lower	Upper			Theoretical	Observed		
				12.8		1247.81		unid.
Ni v	208131	288161.6	1.30×10^{-1}		1249.522			
Zn v	232946	312967	5.28×10^{-2}		1249.675			newly identified
				6.5		1249.98		unid.
Ni v	208163.7	288161.6	5.58×10^{-2}		1250.033			
				13.8		1250.40		unid.
Ni v	208046.4	288021.6	3.50×10^{-1}		1250.388			blend with Zn v
Zn v	231831	311796	9.46×10^{-3}		1250.539			blend with Ni v, newly identified
Ni v	217048.7	296932.9	2.74×10^{-1}		1251.812			
Ni v	232910.8	312778.2	1.69×10^{-1}		1252.075			
Ni v	208046.4	287906.9	1.62×10^{-1}		1252.183			
Ni v	229408.8	309264	8.26×10^{-2}		1252.267			
Ni v	217048.7	296897	2.05×10^{-2}		1252.375			
Ni v	229440.6	309264	1.67×10^{-1}		1252.765			
						1253.38		unid.
Ni v	263700.9	343478.2	1.77×10^{-1}		1253.489			
Ni v	208131	287906.9	4.65×10^{-2}		1253.511			
Kr v	213932.87	293705	3.74×10^{-2}		1253.571			newly identified
Ni v	217129.1	296897	2.43×10^{-1}		1253.637			
Ni v	217101	296847.1	2.52×10^{-1}		1253.980			
				19.0		1254.22		unid.
				7.4		1255.40		unid.
Ba VII	42514	122163	6.18×10^{-4}		1255.520			newly identified
C III	3s 3S_1	4p $^3P_2^o$	4.26×10^{-2}		1256.466			
C III	3s 3S_1	4p $^3P_1^o$	2.56×10^{-2}		1256.542			
C III	3p $^1P_1^o$	5s 1S_0	2.55×10^{-2}		1256.549			
C III	3s 3S_1	4p $^3P_0^o$	8.52×10^{-3}		1256.577			
				14.1		1256.83		unid.
Ni v	208131	287645.9	3.46×10^{-1}		1257.626			
Ni v	243331.5	322820.8	7.67×10^{-2}		1258.031			
Ga IV	149512	228953	4.03×10^{-1}		1258.801			newly identified
Ni v	229413	308804.1	9.65×10^{-2}		1259.587			
Ni v	234082.1	313464.7	8.37×10^{-2}		1259.722			
				84.4		1260.47		unid.
Ni v	234125.4	313464.7	1.98×10^{-1}		1260.409			blend with ?
Si II					1260.422			ISM multi-component
Zr v	391998	471306	1.05		1260.909			
Ni v	212253.4	291541.7	6.11×10^{-2}		1261.220			
Ni v	243331.5	322617.6	1.13×10^{-1}		1261.255			
Ni v	235420.6	314702.2	2.90×10^{-1}		1261.327			

Table A.3. Continued.

Ion	Levels		f	$W_\lambda /$ mÅ	Wavelength / Å		$v_{\text{rad}} /$ km/s	Comment
	Lower	Upper			Theoretical	Observed		
Ni v	279199.5	358475.6	3.28×10^{-1}		1261.414			
Ni v	216189.9	295444.3	3.32×10^{-1}		1261.760			
Zn v	230435	309658	3.99×10^{-2}		1262.252			newly identified
				15.9		1262.38		unid.
Ni v	274738.6	353944.1	1.81×10^{-1}		1262.539			
				13.3		1262.81		unid.
				17.7		1263.27		unid.
				10.8		1263.50		unid.
Mo vi	395181	474296	2.07×10^{-1}		1263.989			
Mo vi	395184	474297	2.04×10^{-1}		1264.023			
				11.0		1264.24		unid.
Ni v	164525.9	243608.5	2.98×10^{-1}		1264.501			
Ga iv	150967	230040	9.57×10^{-2}		1264.654			newly identified
Ni v	243370.5	322436.4	1.14×10^{-1}		1264.768			
Zr v	376898	455925	8.93×10^{-1}	11.2	1265.381	1265.49	25.8	
Zn iv	128730	207737	2.04×10^{-1}		1265.707			newly identified
				8.5		1266.00		unid.
Ni v	247049.1	326029.9	1.14×10^{-1}		1266.131			
Ni v	208163.7	287127.2	3.11×10^{-1}	12.3	1266.408	1266.52	26.5	
Ni v	240193.8	319138.7	7.81×10^{-2}		1266.706			
Ni v	212455.7	291390	3.00×10^{-1}		1266.876			
Ga iv	156025	234940	1.26×10^{-1}		1267.189			newly identified
Ni v	229408.8	308317.3	1.59×10^{-1}		1267.291			
				8.0		1267.56		unid.
				9.7		1267.77		unid.
Ni v	229440.6	308317.3	1.60×10^{-1}		1267.802			
Ni v	236454.1	315326.2	1.02×10^{-1}		1267.875			
				18.6		1268.09		unid.
						1268.40		unid.
Ni v	274738.6	353548.7	2.22×10^{-1}		1268.873			
Ni v	241082.2	319860.4	1.63×10^{-1}		1269.387			
Ni v	242290.4	321018.3	1.44×10^{-1}		1270.198			
N iv	2s3p $^3\text{P}_2^o$	2p($^2\text{P}^o$)3p $^3\text{D}_3$	1.39×10^{-1}		1270.270			
Mo vi	316477	395184	1.14×10^{-2}		1270.523			
Ni v	229440.6	308138.8	3.40×10^{-1}	14.0	1270.677	1270.80	29.0	
Ni v	234275.2	312889.4	7.80×10^{-2}		1272.035			
N iv	2s3p $^3\text{P}_1^o$	2p($^2\text{P}^o$)3p $^3\text{D}_2$	1.23×10^{-1}		1272.145			
				6.9		1272.52		unid.
Ni v	242504.3	321081.9	9.12×10^{-2}		1272.627			
Ni v	208131	286706.6	1.33×10^{-2}		1272.660			

Table A.3. Continued.

Ion	Levels		f	$W_\lambda /$ mÅ	Wavelength / Å		$v_{\text{rad}} /$ km/s	Comment
	Lower	Upper			Theoretical	Observed		
Ni v	274773.5	353347.1	8.85×10^{-2}		1272.692			
Zn iv	130366	208921	1.65×10^{-1}	13.8	1272.990	1273.08	21.2	newly identified
Ni v	208164.6	286706.6	3.51×10^{-1}		1273.204			
				15.7		1274.39		unid.
				10.0		1274.83		unid.
Ni v	216596	294939.6	2.88×10^{-1}		1276.428			
				11.8		1276.72		unid.
Ni v	164525.9	242837	2.13×10^{-1}	17.9	1276.958	1277.06	24.0	
				9.7		1277.64		unid.
				8.2		1278.29		unid.
				16.9		1279.04		unid.
Ni v	212095.8	290262	2.31×10^{-1}	10.6	1279.325	1279.45	29.3	
Ni v	208151.5	286293.6	3.95×10^{-1}		1279.720			
Ni v	247104.9	325222.9	1.05×10^{-1}		1280.115			
Ni v	240959.6	319076.2	2.26×10^{-1}		1280.138			
Xe vi	$5p^2 \ ^4P_{5/2}$	$4f \ ^2F_{7/2}^o$			1280.213			newly identified
Zn iv	131805	209899	1.71×10^{-1}	13.0	1280.500	1280.58	18.7	newly identified
				7.2		1280.78		unid.
				6.8		1281.26		unid.
				7.3		1281.49		unid.
				7.0		1281.62		unid.
				7.5		1281.76		unid.
				4.5		1281.99		unid.
Ni v	229408.8	307399.7	1.14×10^{-1}		1282.201			
Ni v	229413	307399.7	1.08×10^{-1}		1282.270			
Zn iv	151250	229231	1.22×10^{-1}		1282.357			newly identified
Ni v	251654.9	329614.3	1.78×10^{-3}		1282.719			
Zn v	212471	290424	9.80×10^{-3}		1282.832			newly identified
				3.5		1283.77		unid.
Sn v				18.2	1283.810	1283.91	23.4	
Ni v	216590.5	294443.3	2.73×10^{-1}		1284.475			
Ni v	253905.2	331678.2	3.87×10^{-1}		1285.793			
				9.8		1286.64		unid.
Ni v	232545.9	310212.6	1.60×10^{-1}		1287.553			
Ni v	268273.9	345936.1	3.03×10^{-1}		1287.628			
Ni v	216434.7	294086	2.41×10^{-1}		1287.808			
				6.0		1288.22		unid.
				9.1		1288.37		unid.
Zn iv	132777	210187	2.44×10^{-1}		1291.826			newly identified
				6.6		1292.01		unid.
				5.6		1292.19		unid.

Table A.3. Continued.

Ion	Levels		f	$W_\lambda /$ mÅ	Wavelength / Å		$v_{\text{rad}} /$ km/s	Comment
	Lower	Upper			Theoretical	Observed		
Zn iv	130366	207737	1.11×10^{-1}	25.8	1292.476			newly identified
Sn v					1294.360	1294.45	20.8	
Ni v	212095.8	289298	1.20×10^{-1}		1295.300			newly identified unid. blend with C iii blend with C iii
Zn v	221631	298801	1.03×10^{-1}		1295.850			
						1296.10		
Ni v	212095.8	289247.1	4.28×10^{-2}		1296.154			
Ni v	242504.3	319652.7	8.59×10^{-2}		1296.203			
C iii	3d 3D_2	5f $^3F_3^o$	2.04×10^{-1}		1296.322			
C iii	3d 3D_1	5f $^3F_2^o$	2.29×10^{-1}		1296.327			
C iii	3d 3D_3	5f $^3F_4^o$	2.10×10^{-1}		1296.333			
C iii	3d 3D_2	5f $^3F_2^o$	2.59×10^{-2}		1296.345			
C iii	3d 3D_3	5f $^3F_3^o$	1.85×10^{-2}		1296.369			
C iii	3d 3D_3	5f $^3F_2^o$	4.21×10^{-4}		1296.392			
Zn iv	131805	208921	1.67×10^{-1}		1296.734			newly identified
Ni v	242862.6	319860.4	1.61×10^{-1}		1298.738			
Xe vi	5p $^2P_{3/2}^o$	5p $^4P_{1/2}$			1298.921			
Ga iv	153086	230040	3.26×10^{-1}		1299.476			newly identified
Ni v	178019.8	254885	1.79×10^{-1}		1300.979			
Zn iv	148180	225033	3.10×10^{-1}		1301.189			newly identified ISM multi-component
O i					1302.167			
Ni v	242862.6	319652.7	5.50×10^{-2}		1302.251			
Ni v	212095.8	288877.9	7.57×10^{-2}		1302.387			
Zn v	222042	298801	8.34×10^{-2}		1302.786			newly identified
Ni v	235736.5	312463.3	2.32×10^{-1}	2.2	1303.326	1303.43	23.9	
Ga iv	150967	227681	3.17×10^{-1}	5.4	1303.540	1303.66	27.6	newly identified
Zr v	378753	455444	9.01×10^{-1}	16.1	1303.933	1304.05	26.9	
Ni v	247165	323853.1	7.66×10^{-2}		1303.983			unid. unid.
				7.1 27.2		1304.19 1304.44		
Ni v	229408.8	306049	4.36×10^{-2}		1304.798			
Ni v	229413	306049	1.78×10^{-1}		1304.870			
Ni v	212253.4	288877.9	1.26×10^{-1}		1305.066			
Ni v	229408.8	305996.3	1.66×10^{-1}		1305.696			
Ni v	243370.5	319926.5	1.30×10^{-3}		1306.233			
Ni v	229440.6	305996.3	1.24×10^{-1}		1306.238			
Ni v	208046.4	284579.5	2.83×10^{-1}		1306.624			blend with Zn iv, blend with Zr v blend with Ni v, blend with Zr v, newly identified
Zn iv	128730	205261	3.80×10^{-1}		1306.657			
Zr v	395995	472520	1.00	16.1	1306.762			blend with Ni v, blend with Zn iv
Ni v	178019.8	254495.6	2.94×10^{-1}	8.1	1307.603	1307.71	24.5	

Table A.3. Continued.

Ion	Levels		f	$W_\lambda /$ mÅ	Wavelength / Å		$v_{\text{rad}} /$ km/s	Comment
	Lower	Upper			Theoretical	Observed		
C III	$2p^2 \ ^1S_0$	$2s3p \ ^1P^o_1$	2.52×10^{-2}	8.9		1308.07		unid.
					1308.705			
				6.8		1309.08		unid.
				3.8		1309.18		unid.
Zn V	$2s3p \ ^1P^o_1$	$2p(^2P^o_{1/2})3p \ ^1P_1$	1.47×10^{-2}	2.6		1309.26		unid.
					1309.233			newly identified
					1309.555			
					1309.653			
Ni V	208046.4	284402.5	3.96×10^{-2}		1309.689			
Ni V	243266.2	319620.2	1.60×10^{-1}					
Ni V				3.5		1310.00		unid.
					1310.092			
					1310.252			
					1311.027			
Ni V	242862.6	319138.7	6.10×10^{-2}					
Ni V	208131	284402.5	2.40×10^{-1}	14.8	1311.106	1311.21	23.8	
Ni V				3.2		1312.39		unid.
					1312.646			
					1312.717			
					1312.718			
Ni V	229408.8	305590.8	9.64×10^{-2}		1312.718			
Ni V	208131	284308.9	5.48×10^{-2}		1313.280			
Ni V	229413	305590.8	2.17×10^{-1}					
Ni V	208163.7	284308.9	2.21×10^{-1}					
Ni V				18.3		1314.01		unid.
				7.5	1314.330	1314.46	29.7	
					1314.537	1314.64	23.5	
					1314.682			
Sn IV	$5s \ ^2S_{1/2}$	$5p \ ^2P^o_{3/2}$	6.00×10^{-1}	11.4	1314.537	1314.64	23.5	
Ni V	208151.5	284215.5	2.17×10^{-1}		1314.682			
C IV	$4p \ ^2P^o_{1/2}$	$7d \ ^2D_{3/2}$	5.89×10^{-2}		1315.623			
Ni V	225545.1	301553	3.32×10^{-1}		1315.653			blend with C IV
C IV	$4p \ ^2P^o_{3/2}$	$7d \ ^2D_{3/2}$	5.88×10^{-3}		1315.849			
C IV	$4p \ ^2P^o_{3/2}$	$7d \ ^2D_{5/2}$	5.29×10^{-2}		1315.855			
Ni V	225616.5	301553	6.38×10^{-2}		1316.890			
Ni V	232655.6	308592	1.42×10^{-1}		1316.892			
Ni V	221087.6	297013.9	4.55×10^{-2}		1317.067			
Ni V				5.7		1317.45		unid.
				7.7	1317.447	1317.56	25.7	
					1318.001			newly identified
					1318.204			newly identified
Zn V	135951	211824	1.73×10^{-1}					
Zn V	222940	298801	5.79×10^{-2}		1318.327			
Ni V	225616.5	301470.2	3.22×10^{-1}		1318.515	1318.62	23.9	
Ni V	178019.8	253862.7	4.05×10^{-1}	11.4		1319.03		unid.
Kr V				9.6		1319.54		unid.
					1319.923			newly identified
						1320.14		unid.

Table A.3. Continued.

Ion	Levels		f	$W_\lambda /$ mÅ	Wavelength / Å		$v_{\text{rad}} /$ km/s	Comment
	Lower	Upper			Theoretical	Observed		
Ni v	225200.7	300918.1	3.27×10^{-1}		1320.700			blend with Zn iv
Zn iv	128730	204447	1.10×10^{-1}		1320.704			blend with Ni v, newly identified
Ni v	212253.4	287960	4.38×10^{-2}		1320.889			blend with Zn iv
Zn iv	138479	214167	2.77×10^{-1}	9.7 7.1	1321.215	1321.32 1322.25	23.8	blend with Ni v, newly identified unid.
Zn iv	130366	205991	1.37×10^{-1}		1322.316			newly identified
Zn iv	135951	211570	1.98×10^{-1}		1322.428			newly identified
Ni v	236454.1	312008.3	9.08×10^{-2}	7.6	1323.553	1323.66	24.2	
Ni v	241773.6	317327.3	1.52×10^{-1}	7.6	1323.562	1323.66	22.2	
Zr v	382985	458524	7.96×10^{-1}	18.8	1323.826	1323.94	25.8	
Ni v	217101	292631	3.50×10^{-1}		1323.977			
Zn v	208715	284116	9.90×10^{-3}		1326.253			newly identified
Zn iv	131805	207175	1.08×10^{-1}		1326.774			newly identified
N iv	2s3d 3D_1	2p($^2P^o$)3d $^3F_2^o$	1.46×10^{-2}	12.8	1326.957	1327.08	27.8	uncertain
Zn iv	135951	211190	1.11×10^{-1}		1329.110			newly identified
Ni v	217129.1	292353.4	3.28×10^{-1}		1329.358			
Zn v	208715	283933	4.42×10^{-3}		1329.471			newly identified
Zn iv	160919	236109	2.17×10^{-1}		1329.959			newly identified
Zn iv	157075	232246	2.56×10^{-1}		1330.302			newly identified
Zr v	327617	402688	6.65×10^{-2}		1332.065			
Zn iv	157930	232938	5.48×10^{-1}		1333.180			newly identified
Zn iv	138479	213480	1.59×10^{-1}	13.3	1333.326	1333.45	27.9	newly identified
Ni v	233839.2	308804.1	1.31×10^{-1}		1333.958			
Ni v	241773.6	316726.6	1.38×10^{-1}		1334.169			
Ni v	225616.5	300563.3	4.14×10^{-2}		1334.280			
C ii					1334.532			ISM multi-component
Ni v	241082.2	315990.5	1.60×10^{-1}		1334.966			
				22.8		1335.83		unid.
Ni v	217048.7	291891.4	3.25×10^{-1}	14.1	1336.136	1336.28	32.3	
Ga iv	149512	224243	2.02×10^{-1}	9.0	1338.129	1338.25	27.1	newly identified
O iv	2s2p 2 $^2P_{1/2}$	2p 3 $^2D_{3/2}^o$	1.17×10^{-1}	91.9 11.3	1338.615	1338.75 1339.18	30.2	unid.
Zn iv	157075	231693	3.70×10^{-1}		1340.156			newly identified
Ni v	225616.5	300224.9	1.26×10^{-1}		1340.332			
Ni v	216189.9	290757	8.26×10^{-2}		1341.074			
Zn v	241829	316339	1.10×10^{-2}		1342.104			newly identified
Ni v	217048.7	291554.6	2.03×10^{-1}		1342.176			
O iv	2s2p 2 $^2P_{3/2}$	2p 3 $^2D_{3/2}^o$	1.16×10^{-2}	54.9	1342.990	1343.12	29.0	
O iv	2s2p 2 $^2P_{3/2}$	2p 3 $^2D_{5/2}^o$	1.04×10^{-1}	106.7	1343.514	1343.65	30.4	
Zn iv	149191	223609	3.61×10^{-1}		1343.750			newly identified

Table A.3. Continued.

Ion	Levels		f	$W_\lambda /$ mÅ	Wavelength / Å		$v_{\text{rad}} /$ km/s	Comment
	Lower	Upper			Theoretical	Observed		
Ni v	240959.6	315370.1	1.30×10^{-1}		1343.896			
Zn iv	132777	207175	2.94×10^{-1}		1344.122			newly identified
Zn v	240446	314838	4.45×10^{-2}		1344.241			newly identified
O iii	3p $^3\text{P}_2$	3p $^3\text{D}_3^0$	7.89×10^{-2}		1344.943			
O iii	3p $^3\text{P}_1$	3p $^3\text{D}_2^0$	7.05×10^{-2}		1344.962			
				14.4		1345.78		unid.
				16.0		1346.26		unid.
Ni v	217129.1	291328.5	1.82×10^{-1}		1347.720			
C iii	3p $^1\text{P}_1^0$	3p' $^1\text{D}_2$	3.03×10^{-2}	16.7	1347.947	1348.07	27.4	blend with Zn iv
Zn iv	131805	205991	2.15×10^{-1}	16.7	1347.954	1348.07	25.8	blend with C iii, newly identified
Zn iv	130366	204447	1.98×10^{-1}	7.9	1349.876	1350.00	27.5	newly identified
Ni v	216189.9	290262	6.02×10^{-2}		1350.036			
C iv	4d $^2\text{D}_{3/2}$	4f $^2\text{F}_{5/2}^0$	7.22×10^{-2}		1351.214			
C iv	4d $^2\text{D}_{5/2}$	4f $^2\text{F}_{5/2}^0$	3.44×10^{-3}		1351.287			
C iv	4d $^2\text{D}_{5/2}$	4f $^2\text{F}_{7/2}^0$	6.88×10^{-2}		1351.292			
C iv	4f $^2\text{F}_{7/2}^0$	7g $^2\text{G}_{9/2}$	5.65×10^{-2}		1352.975			
C iv	4f $^2\text{F}_{7/2}^0$	7g $^2\text{G}_{7/2}$	1.64×10^{-3}		1352.975			
C iv	4f $^2\text{F}_{5/2}^0$	7g $^2\text{G}_{7/2}$	5.81×10^{-2}		1352.975			
C iv	4f $^2\text{F}_{5/2}^0$	7d $^2\text{D}_{3/2}$	5.37×10^{-4}		1353.427			
C iv	4f $^2\text{F}_{7/2}^0$	7d $^2\text{D}_{5/2}$	5.75×10^{-4}		1353.433			
C iv	4f $^2\text{F}_{5/2}^0$	7d $^2\text{D}_{5/2}$	3.85×10^{-5}		1353.433			
Zr v	402688	476677	1.05		1355.216			
				9.7		1355.74		unid.
Zr v	328941	402688	4.39×10^{-2}		1355.975			
Zn iv	160886	234623	3.72×10^{-1}		1356.171			newly identified
				7.4		1357.45		unid.
Zn iv	131805	205453	1.79×10^{-1}	23.0	1357.801	1357.92	26.3	newly identified
Zn iv	148180	221737	2.35×10^{-1}	11.2	1359.477	1359.61	29.3	newly identified
Zn iv	138479	211824	1.39×10^{-1}		1363.432			newly identified
Zn iv	130366	203685	2.01×10^{-1}	12.7	1363.912	1364.06	32.5	newly identified
				3.9		1364.33		unid.
						1364.65		unid.
				9.7		1364.97		unid.
Zn iv	148180	221426	1.18×10^{-1}	11.7	1365.253	1365.38	27.9	newly identified
Zn iv	135951	208970	3.07×10^{-1}	9.3	1369.510	1369.63	26.3	newly identified
				15.3		1370.26		unid.
				2.5		1370.61		unid.
O v	2s2p $^1\text{P}_1^0$	2p ² $^1\text{D}_2$	1.57×10^{-1}	90.9	1371.294	1371.43	29.7	
Sr v				8.3	1372.838	1372.96	26.6	

Table A.3. Continued.

Ion	Levels		f	$W_\lambda /$ mÅ	Wavelength / Å		$v_{\text{rad}} /$ km/s	Comment
	Lower	Upper			Theoretical	Observed		
Zn iv	138479	211190	2.47×10^{-1}	5.3	1375.325			newly identified unid.
Zr v	382985	455631	3.17×10^{-1}		1376.544	1376.45		
				6.3		1376.79		unid.
						1377.50		unid.
Zn iv	128730	201319	2.29×10^{-1}	15.7	1377.615	1377.75	29.4	newly identified
				9.8		1379.19		unid.
C iii	3d 1D_2	5f 1F_3	3.46×10^{-1}	37.7	1381.652	1381.76	23.4	
Kr v	211336.57	283559	5.14×10^{-2}	10.6	1384.611	1384.72	23.6	
Zn iv	160919	232981	3.61×10^{-1}		1387.694			newly identified
Kr v	213932.87	285981	7.46×10^{-2}	7.5	1387.961	1388.07	23.5	
				14.1		1390.73		unid.
				14.2		1390.94		unid.
Ni v	221087.6	292983	1.41×10^{-1}		1390.910			
Kr v	216874.54	288683	4.28×10^{-2}		1392.594	1392.77	38.3	
Kr v	219381.57	291138	9.66×10^{-2}		1393.603			
Si iv	3s $^2S_{1/2}$	3p $^2P_{3/2}$	5.13×10^{-1}	82.1	1393.755	1393.87	24.7	
				12.8		1395.98		unid.
						1396.48		unid.
Kr v	219823.27	291138	2.40×10^{-2}	8.0	1402.235	1402.32	18.2	newly identified
				14.5		1402.53		unid.
Si iv	3s $^2S_{1/2}$	3p $^2P_{1/2}$	2.55×10^{-1}	62.4	1402.770	1402.90	27.8	
				13.0		1408.56		unid.
				13.9		1409.60		unid.
				17.4		1413.09		unid.
				7.0		1413.31		unid.
Sr v				12.8	1413.882	1414.02	29.3	
						1423.36		unid.
						1423.48		unid.
				9.9		1424.44		unid.
				7.0		1424.95		unid.
C iii	3d 3D_1	3d' $^3P_0^o$	3.40×10^{-2}		1425.903			
C iii	3d 3D_1	3d' $^3P_1^o$	3.56×10^{-2}		1426.194			
C iii	3d 3D_2	3d' $^3P_1^o$	4.60×10^{-2}		1426.216			
C iii	2s3s 3S_1	2p($^2P^o$)3s $^3P_1^o$	1.62×10^{-1}	27.0	1426.446	1426.58	28.2	
C iii	3d 3D_1	3d' $^3P_2^o$	1.03×10^{-3}		1426.716			
C iii	3d 3D_2	3d' $^3P_2^o$	1.10×10^{-2}		1426.739			
C iii	3d 3D_3	3d' $^3P_2^o$	4.77×10^{-2}		1426.796			
Mo vi	316477	386552	7.53×10^{-4}	7.6	1427.030	1427.15	25.2	
C iii	2s3s 3S_1	2p($^2P^o$)3s $^3P_1^o$	9.78×10^{-2}	39.5	1427.839	1427.97	27.5	
C iii	3p $^3P_1^o$	3p' 3P_2	4.56×10^{-2}		1427.911			

Table A.3. Continued.

Ion	Levels		f	$W_\lambda /$ mÅ	Wavelength / Å		$v_{\text{rad}} /$ km/s	Comment
	Lower	Upper			Theoretical	Observed		
C III	3p $^3\text{P}_2^o$	3p' $^3\text{P}_2$	8.22×10^{-2}	23.8	1428.178	1428.31	27.7	
C III	2s3s $^3\text{S}_1$	2p($^2\text{P}^o$)3s $^3\text{P}_0^o$	3.26×10^{-2}		1428.498			
C III	3p $^3\text{P}_0^o$	3p' $^3\text{P}_1$	1.10×10^{-1}		1428.553			
C III	3p $^3\text{P}_1^o$	3p' $^3\text{P}_1$	2.74×10^{-2}		1428.668			
C III	3p $^3\text{P}_2^o$	3p' $^3\text{P}_1$	2.74×10^{-2}		1428.935			
C III	3p $^3\text{P}_1^o$	3p' $^3\text{P}_0$	3.66×10^{-2}		1429.099			
				22.2		1431.72		unid.
Sn IV	5s $^2\text{S}_{1/2}$	5p $^2\text{P}_{1/2}^o$	3.00×10^{-1}	15.1	1437.525	1437.64	24.0	
Kr V	213932.87	283439.05	1.10×10^{-2}	8.0	1438.722	1438.83	22.5	newly identified
C IV	4s $^2\text{S}_{1/2}$	6p $^2\text{P}_{3/2}^o$	4.70×10^{-2}		1440.283			
C IV	4s $^2\text{S}_{1/2}$	6p $^2\text{P}_{1/2}^o$	2.35×10^{-2}		1440.364			
				7.7		1447.25		unid.
						1451.78		unid.
						1454.45		unid.
Ba VII	173154	241412	1.46×10^{-2}		1465.045			newly identified
						1475.13		unid.
						1475.29		unid.
						1475.41		unid.
						1475.50		unid.
						1477.59		unid.
C III	3d $^3\text{D}_2$	3d' $^3\text{D}_3^o$	1.92×10^{-2}		1477.626			
C III	3d $^3\text{D}_3$	3d' $^3\text{D}_3^o$	1.10×10^{-1}	32.2	1477.688	1477.810	24.8	
Ba VII	156151	223820	1.72×10^{-2}		1477.775			newly identified
C III	3d $^3\text{D}_1$	3d' $^3\text{D}_2^o$	3.09×10^{-2}		1478.021			
C III	3d $^3\text{D}_2$	3d' $^3\text{D}_2^o$	8.56×10^{-2}	38.7	1478.045	1478.170	25.4	
C III	3d $^3\text{D}_3$	3d' $^3\text{D}_2^o$	1.37×10^{-2}		1478.106			
C III	3d $^3\text{D}_1$	3d' $^3\text{D}_1^o$	9.25×10^{-2}		1478.303			
C III	3d $^3\text{D}_2$	3d' $^3\text{D}_1^o$	1.86×10^{-2}		1478.327			
Mo VI	119726	187331	6.15×10^{-1}	38.8	1479.168	1479.30	26.8	
				15.6		1479.49		unid.
				21.8		1485.53		unid.
Ge IV	4d $^2\text{D}_{3/2}$	4f $^2\text{F}_{5/2}^o$			1494.889	1494.97	16.2	
C III	3d $^1\text{D}_2$	5p $^1\text{P}_1^o$	2.98×10^{-2}		1497.563			
Ge IV	4d $^2\text{D}_{5/2}$	4f $^2\text{F}_{5/2}^o$			1500.519			newly identified
Ge IV	4d $^2\text{D}_{5/2}$	4f $^2\text{F}_{7/2}^o$			1500.609			newly identified
S V	3p $^1\text{P}^o$	3p' ^1D	1.04×10^{-1}	45.0	1501.799	1501.92	24.2	
				78.5		1511.07		unid.
Zr VI	393555	459581	2.70×10^{-1}		1514.568			
Kr V	278928	344908	8.37×10^{-1}		1515.611			
Zr VI	369712	435428	1.99×10^{-1}		1521.699			

Table A.3. Continued.

Ion	Levels		f	$W_\lambda /$ mÅ	Wavelength / Å		$v_{\text{rad}} /$ km/s	Comment
	Lower	Upper			Theoretical	Observed		
Ba VII	178316	243933	1.07×10^{-2}		1524.009			newly identified
				21.4		1526.05		unid.
Si II					1526.707			ISM multi-component
C III	3p $^1P_1^o$	4d 1D_2	2.03×10^{-1}	23.4	1531.835	1531.97	26.4	
				22.9		1536.23		unid.
C III	3d 1D_2	3d' $^1F_3^o$	6.86×10^{-2}	56.6	1541.115	1541.26	28.2	
C IV	2s $^2S_{1/2}$	2p $^2P_{3/2}^o$	1.90×10^{-1}	245.9	1548.203	1548.33	24.6	
C IV	2s $^2S_{1/2}$	2p $^2P_{1/2}^o$	9.52×10^{-2}	217.7	1550.772	1550.90	24.8	
						1561.93		unid.
						1563.99		unid.
Kr V	288683	352537	6.65×10^{-1}		1566.073			
				27.1		1567.70		unid.
C III	3d 3D_3	3d' $^3F_4^o$	2.28×10^{-1}	36.5	1576.479	1576.61	24.9	
C III	3p $^3P_2^o$	3p' 3D_3	1.07×10^{-2}		1576.888			
C III	3d 3D_2	3d' $^3F_3^o$	2.21×10^{-1}		1577.297			
C III	3d 3D_3	3d' $^3F_3^o$	2.01×10^{-1}		1577.366			
C III	3p $^3P_1^o$	3p' 3D_2	9.58×10^{-1}		1577.532			
C III	3p $^3P_2^o$	3p' 3D_2	1.92×10^{-3}		1577.858			
C III	3d 3D_1	3d' $^3F_2^o$	2.49×10^{-1}		1577.880			
C III	3d 3D_2	3d' $^3F_2^o$	2.81×10^{-2}		1577.907			
C III	3d 3D_3	3d' $^3F_2^o$	4.56×10^{-4}		1577.977			
C III	3p $^3P_0^o$	3p' 3D_1	1.28×10^{-2}		1578.001			
C III	3p $^3P_1^o$	3p' 3D_1	3.20×10^{-3}		1578.142			
Ba VII	178140	241412	4.22×10^{-3}		1580.480			newly identified
Ba VII	156256	219528	2.05×10^{-3}		1580.483			newly identified
						1582.54		unid.
Kr V	291138	354291	3.56×10^{-1}		1583.456			
C IV	4p $^2P_{1/2}^o$	6d $^2D_{3/2}$	1.36×10^{-1}		1585.811			
C IV	4p $^2P_{3/2}^o$	6d $^2D_{5/2}$	1.22×10^{-1}		1586.111			
C IV	4p $^2P_{3/2}^o$	6d $^2D_{3/2}$	1.35×10^{-2}		1586.141			
Mo V	94835	157851	1.46×10^{-1}		1586.898			
Kr V	283677	346599	9.57×10^{-1}		1589.269			
Mo V	99380	162257	1.66×10^{-1}		1590.414			
C III	3s 1S_0	3s' $^1P_1^o$	6.85×10^{-1}	37.5	1591.443	1591.59	27.7	
Zr VI	364827	427649	4.28×10^{-1}		1591.799			
Kr V	291138	353957	6.18×10^{-1}		1591.875			
Mo VI	119726	182404	2.81×10^{-1}	27.3	1595.435	1595.58	27.2	
Zr IV	84461	147002	9.73×10^{-1}		1598.948			
						1600.88		unid.
						1610.42		unid.

Table A.3. Continued.

Ion	Levels		f	$W_\lambda /$ mÅ	Wavelength / Å		$v_{\text{rad}} /$ km/s	Comment
	Lower	Upper			Theoretical	Observed		
						1610.70		unid.
						1616.99		unid.
C III	3p $^3\text{P}_2^o$	4d $^3\text{D}_3$	4.57×10^{-1}	46.1	1620.069	1620.18	20.5	
C III	3p $^3\text{P}_1^o$	4d $^3\text{D}_2$	4.03×10^{-1}	19.9	1620.338	1620.46	22.6	
C III	3p $^3\text{P}_0^o$	4d $^3\text{D}_1$	5.44×10^{-1}		1620.594			
C III	3p $^3\text{P}_2^o$	4d $^3\text{D}_2$	8.18×10^{-2}		1620.681			
C III	3p $^3\text{P}_1^o$	4d $^3\text{D}_1$	1.36×10^{-1}		1620.743			
C III	3p $^3\text{P}_2^o$	4d $^3\text{D}_1$	5.49×10^{-3}		1621.087			
Zr V	327617	388853	1.21×10^{-1}		1633.027			
C IV	4d $^2\text{D}_{3/2}$	6f $^2\text{F}_{5/2}^o$	1.86×10^{-1}		1637.543			
C IV	4d $^2\text{D}_{5/2}$	6f $^2\text{F}_{5/2}^o$	8.85×10^{-3}		1637.650			
C IV	4d $^2\text{D}_{5/2}$	6f $^2\text{F}_{7/2}^o$	1.77×10^{-1}		1637.650			
He II	2	3	6.41×10^{-1}	254.3	1640.377	1640.54	29.8	
Mo V	99380	159857	3.81×10^{-1}		1653.541			
C IV	4p $^2\text{P}_{1/2}^o$	6s $^2\text{S}_{1/2}$	2.46×10^{-2}		1653.633			
C IV	4p $^2\text{P}_{3/2}^o$	6s $^2\text{S}_{1/2}$	2.46×10^{-2}		1653.992			
C IV	4d $^2\text{D}_{3/2}$	6p $^2\text{P}_{3/2}^o$	1.35×10^{-3}		1654.457			
C IV	4d $^2\text{D}_{3/2}$	6p $^2\text{P}_{1/2}^o$	6.75×10^{-3}		1654.564			
C IV	4d $^2\text{D}_{5/2}$	6p $^2\text{P}_{3/2}^o$	8.10×10^{-3}		1654.566			
				29.5		1659.43		unid.
Mo V	94835	155032	3.93×10^{-1}		1661.215	1661.37	28.0	
Xe VI	5p ² $^2\text{D}_{3/2}$	4f $^2\text{F}_{5/2}^o$			1663.116			newly identified
Xe VI	5d' $^2\text{F}_{5/2}^o$	5g $^2\text{G}_{7/2}$	3.02×10^{-1}		1663.146			newly identified
				58.4		1667.83		unid.
Mo V	93111	153040	2.83×10^{-1}		1668.662			
				30.4		1669.99		unid.
						1673.23		unid.
Zr VI	393555	453000	4.00×10^{-1}		1682.241			
N IV	2s2p $^1\text{P}_1^o$	2p ² $^1\text{D}_2$	1.71×10^{-1}	106.7	1718.550	1718.69	24.4	
Zr V	325015	382985	2.14×10^{-1}		1725.024			uncertain
Zr VI	364827	421991	2.77×10^{-1}	79.8	1749.350	1749.50	26.7	uncertain
						1751.72		unid.
						1752.87		unid.
						1757.05		unid.
				138.8		1757.86		unid.
				37.6		1760.23		unid.
						1761.20		unid.
Kr V	250993	307667	2.31×10^{-1}		1764.478			
				27.0		1767.98		unid.

Table A.3. Continued.

Ion	Levels		f	$W_\lambda /$ mÅ	Wavelength / Å		$v_{\text{rad}} /$ km/s	Comment
	Lower	Upper			Theoretical	Observed		
Ba VII	157675	213712	2.22×10^{-2}		1784.535			newly identified
				49.4		1796.62		unid.
				34.9		1803.15		unid.
						1807.71		unid.
				33.0		1808.36		unid.
Ba VII	152397	206668	1.50×10^{-2}		1842.595	1819.61		unid.
						1849.26		newly identified
						1851.95		unid.
						1855.49		unid.
				27.3		1855.77		unid.
Xe VI	$5p^2 \ ^2D_{5/2}$	$5d \ ^2D_{5/2}$		38.6	1884.016	1879.01		unid.
								newly identified
				23.6		1885.53		unid.
C III	$2s3p \ ^1P_1^o$	$2s4s \ ^1S_0$	9.68×10^{-2}	10.2	1894.290	1888.08		unid.
				30.9		1901.53		unid.
				16.3		1901.77		unid.
				25.6		1901.97		unid.
				37.5		1902.29		unid.
C III	$3d \ ^3D_3$	$4f \ ^3F_4^o$	5.77×10^{-1}		1922.957			
C III	$3d \ ^3D_2$	$4f \ ^3F_3^o$	5.58×10^{-1}		1923.164			
C III	$3d \ ^3D_3$	$4f \ ^3F_3^o$	5.08×10^{-2}		1923.268			
C III	$3d \ ^3D_1$	$4f \ ^3F_2^o$	6.29×10^{-1}		1923.341			
C III	$3d \ ^3D_2$	$4f \ ^3F_2^o$	7.11×10^{-2}		1923.382			
C III	$3d \ ^3D_3$	$4f \ ^3F_2^o$	1.15×10^{-3}		1923.486			
Kr VI	275380	326657	6.59×10^{-1}	19.3	1950.192	1937.28		unid.
				93.3		1957.24		newly identified
				20.3		1967.57		unid.
				37.7		1984.64		unid.
C III	$3p \ ^3P_0^o$	$4s \ ^3S_1$	1.39×10^{-1}		2009.985			
C III	$3p \ ^3P_1^o$	$4s \ ^3S_1$	1.39×10^{-1}		2010.214			
C III	$3p \ ^3P_2^o$	$4s \ ^3S_1$	1.39×10^{-1}	45.0	2010.743	2010.91	24.9	
				15.9		2011.39		unid.
				17.9		2011.83		unid.
				12.7		2012.15		unid.
						2029.38		unid.
				19.9		2051.02		unid.
				38.8		2051.89		unid.
				23.3		2066.42		unid.

Table A.3. Continued.

Ion	Levels		f	$W_\lambda /$ mÅ	Wavelength / Å		$v_{\text{rad}} /$ km/s	Comment
	Lower	Upper			Theoretical	Observed		
C III	3d 3D_1	4p $^3P_2^o$	7.22×10^{-4}		2092.467			
C III	3d 3D_2	4p $^3P_2^o$	7.69×10^{-3}		2092.516			
C III	3d 3D_3	4p $^3P_2^o$	3.34×10^{-2}		2092.639			
C III	3d 3D_1	4p $^3P_1^o$	1.80×10^{-2}		2092.677			
C III	3d 3D_2	4p $^3P_1^o$	3.23×10^{-2}		2092.725			
C III	3d 3D_1	4p $^3P_0^o$	2.39×10^{-2}		2092.776			
				27.3		2098.66		unid.
C IV	4s $^2S_{1/2}$	5p $^2P_{3/2}^o$	1.43×10^{-1}		2104.607			
C IV	4s $^2S_{1/2}$	5p $^2P_{1/2}^o$	7.14×10^{-2}		2104.922			
Xe VI	6s $^2S_{1/2}$	6p $^2P_{3/2}^o$	7.40×10^{-1}		2135.479			newly identified
						2146.69		unid.
C III	3d 1D_2	4f $^1F_3^o$	7.96×10^{-1}	76.5	2163.605	2163.84	32.6	
				8.3		2212.24		unid.
				5.9		2212.49		unid.
				5.5		2212.92		unid.
				19.1		2240.01		unid.
C III	2p $^1P_1^o$	2p 1D_2	1.80×10^{-1}	109.9	2297.578	2297.78	26.4	
				21.5		2314.97		unid.
C IV	5d $^2D_{3/2}$	8f $^2F_{5/2}^o$	8.12×10^{-2}		2333.504			
C IV	5d $^2D_{5/2}$	8f $^2F_{5/2}^o$	3.87×10^{-3}		2333.597			
C IV	5d $^2D_{5/2}$	8f $^2F_{7/2}^o$	7.73×10^{-2}		2333.597			
C IV	5f $^2F_{7/2}^o$	8g $^2G_{7/2}$	2.39×10^{-3}		2336.247			
C IV	5f $^2F_{7/2}^o$	8g $^2G_{9/2}$	8.23×10^{-2}		2336.247			
C IV	5f $^2F_{5/2}^o$	8g $^2G_{7/2}$	8.46×10^{-2}		2336.247			
C IV	5g $^2G_{7/2}$	8h $^2H_{9/2}^o$	5.98×10^{-2}		2336.700			
C IV	5g $^2G_{9/2}$	8h $^2H_{9/2}^o$	1.12×10^{-3}		2336.700			
C IV	5g $^2G_{9/2}$	8h $^2H_{11/2}^o$	5.87×10^{-2}		2336.700			
C IV	5p $^2P_{1/2}^o$	8s $^2S_{1/2}$	1.32×10^{-2}		2336.722			
C IV	5g $^2G_{7/2}$	8f $^2F_{5/2}^o$	3.77×10^{-4}		2336.787			
C IV	5g $^2G_{7/2}$	8f $^2F_{7/2}^o$	1.42×10^{-5}		2336.787			
C IV	5g $^2G_{9/2}$	8f $^2F_{7/2}^o$	3.91×10^{-4}		2336.787			
C IV	5f $^2F_{5/2}^o$	8d $^2D_{5/2}$	1.11×10^{-4}		2337.066			
C IV	5f $^2F_{5/2}^o$	8d $^2D_{3/2}$	1.56×10^{-3}		2337.066			
C IV	5f $^2F_{7/2}^o$	8d $^2D_{5/2}$	1.67×10^{-3}		2337.066			
C IV	5p $^2P_{3/2}^o$	8s $^2S_{1/2}$	1.32×10^{-2}		2337.109			
				46.5		2344.31		unid.
				73.5		2382.82		unid.
He II	3	8	1.60×10^{-2}		2386.221			

Table A.3. Continued.

Ion	Levels		f	$W_\lambda /$ mÅ	Wavelength / Å		$v_{\text{rad}} /$ km/s	Comment
	Lower	Upper			Theoretical	Observed		
C IV	4p $^2\text{P}_{1/2}^o$	5d $^2\text{D}_{3/2}$	5.23×10^{-1}		2405.170			
C IV	4p $^2\text{P}_{3/2}^o$	5d $^2\text{D}_{5/2}$	4.61×10^{-1}		2405.830			
C IV	4p $^2\text{P}_{3/2}^o$	5d $^2\text{D}_{3/2}$	5.12×10^{-2}		2405.928			
O IV	4f $^2\text{F}_{5/2}^o$	5g $^2\text{G}_{7/2}$	1.20		2450.116			
O IV	4f $^2\text{F}_{7/2}^o$	5g $^2\text{G}_{7/2}$	3.38×10^{-2}		2450.782			
O IV	4f $^2\text{F}_{7/2}^o$	5g $^2\text{G}_{9/2}$	1.17		2450.782			
				17.6		2460.82		unid. newly identified
Ge IV	5p $^2\text{P}_{3/2}^o$	5d $^2\text{D}_{5/2}$			2488.691			
He II	3	7	2.77×10^{-2}		2512.059			
						2524.41 2524.72		unid. unid.
C IV	4d $^2\text{D}_{3/2}$	5f $^2\text{F}_{5/2}^o$	8.86×10^{-1}		2525.017			
C IV	4d $^2\text{D}_{5/2}$	5f $^2\text{F}_{5/2}^o$	4.22×10^{-2}		2525.272			
C IV	4d $^2\text{D}_{5/2}$	5f $^2\text{F}_{7/2}^o$	8.44×10^{-1}		2525.272			
C IV	4f $^2\text{F}_{7/2}^o$	5g $^2\text{G}_{9/2}$	1.30		2530.736			
C IV	4f $^2\text{F}_{7/2}^o$	5g $^2\text{G}_{7/2}$	3.78×10^{-2}		2530.736			
C IV	4f $^2\text{F}_{5/2}^o$	5g $^2\text{G}_{7/2}$	1.34		2530.736			
C IV	4f $^2\text{F}_{7/2}^o$	5d $^2\text{D}_{5/2}$	9.08×10^{-3}		2534.488			
C IV	4f $^2\text{F}_{5/2}^o$	5d $^2\text{D}_{5/2}$	6.05×10^{-4}		2534.488			
C IV	4f $^2\text{F}_{5/2}^o$	5d $^2\text{D}_{3/2}$	8.47×10^{-3}		2534.597			
				6.7		2586.31 2586.65 2586.83 2595.53		unid. unid. unid. unid.
				18.4				
C IV	4d $^2\text{D}_{3/2}$	5p $^2\text{P}_{3/2}$	6.74×10^{-3}		2595.596			
C IV	4d $^2\text{D}_{5/2}$	5p $^2\text{P}_{3/2}$	4.06×10^{-2}		2595.865			
C IV	4d $^2\text{D}_{3/2}$	5p $^2\text{P}_{1/2}$	3.38×10^{-2}		2596.074			
				23.6		2597.57		unid.
				33.0		2598.08		unid.
				45.4		2599.11		unid.
				44.3		2599.80		unid.
				67.1		2600.27		unid.
C IV	4p $^2\text{P}_{1/2}^o$	5s $^2\text{S}_{1/2}$	1.28×10^{-1}		2698.516			
C IV	4p $^2\text{P}_{3/2}^o$	5s $^2\text{S}_{1/2}$	1.28×10^{-1}		2699.471			
He II	3	6	5.59×10^{-2}		2734.220			
Mg II					2796.352			ISM multi-component
Mg II					2803.531			ISM multi-component
C IV	5p $^2\text{P}_{1/2}^o$	7d $^2\text{D}_{3/2}$	1.40×10^{-1}		2819.687			

Table A.3. Continued.

Ion	Levels		f	$W_\lambda /$ mÅ	Wavelength / Å		$v_{\text{rad}} /$ km/s	Comment
	Lower	Upper			Theoretical	Observed		
C iv	5p $^2\text{P}_{3/2}^o$	7d $^2\text{D}_{3/2}$	1.40×10^{-2}		2820.251			
C iv	5p $^2\text{P}_{3/2}^o$	7d $^2\text{D}_{5/2}$	1.26×10^{-1}		2820.278			
O iv	3s $^4\text{P}_{5/2}^o$	3p $^4\text{S}_{3/2}$	6.83×10^{-2}		2837.105			
				54.5		2881.55		unid.
C iv	5d $^2\text{D}_{3/2}$	7f $^2\text{F}_{5/2}^o$	1.96×10^{-1}		2902.303			
C iv	5d $^2\text{D}_{5/2}$	7f $^2\text{F}_{5/2}^o$	9.34×10^{-3}		2902.446			
C iv	5d $^2\text{D}_{5/2}$	7f $^2\text{F}_{7/2}^o$	1.87×10^{-1}		2902.466			
C iv	5f $^2\text{F}_{7/2}^o$	7g $^2\text{G}_{9/2}$	2.21×10^{-1}		2906.502			
C iv	5f $^2\text{F}_{7/2}^o$	7g $^2\text{G}_{7/2}$	6.42×10^{-3}		2906.502			
C iv	5f $^2\text{F}_{5/2}^o$	7g $^2\text{G}_{7/2}$	2.27×10^{-1}		2906.502			
C iv	5g $^2\text{G}_{7/2}$	7h $^2\text{H}_{9/2}^o$	2.00×10^{-1}		2907.193			
C iv	5g $^2\text{G}_{9/2}$	7h $^2\text{H}_{9/2}^o$	3.73×10^{-3}		2907.193			
C iv	5g $^2\text{G}_{9/2}$	7h $^2\text{H}_{11/2}^o$	1.96×10^{-1}		2907.193			
C iv	5g $^2\text{G}_{7/2}$	7f $^2\text{F}_{5/2}^o$	1.13×10^{-3}		2907.382			
C iv	5g $^2\text{G}_{7/2}$	7f $^2\text{F}_{7/2}^o$	4.24×10^{-5}		2907.402			
C iv	5g $^2\text{G}_{9/2}$	7f $^2\text{F}_{7/2}^o$	1.17×10^{-3}		2907.402			
C iv	5f $^2\text{F}_{5/2}^o$	7d $^2\text{D}_{5/2}$	3.01×10^{-4}		2907.589			
C iv	5f $^2\text{F}_{5/2}^o$	7d $^2\text{D}_{3/2}$	4.21×10^{-3}		2907.589			
C iv	5f $^2\text{F}_{7/2}^o$	7d $^2\text{D}_{5/2}$	4.52×10^{-3}		2907.617			
				60.1		2958.83		unid.
O iii	3p $^1\text{P}_1$	3d $^1\text{D}_2^o$	4.20×10^{-1}		2960.559			
C iii	3d $^1\text{D}_2$	3s' $^1\text{P}_1^o$	6.72×10^{-2}	36.9	2982.986	2983.23	24.5	

Table A.4. Like Table A.1, for the optical observations.

Ion	Levels		f	$W_\lambda /$ mÅ	Wavelength / Å		$v_{\text{rad}} /$ km/s	Comment
	Lower	Upper			Theoretical	Observed		
O iv	3s $^2\text{P}_{1/2}^o$	3p $^2\text{D}_{3/2}$	2.84×10^{-1}		3348.055			newly identified
O iv	3s $^2\text{P}_{3/2}^o$	3p $^2\text{D}_{5/2}$	2.55×10^{-1}		3349.110			newly identified
O iv	3s $^4\text{P}_{3/2}^o$	3p $^4\text{D}_{5/2}$	1.83×10^{-1}		3381.212			newly identified
O iv	3s $^4\text{P}_{1/2}^o$	3p $^4\text{D}_{3/2}$	1.45×10^{-1}		3381.304			newly identified
O iv	3s $^4\text{P}_{5/2}^o$	3p $^4\text{D}_{7/2}$	2.32×10^{-1}		3385.518			newly identified
O iv	3s $^4\text{P}_{1/2}^o$	3p $^4\text{D}_{1/2}$	1.45×10^{-1}		3390.191			newly identified
O iv	3s $^4\text{P}_{3/2}^o$	3p $^4\text{D}_{3/2}$	9.29×10^{-2}		3396.803			newly identified
S v	4s ^1S	4p $^1\text{P}^o$	6.37×10^{-1}		3397.334			blend with O iv, newly identified
O iv	3p $^2\text{P}_{1/2}^o$	3d $^2\text{D}_{3/2}$	2.95×10^{-1}		3403.545			newly identified

Table A.4. Continued.

Ion	Levels		f	$W_\lambda /$ mÅ	Wavelength/Å		$v_{\text{rad}} /$ km/s	Comment
	Lower	Upper			Theoretical	Observed		
O IV	3s $4P_{5/2}^o$	3p $4D_{5/2}$	5.22×10^{-2}	49.1	3409.698			newly identified
O IV	3p $2P_{3/2}^o$	3d $2D_{5/2}$	2.65×10^{-1}		3411.688	3412.02	29.2	newly identified
O IV	3p $2P_{3/2}^o$	3d $2D_{3/2}$	2.95×10^{-2}		3413.633			newly identified
C III	4p $3P_0^o$	5d $3D_1$	3.17×10^{-1}		3608.778			newly identified
C III	4p $3P_1^o$	5d $3D_2$	2.38×10^{-1}		3609.051			newly identified
C III	4p $3P_1^o$	5d $3D_1$	7.96×10^{-2}		3609.071			newly identified
C III	4p $3P_2^o$	5d $3D_3$	2.67×10^{-1}		3609.620			newly identified
C III	4p $3P_2^o$	5d $3D_2$	4.78×10^{-2}		3609.676			newly identified
C III	4p $3P_2^o$	5d $3D_1$	3.20×10^{-3}		3609.695			newly identified
C IV	6f $2F_{5/2}^o$	9g $2G_{7/2}$	9.78×10^{-2}		3689.263			newly identified
C IV	6f $2F_{7/2}^o$	9g $2G_{7/2}$	2.76×10^{-3}		3689.263			newly identified
C IV	6f $2F_{7/2}^o$	9g $2G_{9/2}$	9.51×10^{-2}		3689.263			newly identified
C IV	6g $2G_{9/2}$	9h $2H_{11/2}^o$	9.15×10^{-2}		3689.635			newly identified
C IV	6g $2G_{9/2}$	9h $2H_{9/2}^o$	1.74×10^{-3}		3689.636			newly identified
C IV	6g $2G_{7/2}$	9h $2H_{9/2}^o$	9.32×10^{-2}		3689.636			newly identified
C IV	6h $2H_{9/2}^o$	9i $2I_{11/2}$	5.77×10^{-2}		3689.717			newly identified
C IV	6h $2H_{11/2}^o$	9i $2I_{11/2}$	8.54×10^{-4}		3689.717			newly identified
C IV	6h $2H_{11/2}^o$	9i $2I_{13/2}$	5.69×10^{-2}		3689.717			newly identified
C IV	6h $2H_{9/2}^o$	9g $2G_{7/2}$	2.73×10^{-4}		3689.753			newly identified
C IV	6h $2H_{9/2}^o$	9g $2G_{9/2}$	6.36×10^{-6}		3689.753			newly identified
C IV	6h $2H_{11/2}^o$	9g $2G_{9/2}$	2.79×10^{-4}		3689.753			newly identified
C IV	6g $2G_{7/2}$	9f $2F_{5/2}^o$	1.15×10^{-3}		3689.785			newly identified
C IV	6g $2G_{7/2}$	9f $2F_{7/2}^o$	4.34×10^{-5}		3689.785			newly identified
C IV	6g $2G_{9/2}$	9f $2F_{7/2}^o$	1.20×10^{-3}		3689.785			newly identified
O IV	3p $4D_{1/2}$	3d $4F_{3/2}^o$	2.31×10^{-1}		3725.889			newly identified
O IV	3p $4D_{3/2}$	3d $4F_{5/2}^o$	1.85×10^{-1}		3725.945			newly identified
O IV	3p $4D_{5/2}$	3d $4F_{7/2}^o$	1.89×10^{-1}		3729.030			newly identified
O IV	3p $4D_{3/2}$	3d $4F_{3/2}^o$	4.62×10^{-2}		3736.682			newly identified
O IV	3p $4D_{7/2}$	3d $4F_{9/2}^o$	2.06×10^{-1}		3736.850			newly identified
He I	2s $3S$	3p $3P^o$	6.45×10^{-2}		3888.643			newly identified
H I	2	8	8.04×10^{-3}		3889.049			newly identified
C III	4d $3D_3$	5f $3F_4^o$	3.28×10^{-1}		3889.137			blend with H I, newly identified
C III	4d $3D_3$	5f $3F_3^o$	2.89×10^{-2}		3889.462			blend with H I, newly identified
C III	4d $3D_3$	5f $3F_2^o$	6.57×10^{-4}		3889.670			blend with H I, newly identified
C IV	5s $2S_{1/2}$	6p $2P_{3/2}^o$	1.52×10^{-1}		3934.283			newly identified
C IV	5s $2S_{1/2}$	6p $2P_{1/2}^o$	7.62×10^{-2}		3934.887			newly identified
C III	4d $1D_2$	5f $1F_3^o$	3.70×10^{-1}	94.2	4056.061	4056.33	19.9	uncertain, newly identified

Table A.4. Continued.

Ion	Levels		f	$W_\lambda /$ mÅ	Wavelength/ Å		$v_{\text{rad}} /$ km/s	Comment
	Lower	Upper			Theoretical	Observed		
N iv	3p $^1\text{P}^{\circ}_1$	3d $^1\text{D}_2$	2.74×10^{-1}		4057.757			newly identified
C iii	4f $^3\text{F}^{\circ}_2$	5g $^3\text{G}_3$	1.02		4067.939			newly identified
C iii	4f $^3\text{F}^{\circ}_3$	5g $^3\text{G}_3$	6.50×10^{-2}		4068.916			newly identified
C iii	4f $^3\text{F}^{\circ}_3$	5g $^3\text{G}_4$	9.78×10^{-1}		4068.916			newly identified
C iii	4f $^3\text{F}^{\circ}_4$	5g $^3\text{G}_5$	9.92×10^{-1}		4070.260			newly identified
C iii	4f $^3\text{F}^{\circ}_4$	5g $^3\text{G}_3$	9.92×10^{-4}		4070.306			newly identified
C iii	4f $^3\text{F}^{\circ}_4$	5g $^3\text{G}_4$	5.06×10^{-2}		4070.306			newly identified
C iii	4p $^1\text{P}^{\circ}_1$	5d $^1\text{D}_2$	3.40×10^{-1}		4121.845			newly identified
C iii	3p' $^3\text{D}_2$	5f $^3\text{F}^{\circ}_3$	2.23×10^{-1}		4156.504			newly identified
C iii	3p' $^3\text{D}_2$	5f $^3\text{F}^{\circ}_2$	2.84×10^{-2}		4156.741			newly identified
C iii	3p' $^3\text{D}_3$	5f $^3\text{F}^{\circ}_4$	2.31×10^{-1}		4162.877			newly identified
C iii	4f $^1\text{F}^{\circ}_3$	5g $^1\text{G}_4$	1.18		4186.900			newly identified
C iii	3s' $^1\text{P}^{\circ}_1$	3p' $^1\text{D}_2$	5.03×10^{-1}		4325.561			newly identified
He ii	4	10	1.20×10^{-2}		4338.659			Barstow et al. (2000)
C iv	5p $^2\text{P}^{\circ}_{1/2}$	6d $^2\text{D}_{3/2}$	4.14×10^{-1}		4440.335			newly identified
C iv	5p $^2\text{P}^{\circ}_{3/2}$	6d $^2\text{D}_{5/2}$	4.62×10^{-1}		4441.499			newly identified
C iv	5p $^2\text{P}^{\circ}_{3/2}$	6d $^2\text{D}_{3/2}$	5.13×10^{-2}		4441.736			newly identified
C iii	4p $^3\text{P}^{\circ}_0$	5s $^3\text{P}_1$	1.74×10^{-1}		4515.352			newly identified
C iii	4p $^3\text{P}^{\circ}_1$	5s $^3\text{P}_1$	1.74×10^{-1}		4515.811			newly identified
C iii	4p $^3\text{P}^{\circ}_2$	5s $^3\text{P}_1$	1.74×10^{-1}		4516.788			newly identified
C iv	5f $^2\text{F}^{\circ}_{5/2}$	6g $^2\text{G}_{7/2}$	1.18		4657.474			Barstow et al. (2000)
C iv	5f $^2\text{F}^{\circ}_{7/2}$	6g $^2\text{G}_{9/2}$	1.15		4657.606			Barstow et al. (2000)
C iv	5f $^2\text{F}^{\circ}_{7/2}$	6g $^2\text{G}_{7/2}$	3.32×10^{-2}		4657.690			Barstow et al. (2000)
C iv	5g $^2\text{G}_{7/2}$	6h $^2\text{H}^{\circ}_{9/2}$	1.66		4658.147			Barstow et al. (2000)
C iv	5g $^2\text{G}_{9/2}$	6h $^2\text{H}^{\circ}_{11/2}$	1.63		4658.228			Barstow et al. (2000)
C iv	5g $^2\text{G}_{9/2}$	6h $^2\text{H}^{\circ}_{9/2}$	3.10×10^{-2}		4658.278			Barstow et al. (2000)
C iii	3s' $^3\text{P}^{\circ}_1$	3p' $^3\text{P}_1$	7.53×10^{-2}		4659.058			newly identified
C iii	3s' $^3\text{P}^{\circ}_2$	3p' $^3\text{P}_2$	2.26×10^{-1}		4665.860			newly identified
He ii	3	4	8.43×10^{-1}		4686.059			Barstow et al. (2000)
He ii	4	8	3.23×10^{-2}		4859.299			Barstow et al. (2000)
He ii	4	7	6.55×10^{-2}		5411.492			Barstow et al. (2000)
C iii	3p $^1\text{P}^{\circ}_1$	3d $^1\text{D}_2$	3.47×10^{-1}	53.9	5695.916	5696.47	29.2	newly identified
C iv	3s $^2\text{S}_{1/2}$	3p $^2\text{P}^{\circ}_{3/2}$	3.19×10^{-1}	159.2	5801.313	5801.78	24.1	Barstow et al. (2000)
C iv	3s $^2\text{S}_{1/2}$	3p $^2\text{P}^{\circ}_{1/2}$	1.59×10^{-1}		5811.970			Barstow et al. (2000)
N iv	3p' $^3\text{P}_{1/2}$	3d' $^3\text{P}^{\circ}_{2/3}$	1.12×10^{-2}		5812.308			blend with C iv, newly identified
He i	2p $^3\text{P}^{\circ}_0$	3d ^3D	6.11×10^{-1}	264.8	5875.661	5876.10	22.4	Barstow et al. (2000)
He ii	4	6	1.79×10^{-1}		6560.049			Barstow et al. (2000)

Table A.5. Like Table A.1, for the *SofI* observations.

Ion	Levels		f	$W_\lambda /$ mÅ	Wavelength/Å		$v_{\text{rad}} /$ km/s	Comment
	Lower	Upper			Theoretical	Observed		
He II	4	5	1.04		10123.499			
He II	5	7	2.07×10^{-1}		11626.406			

Appendix B: Observed spectra of RE 0503–289 compared with our best model

In the following figures, we show the comparison of our synthetic spectra with the FUSE (Fig.B.1, HST/STIS (Fig.B.2, and optical (Fig.B.3 observations. A visualization via TVIS is available at <http://astro.uni-tuebingen.de/~TVIS/objects/RE0503-289>.

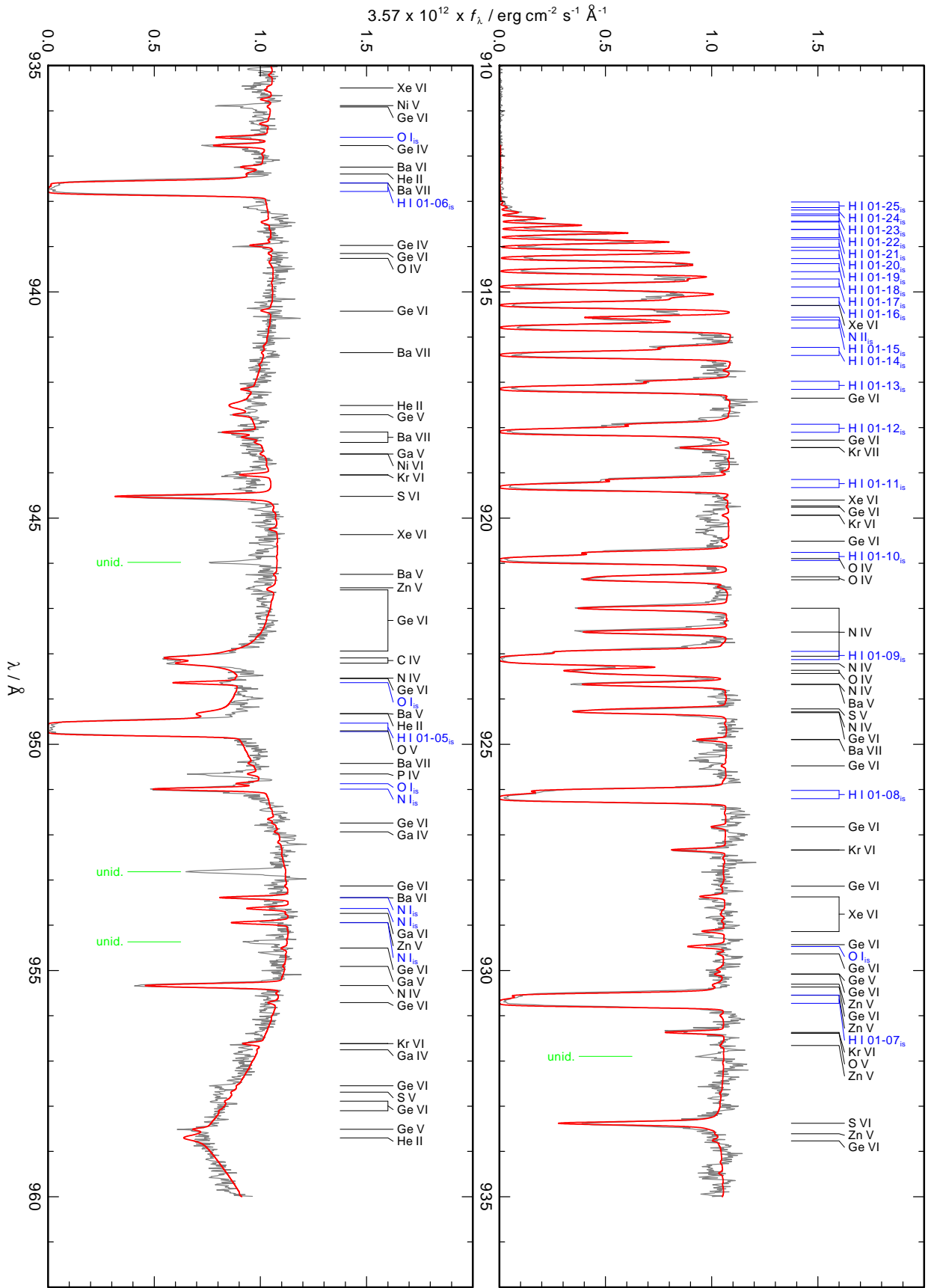
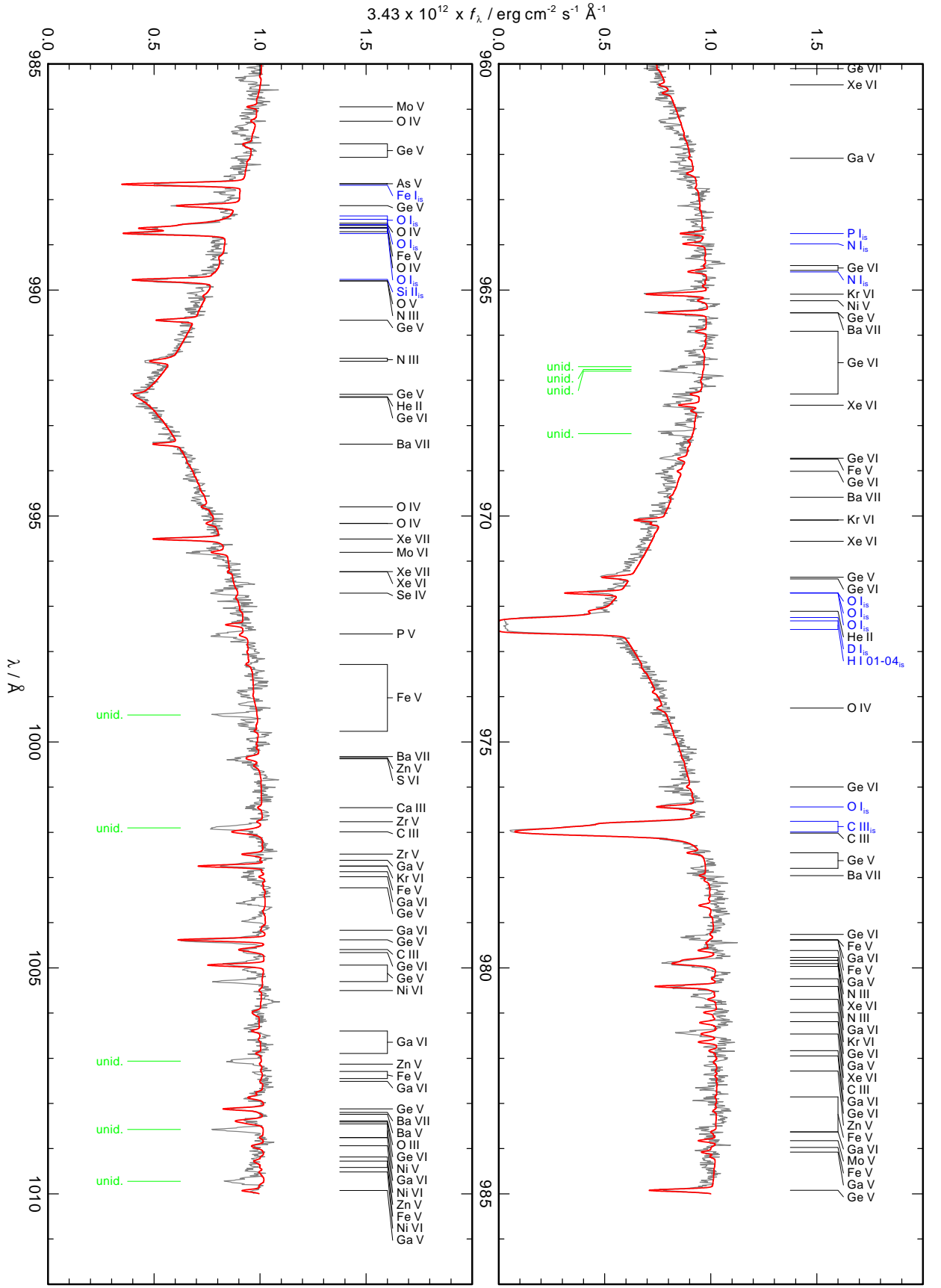


Fig. B.1. FUSE observation (gray) compared with the best model (red). Stellar lines are identified at top. “unid.” denotes unidentified lines.

Fig. B.1. Figure B.1 continued.



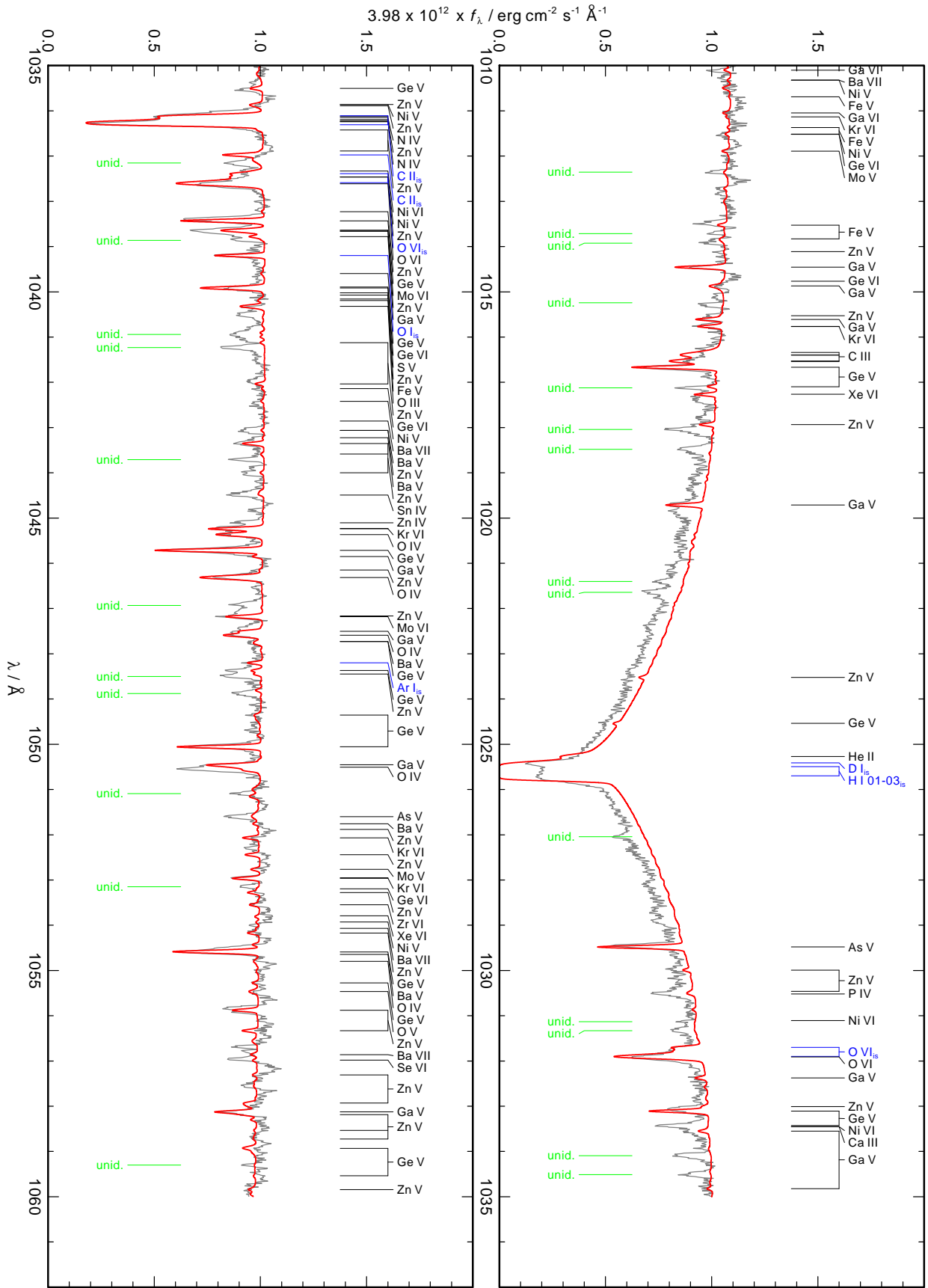


Fig. B.1. Figure B.1 continued.

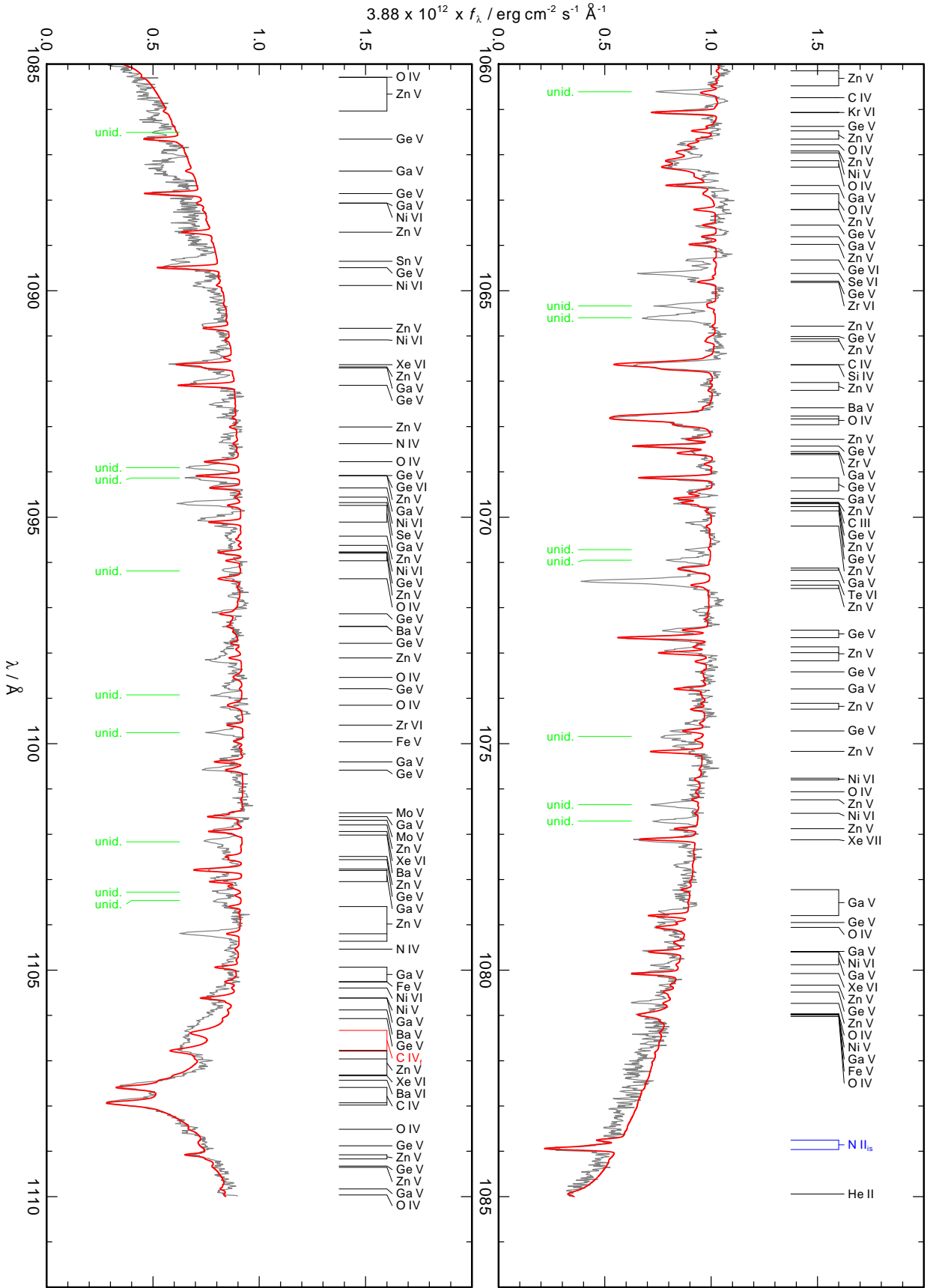


Fig. B.1. Figure B.1 continued.

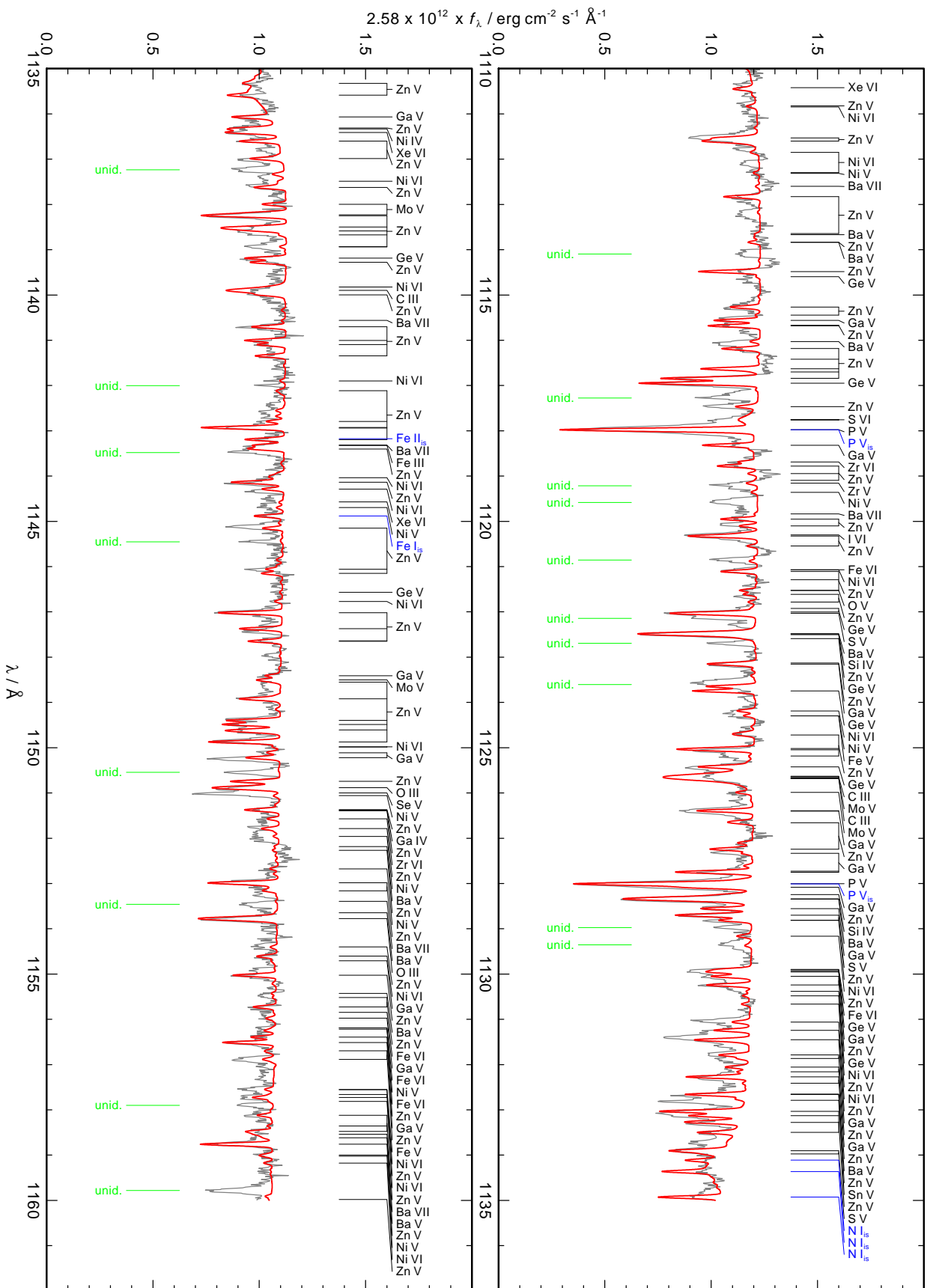
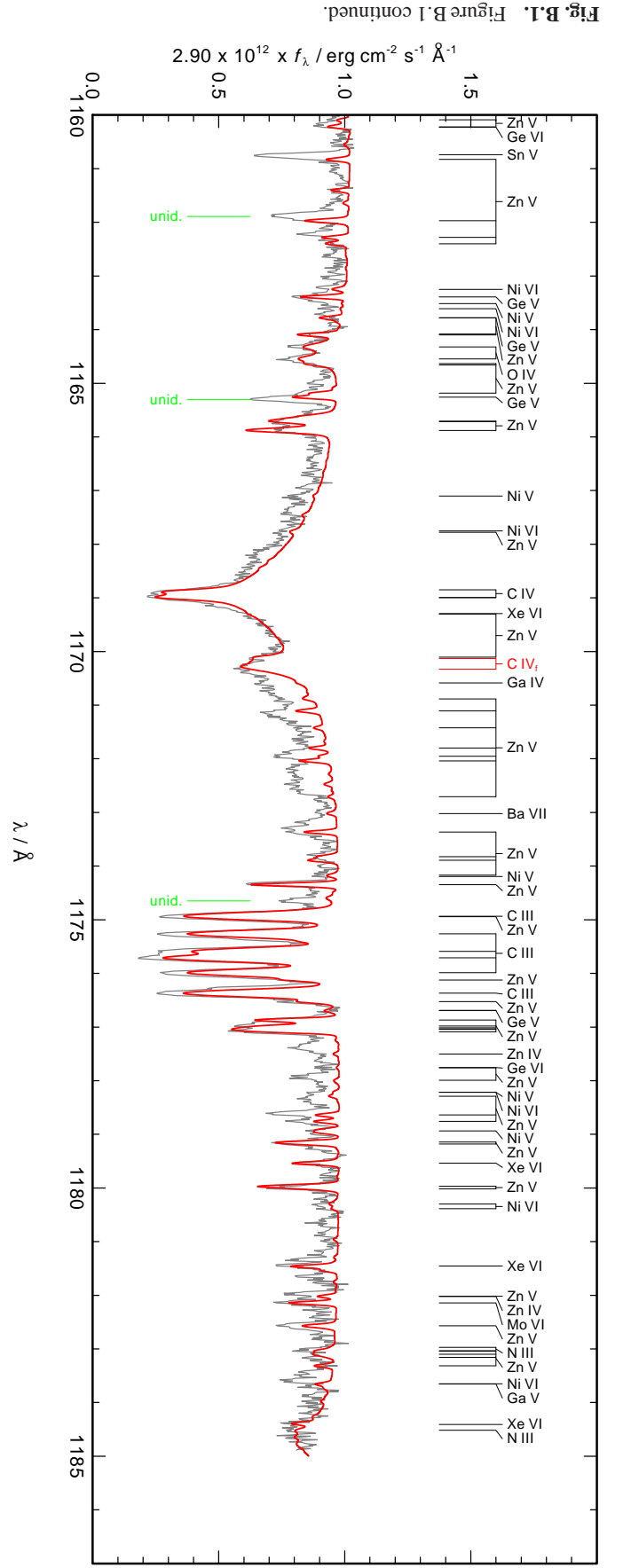


Fig. B.1. Figure B.1 continued.



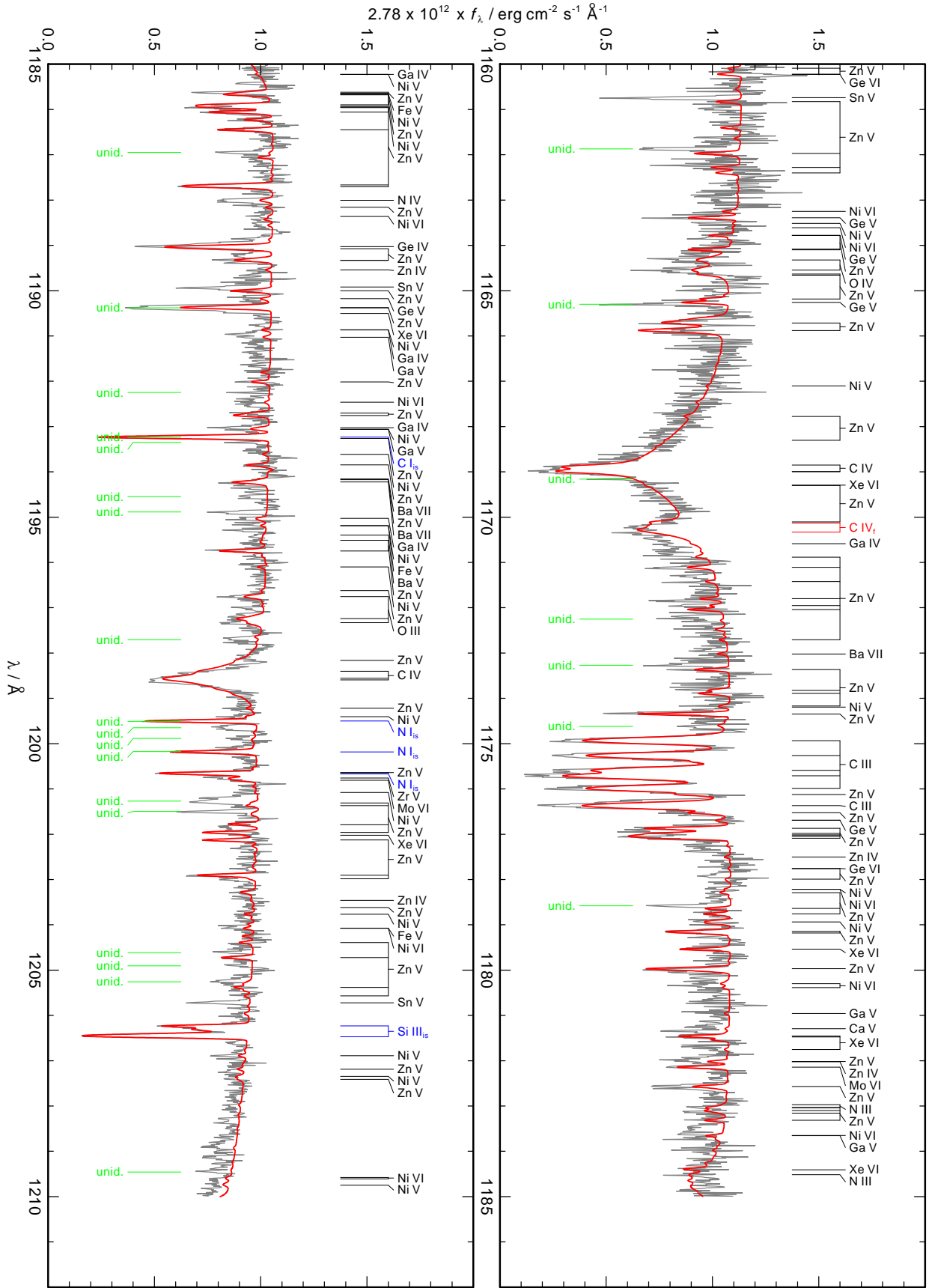
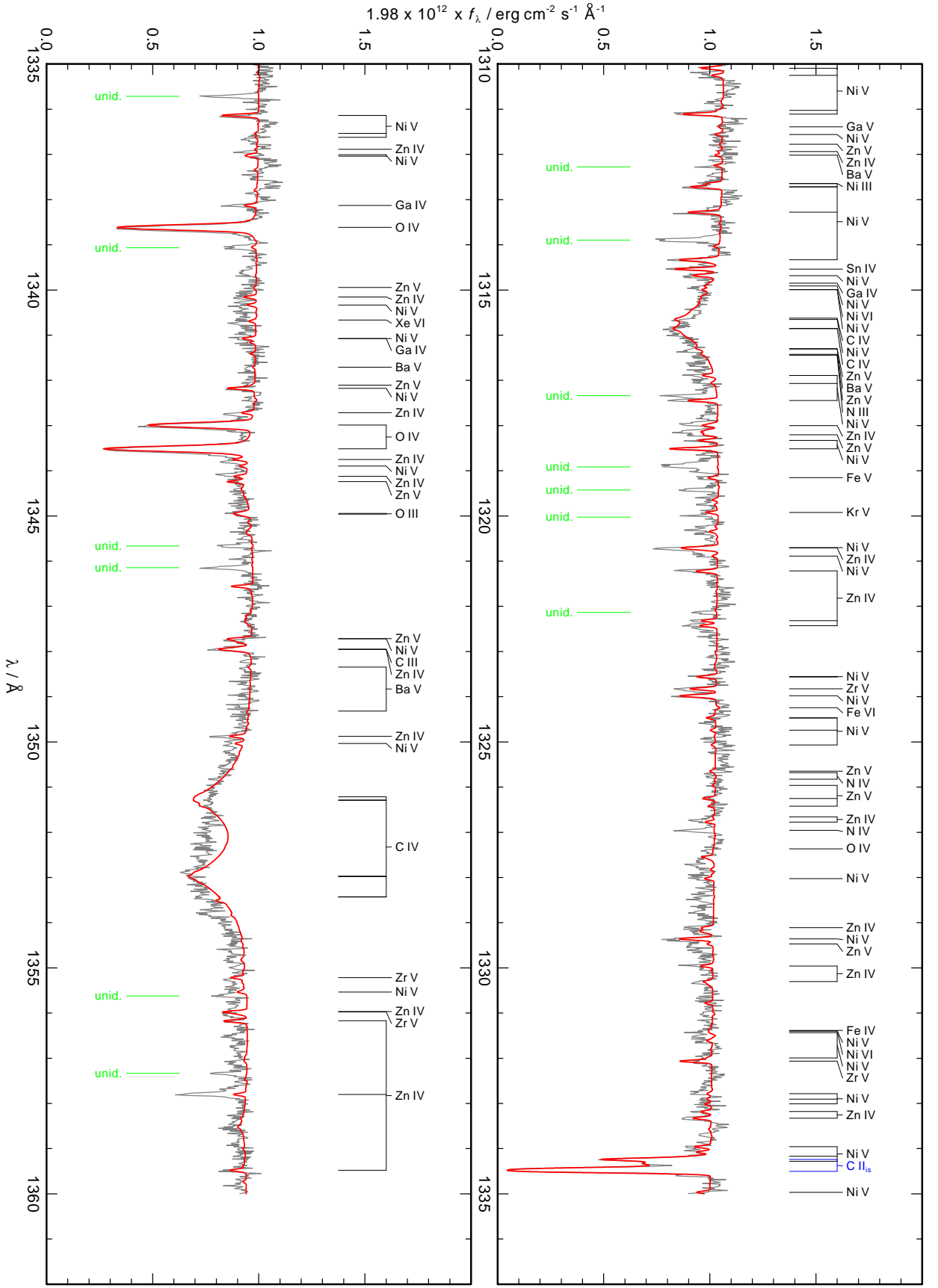


Fig. B.2. HST/STIS observation (gray) compared with the best model (red). Stellar lines are identified at top. "unid." denotes unidentified lines.

Fig. B.2. Figure B.2 continued.



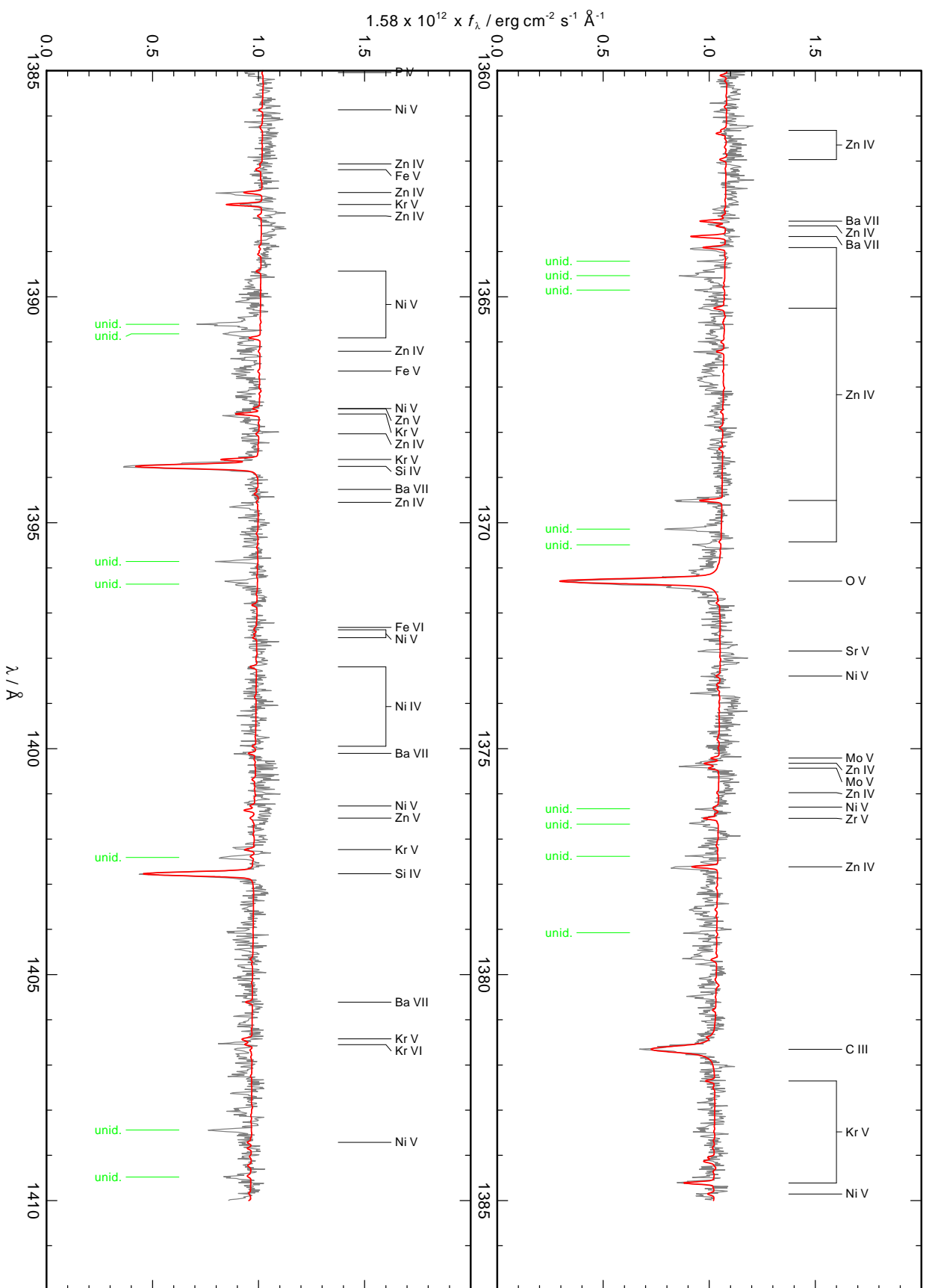
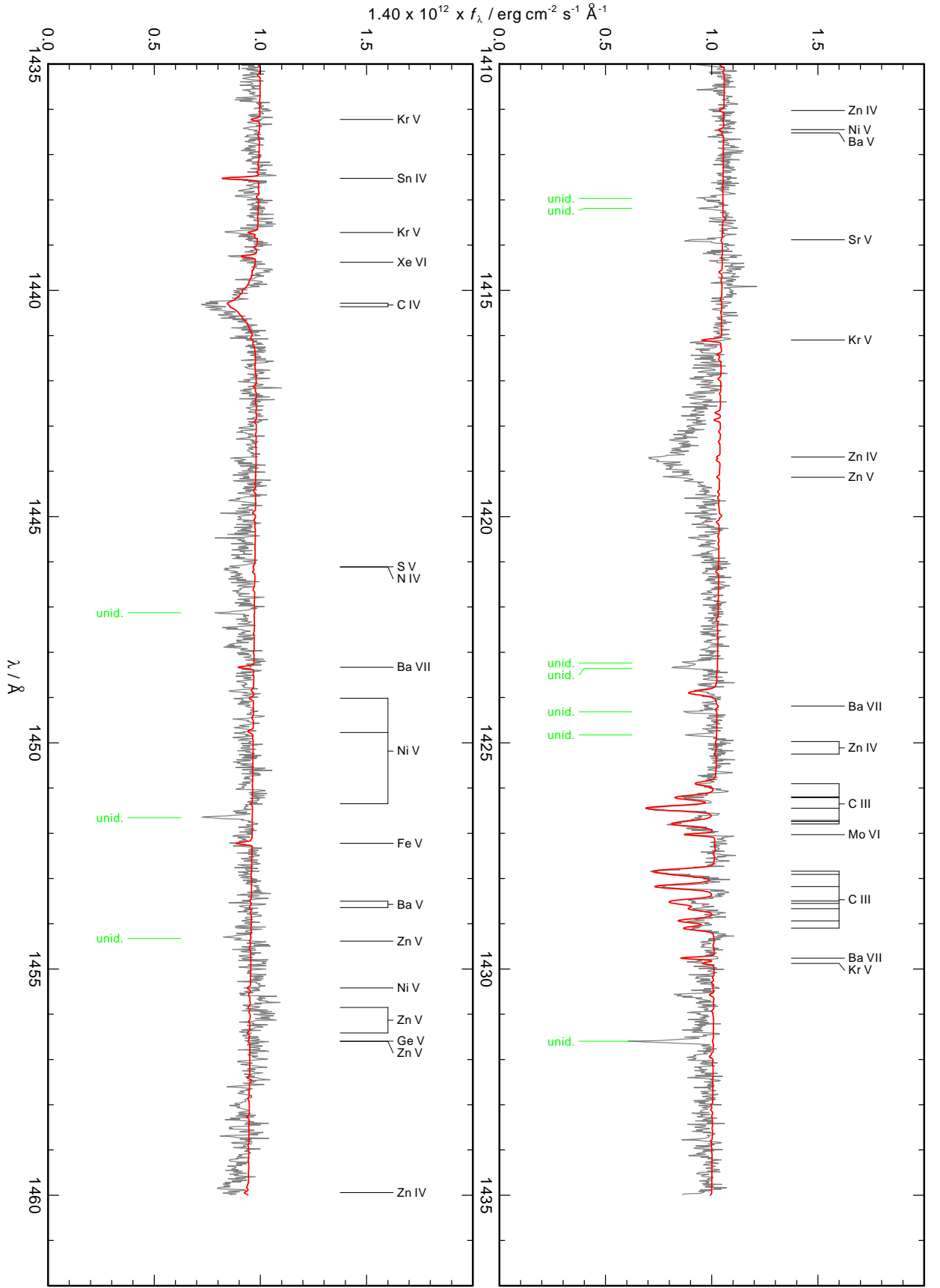


Fig. B.2. Figure B.2 continued.

Fig. B.2. Figure B.2 continued.



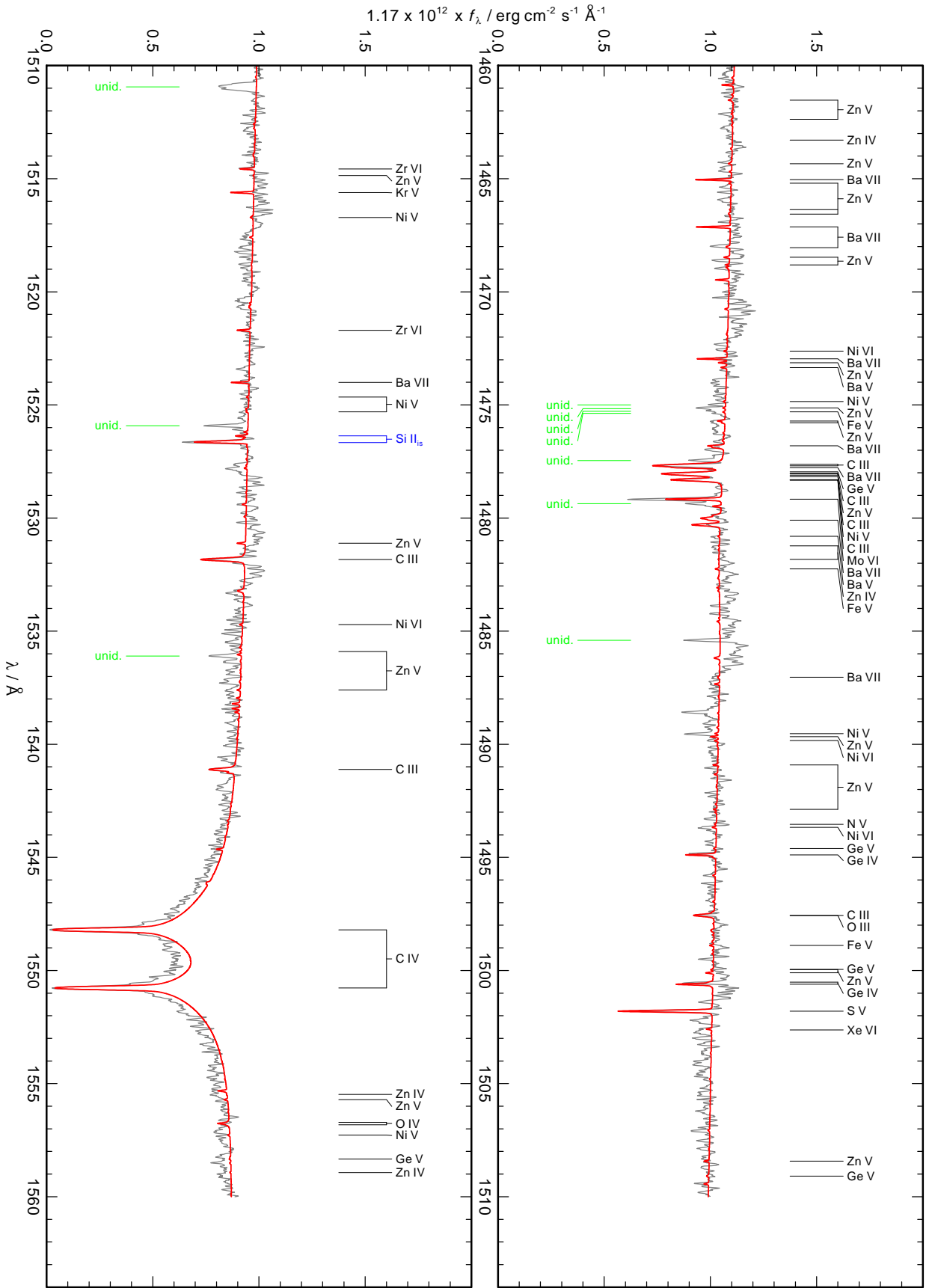
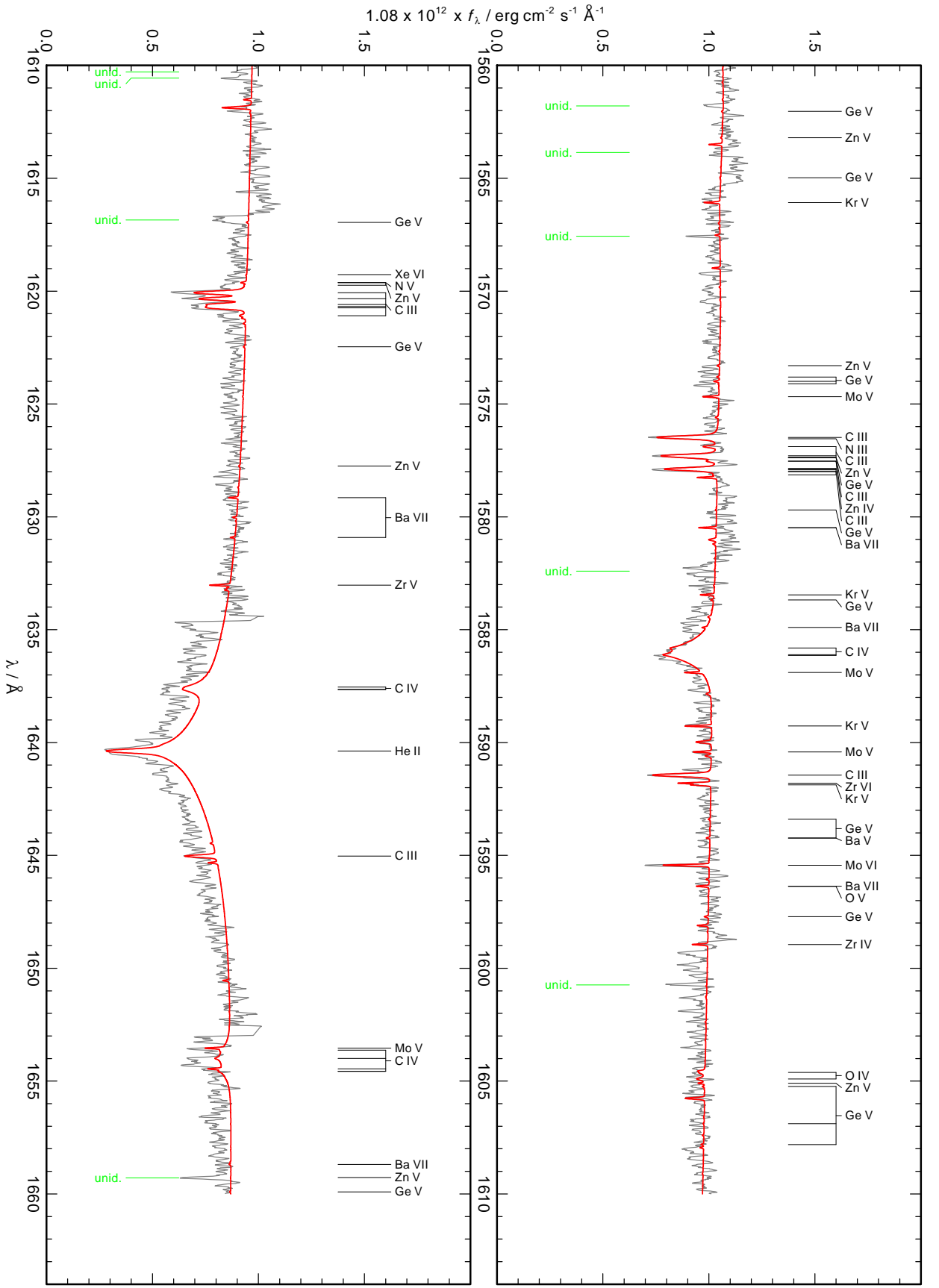


Fig. B.2. Figure B.2 continued.

Fig. B.2. Figure B.2 continued.



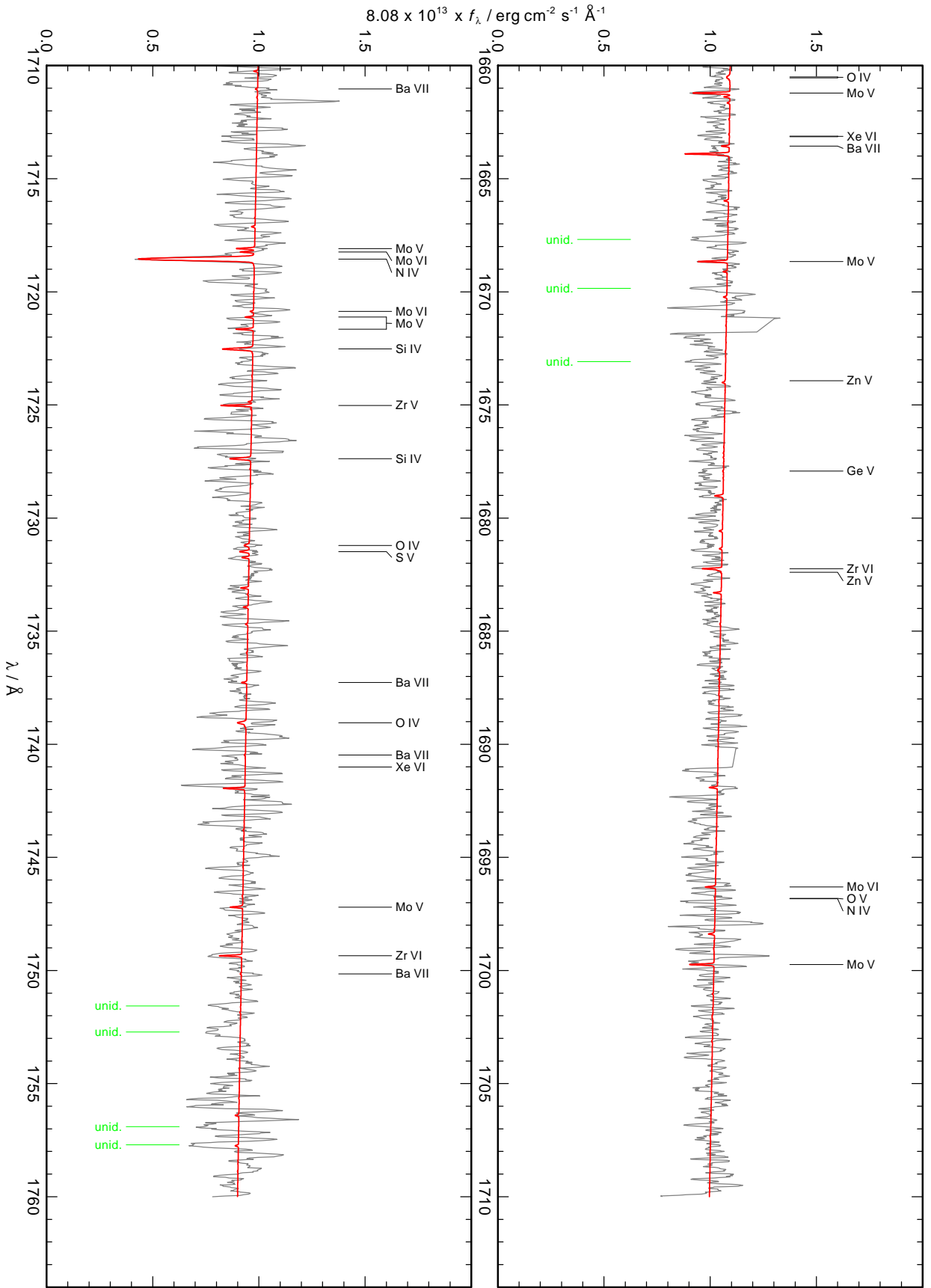


Fig. B.2. Figure B.2 continued.

Fig. B.2. Figure B.2 continued.

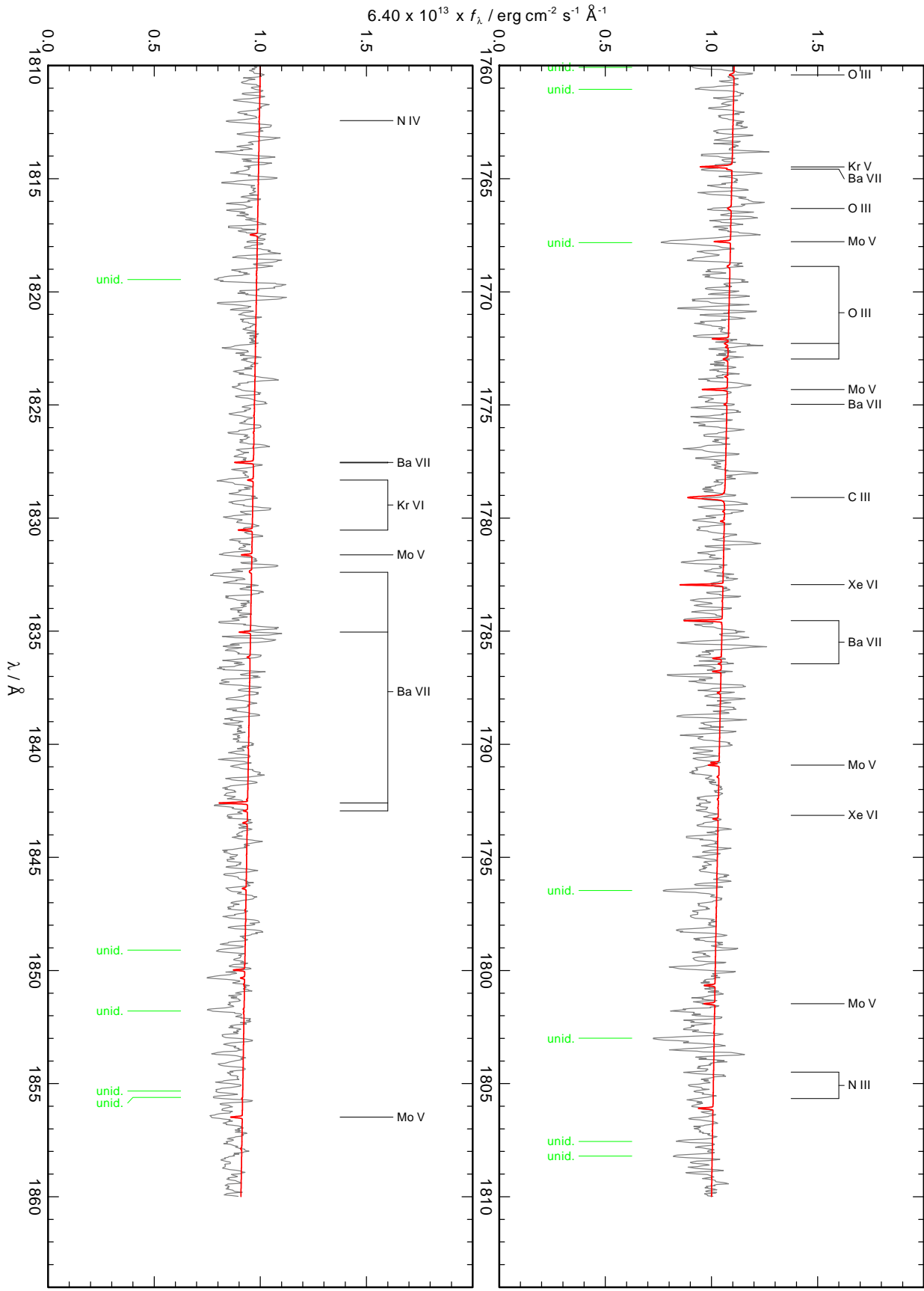
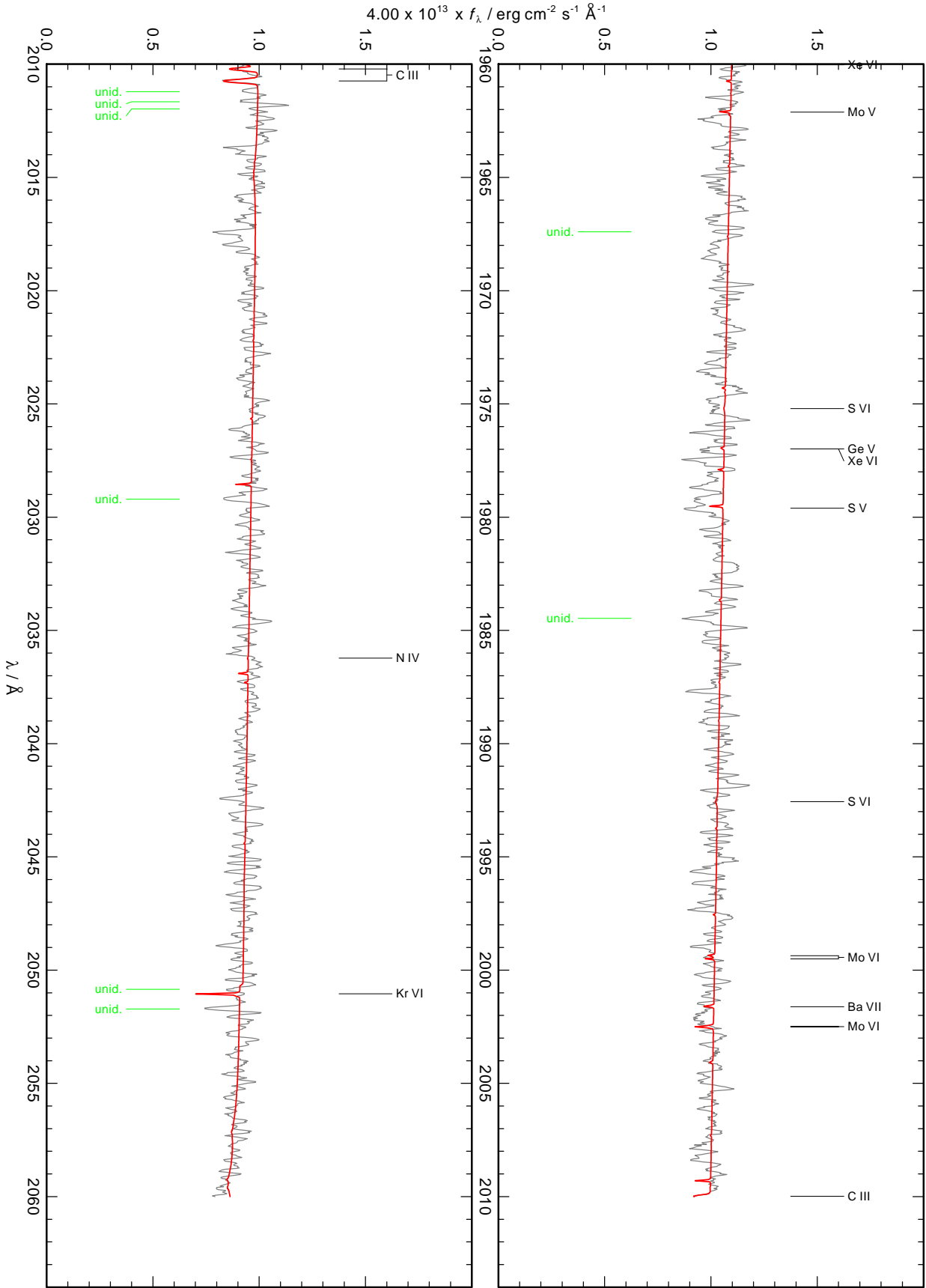




Fig. B.2. Figure B.2 continued.



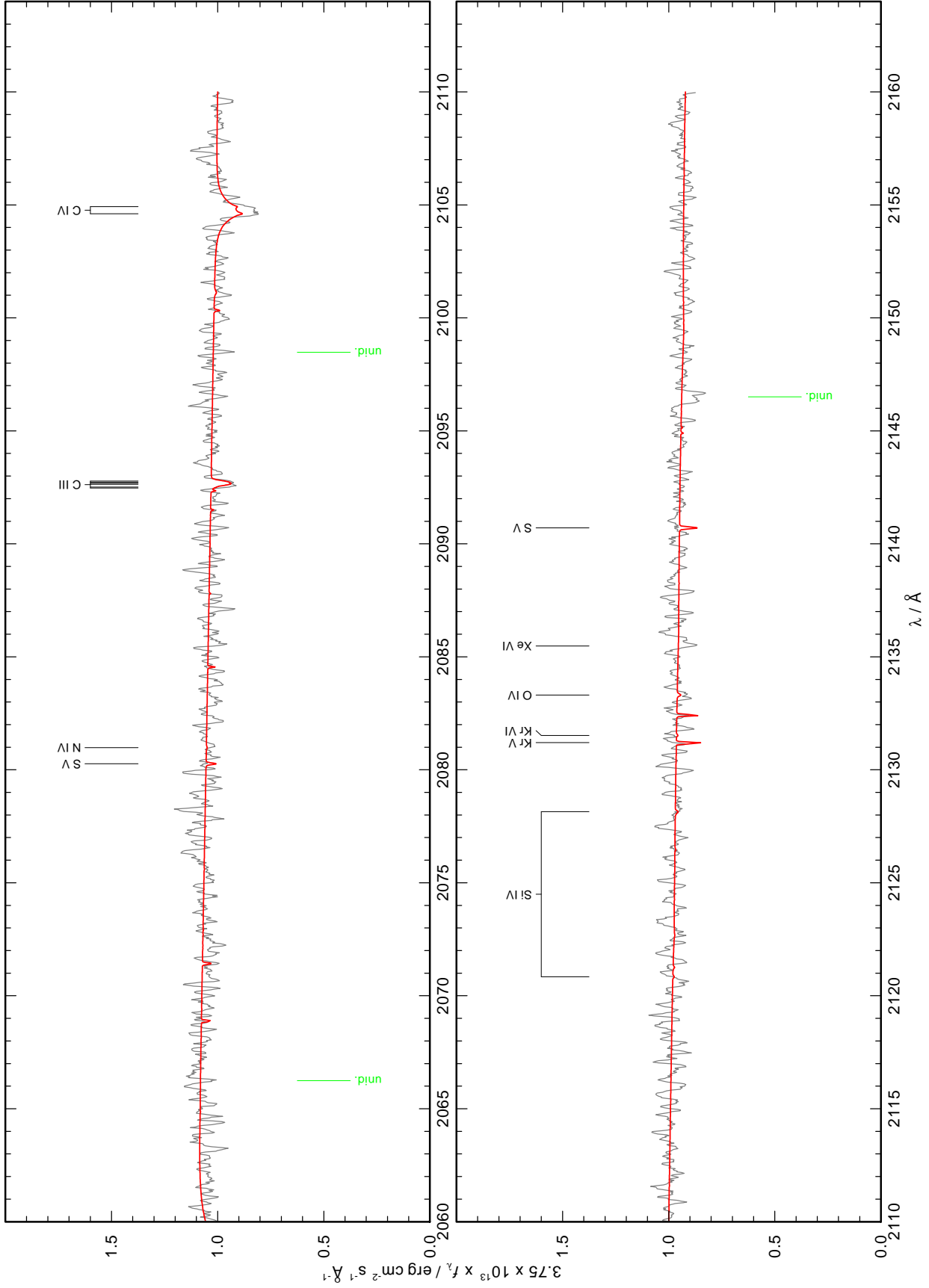


Fig. B.2. Figure B.2 continued.

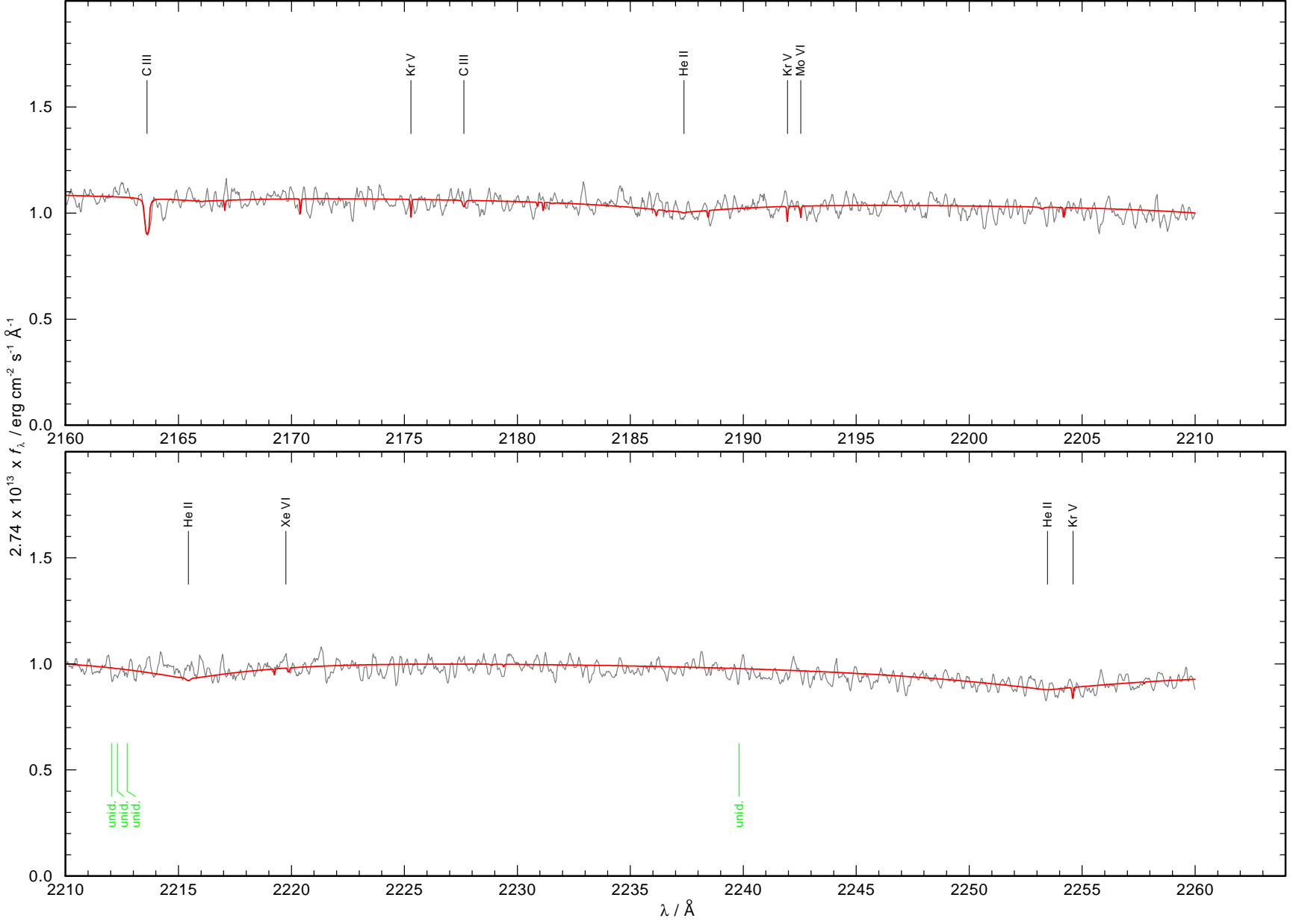


Fig. B.2. Figure B.2 continued.

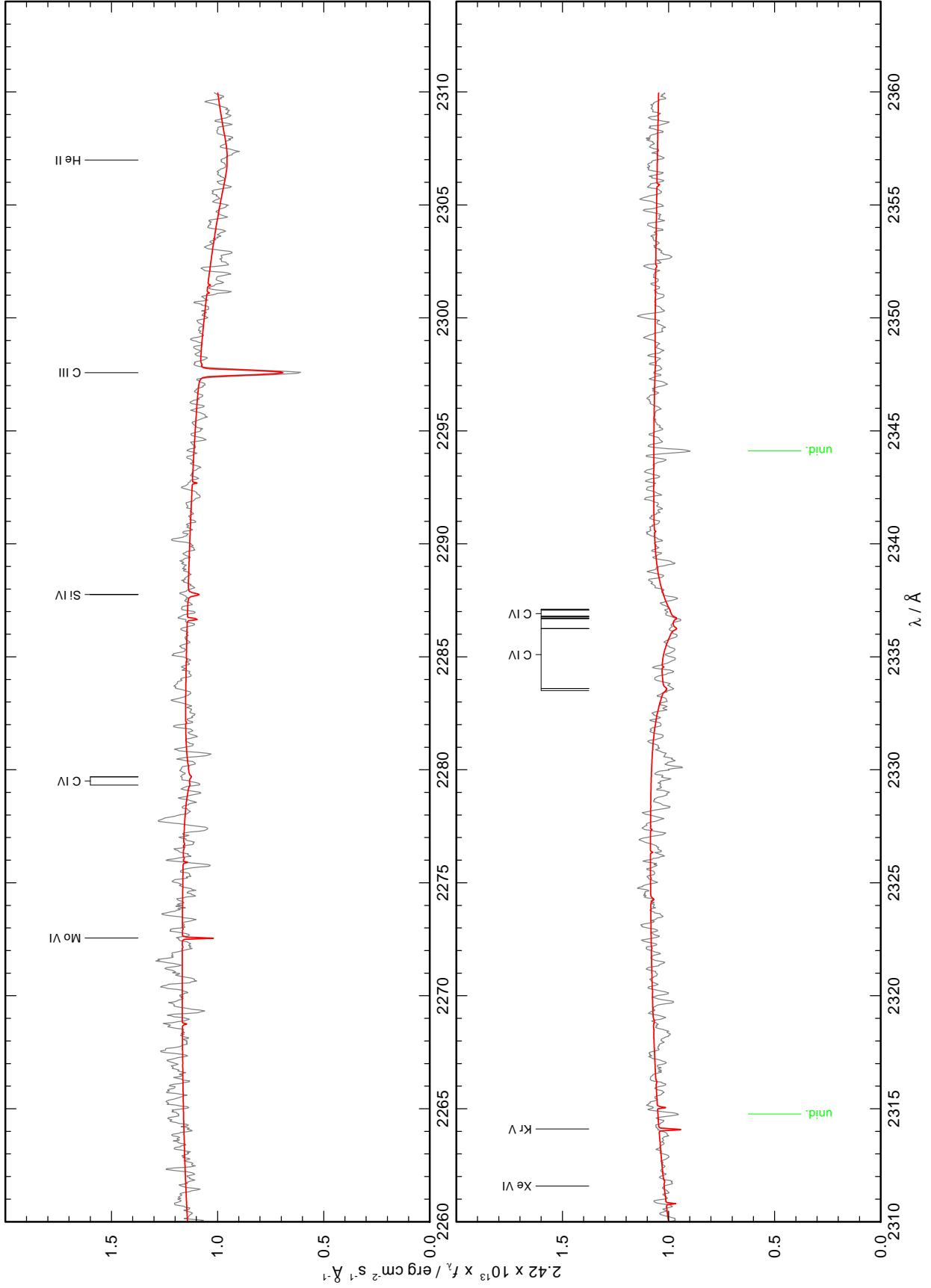


Fig. B.2. Figure B.2 continued.

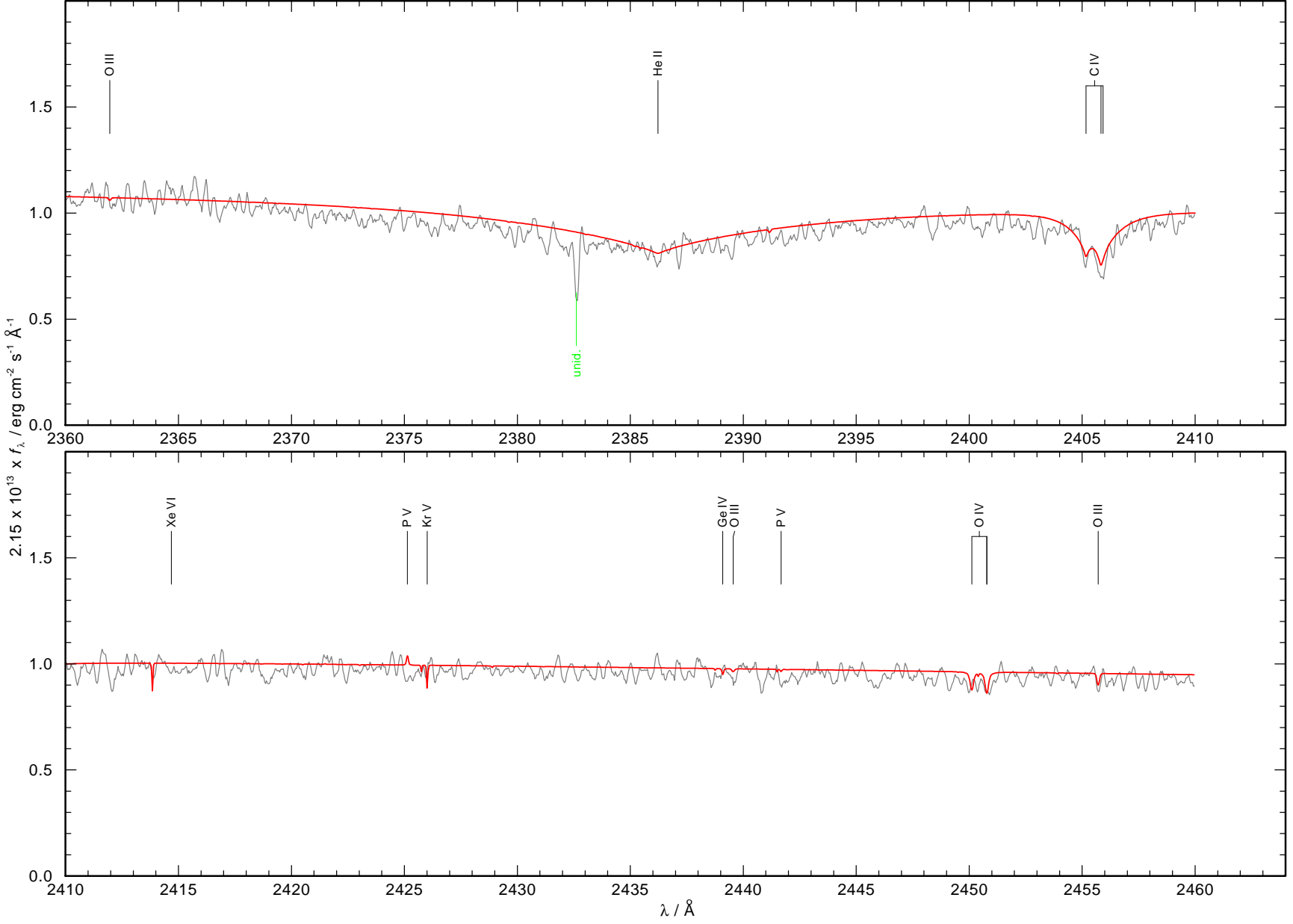


Fig. B.2. Figure B.2 continued.

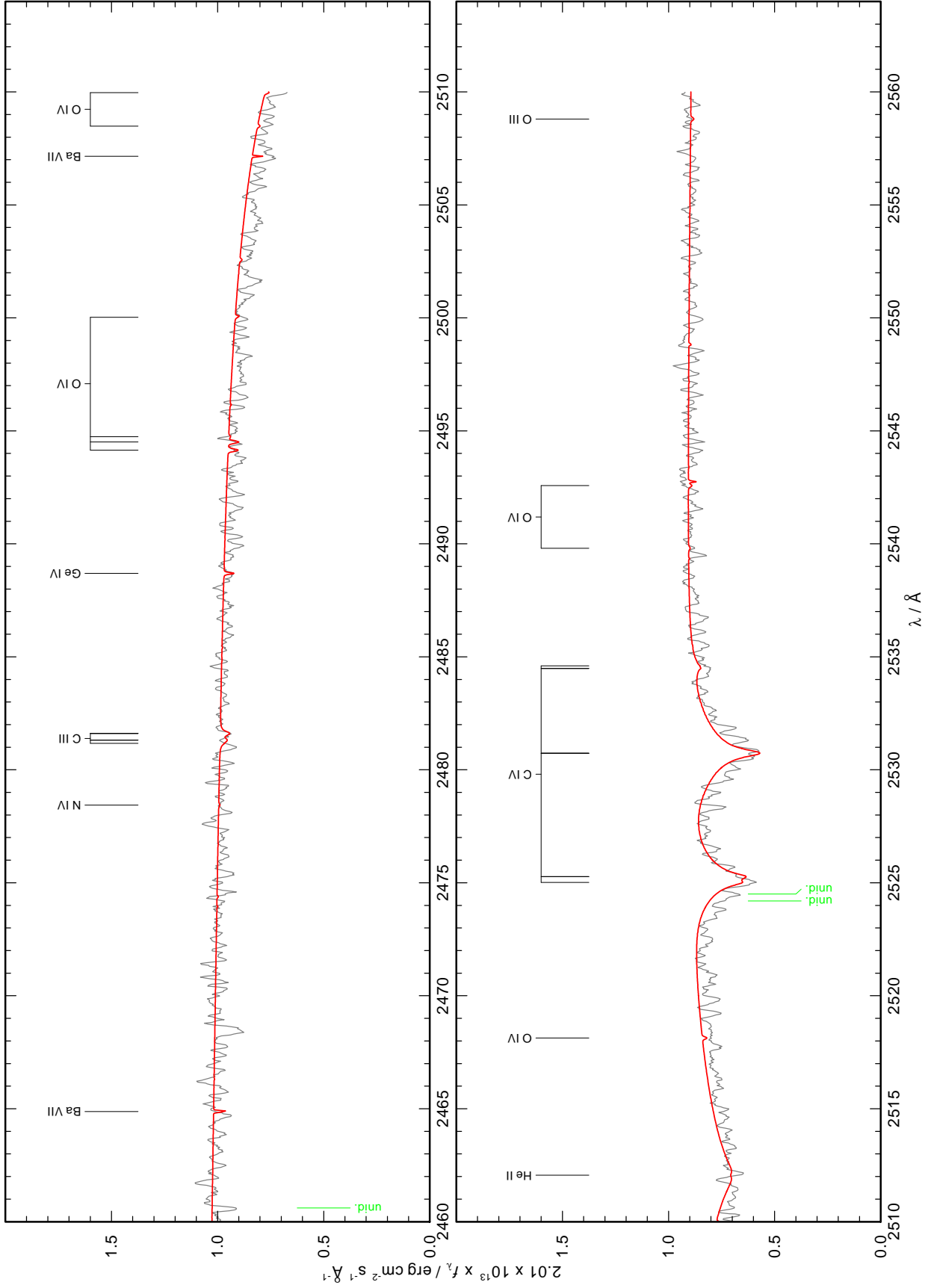


Fig. B.2. Figure B.2 continued.

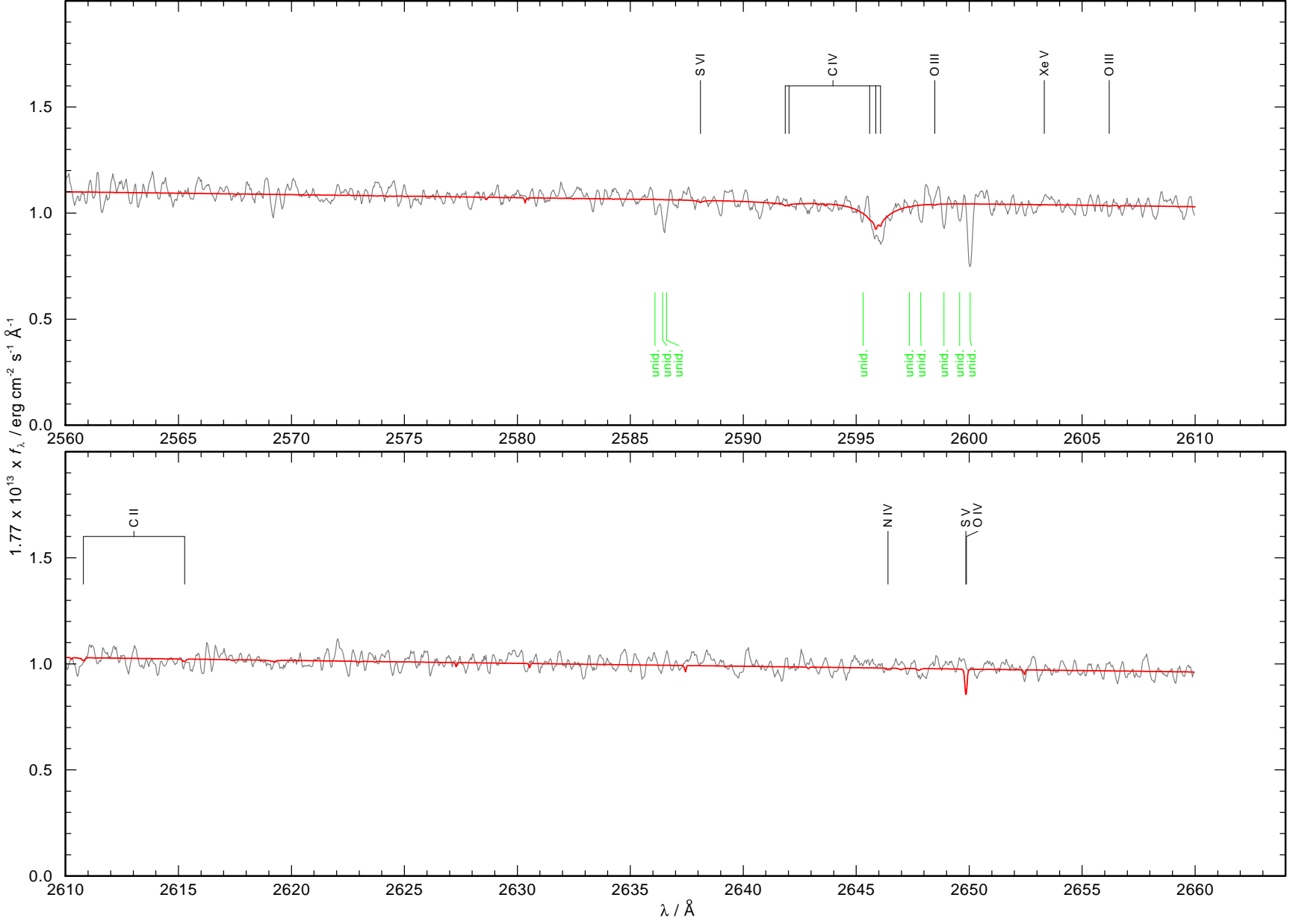


Fig. B.2. Figure B.2 continued.

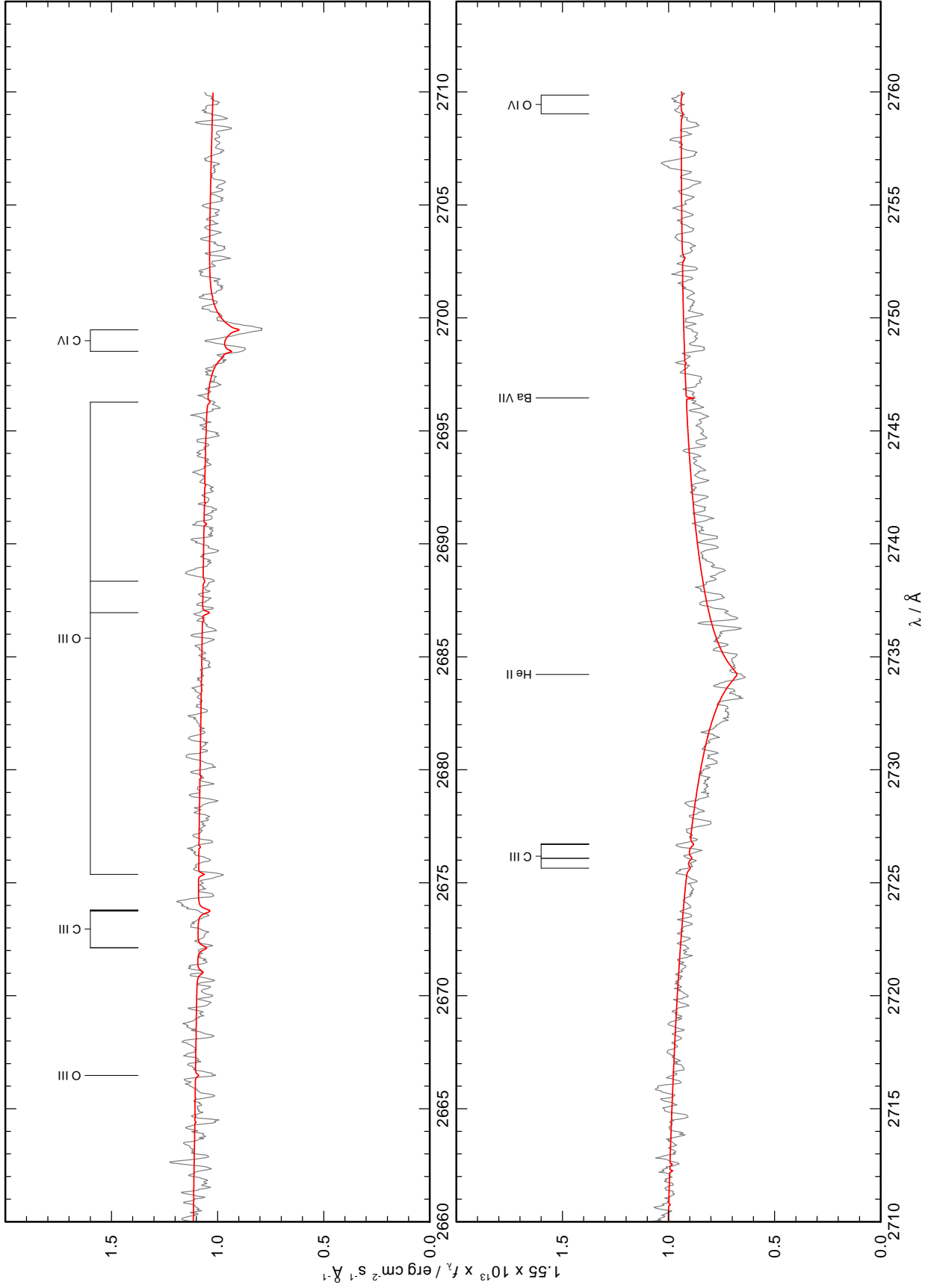


Fig. B.2. Figure B.2 continued.

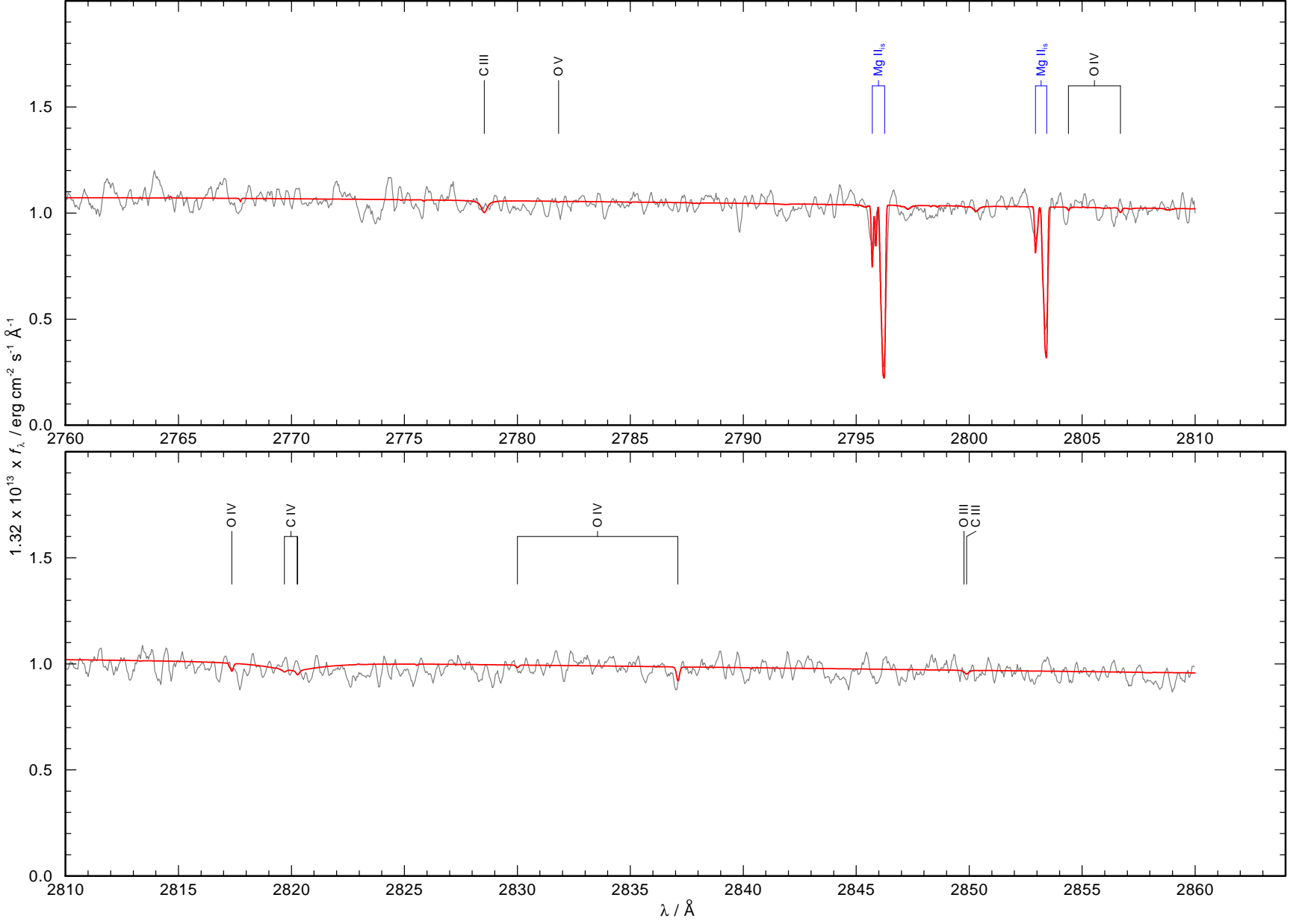


Fig. B.2. Figure B.2 continued.

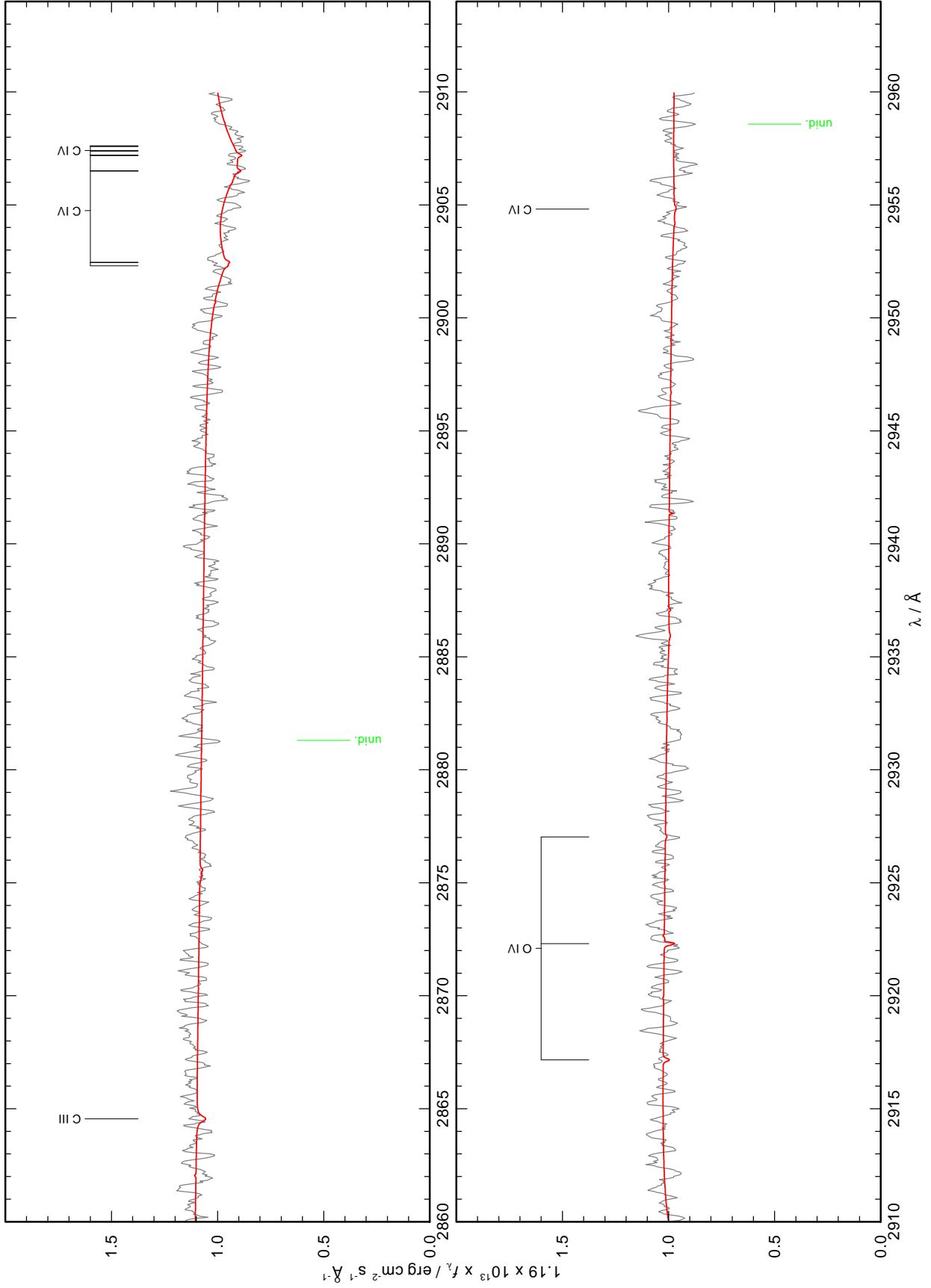


Fig. B.2. Figure B.2 continued.

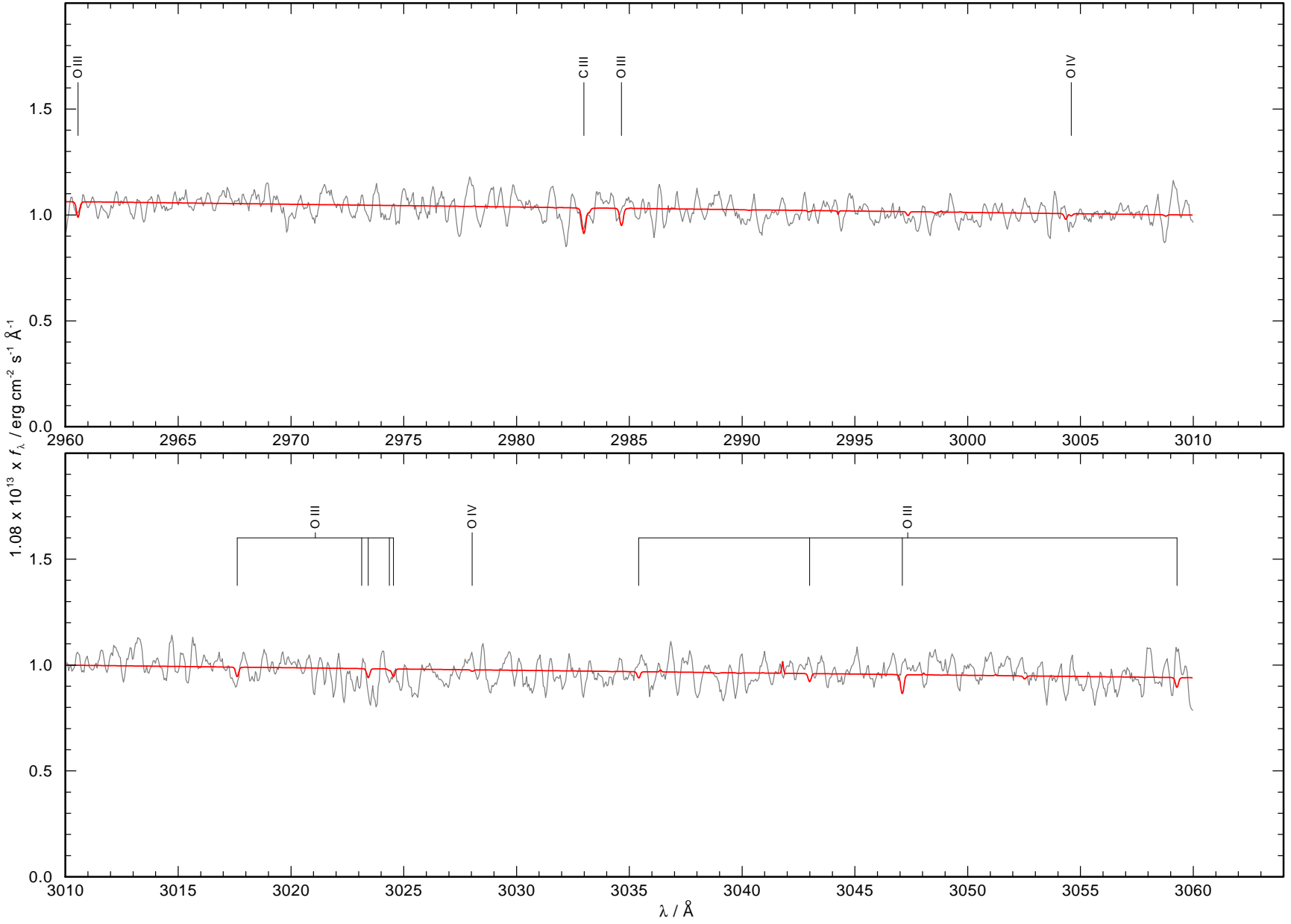


Fig. B.2. Figure B.2 continued.

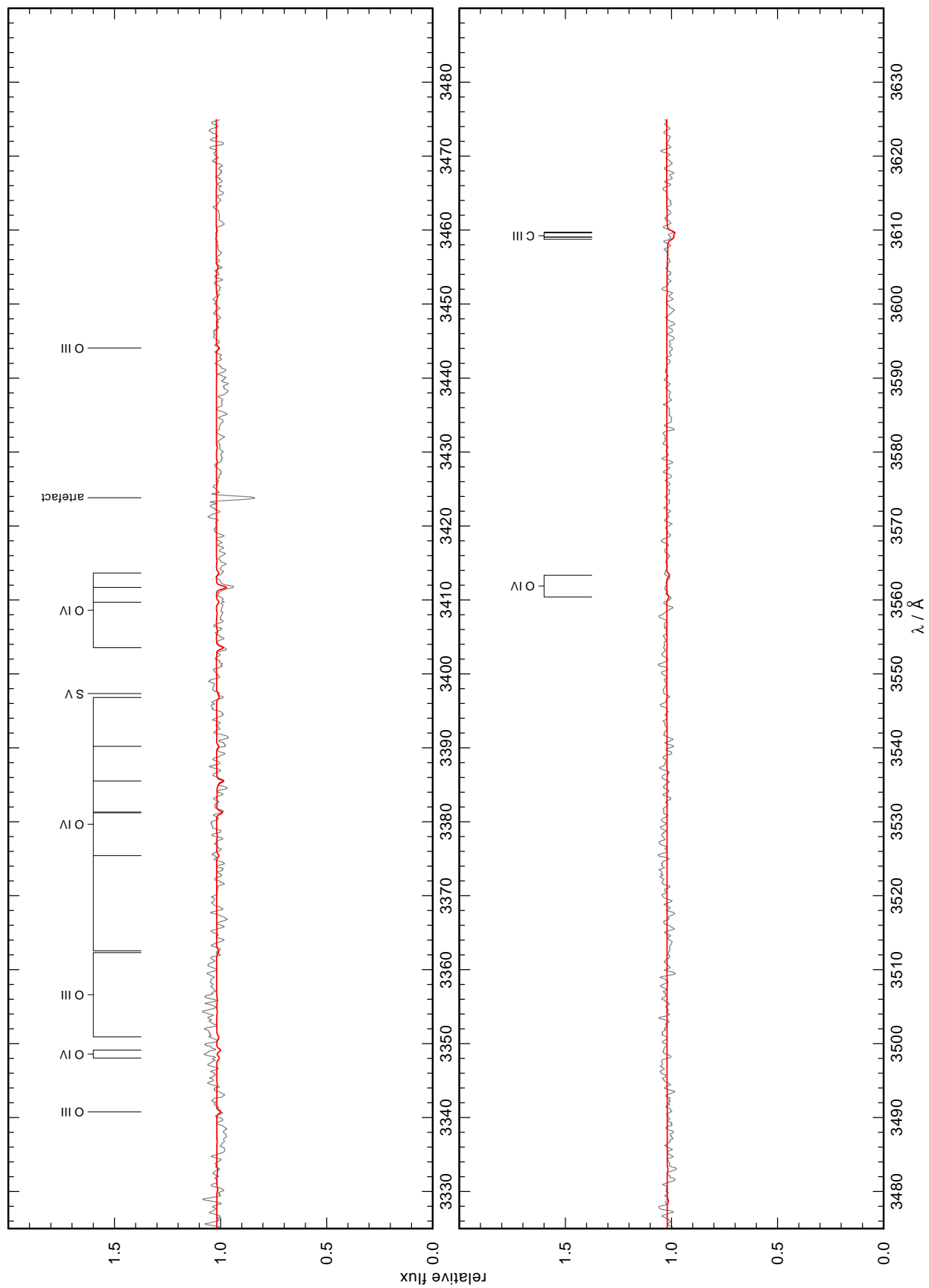


Fig. B.3. Optical (SPY) observation (gray) compared with the best model (red). Stellar lines are identified at top. “unid.” denotes unidentified lines.

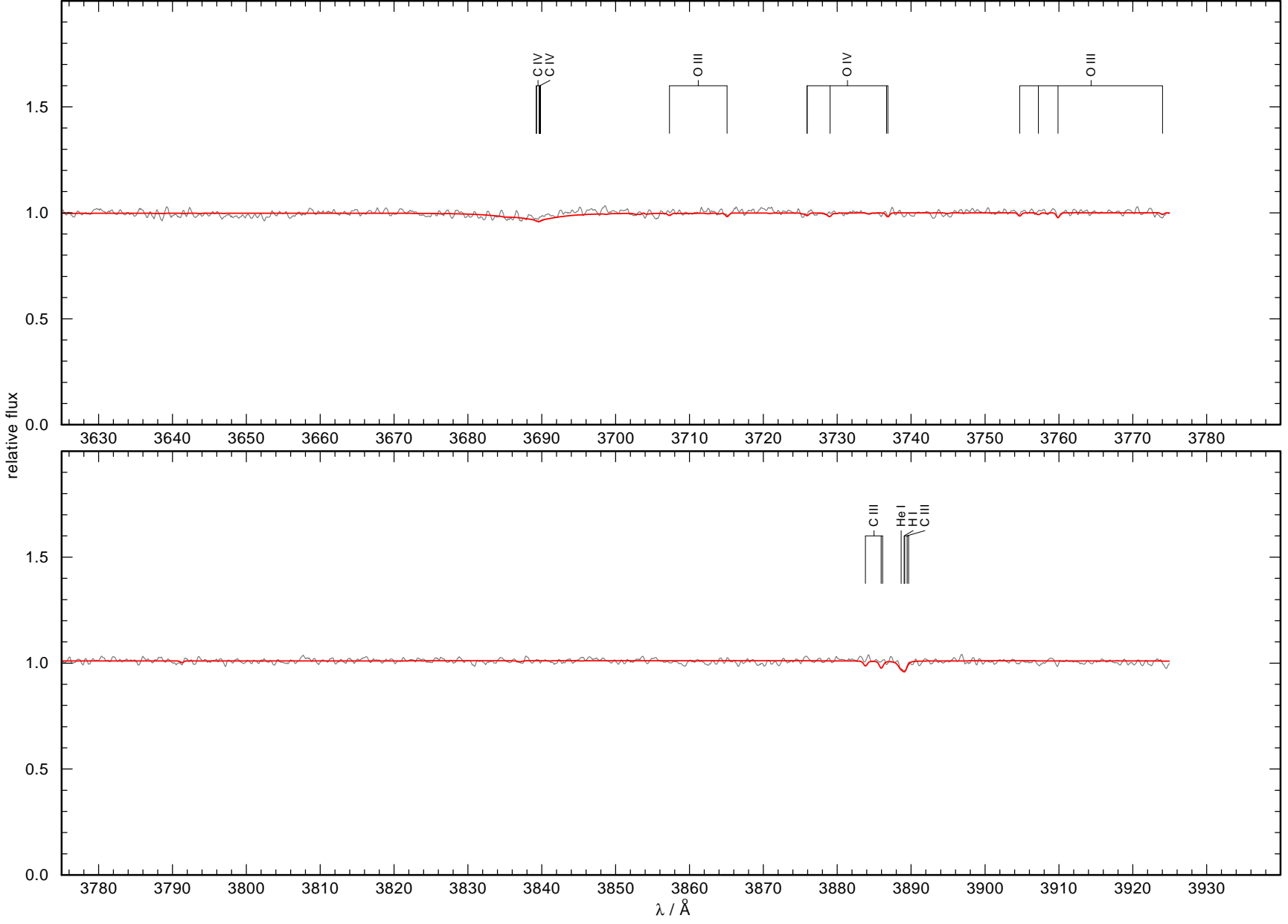


Fig. B.3. Figure B.3 continued.

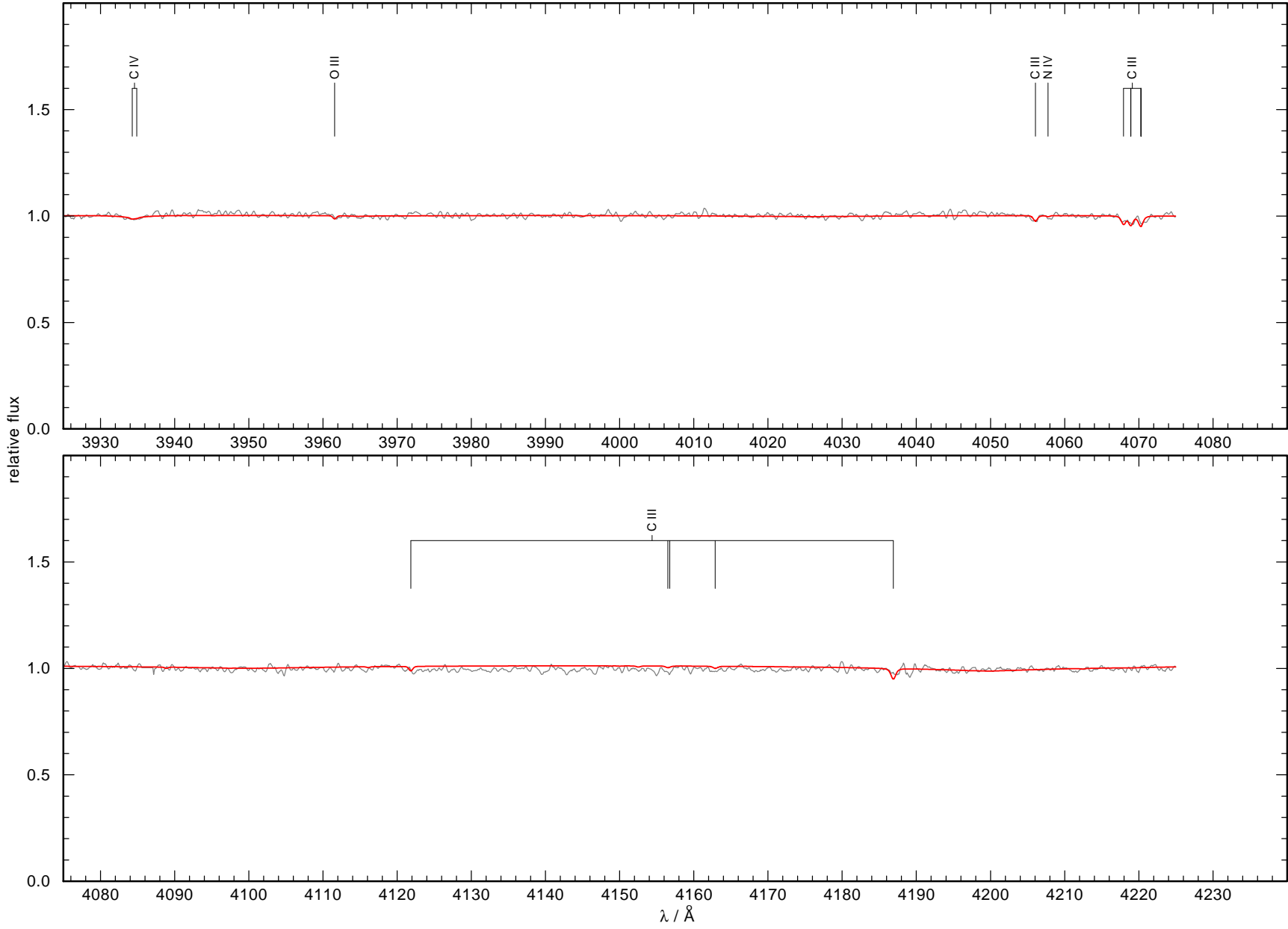


Fig. B.3. Figure B.3 continued.

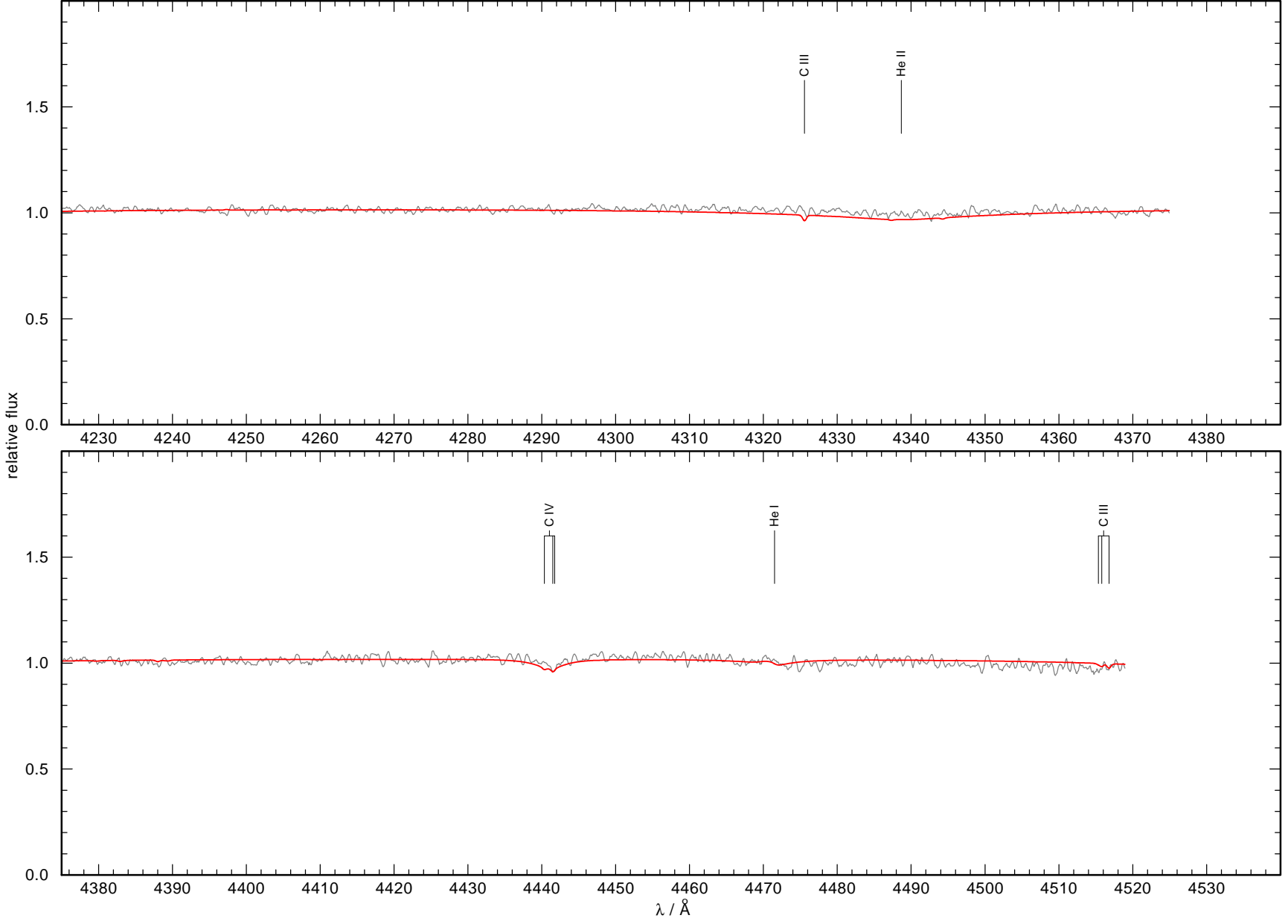


Fig. B.3. Figure B.3 continued.

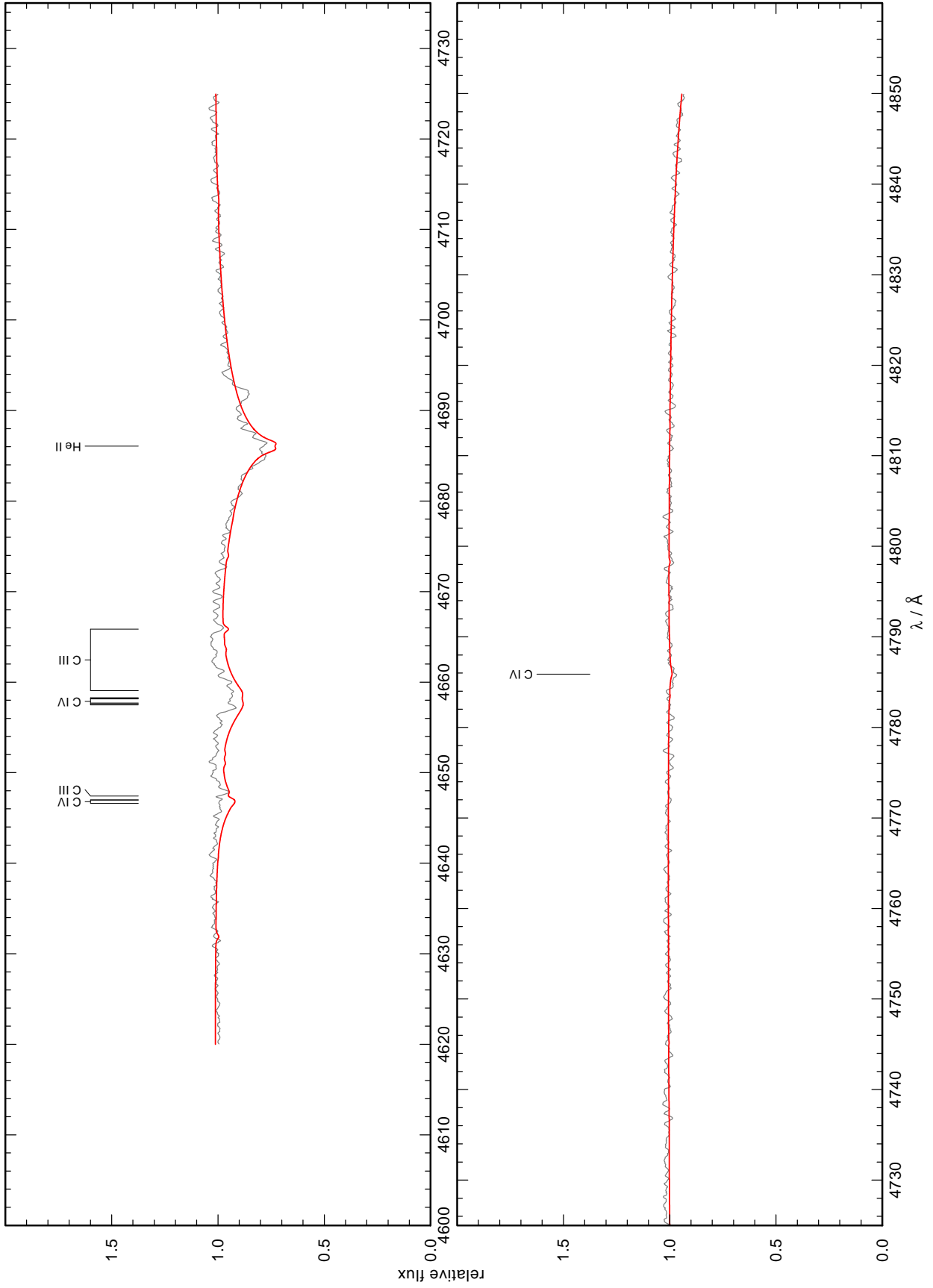


Fig. B.3. Figure B.3 continued.

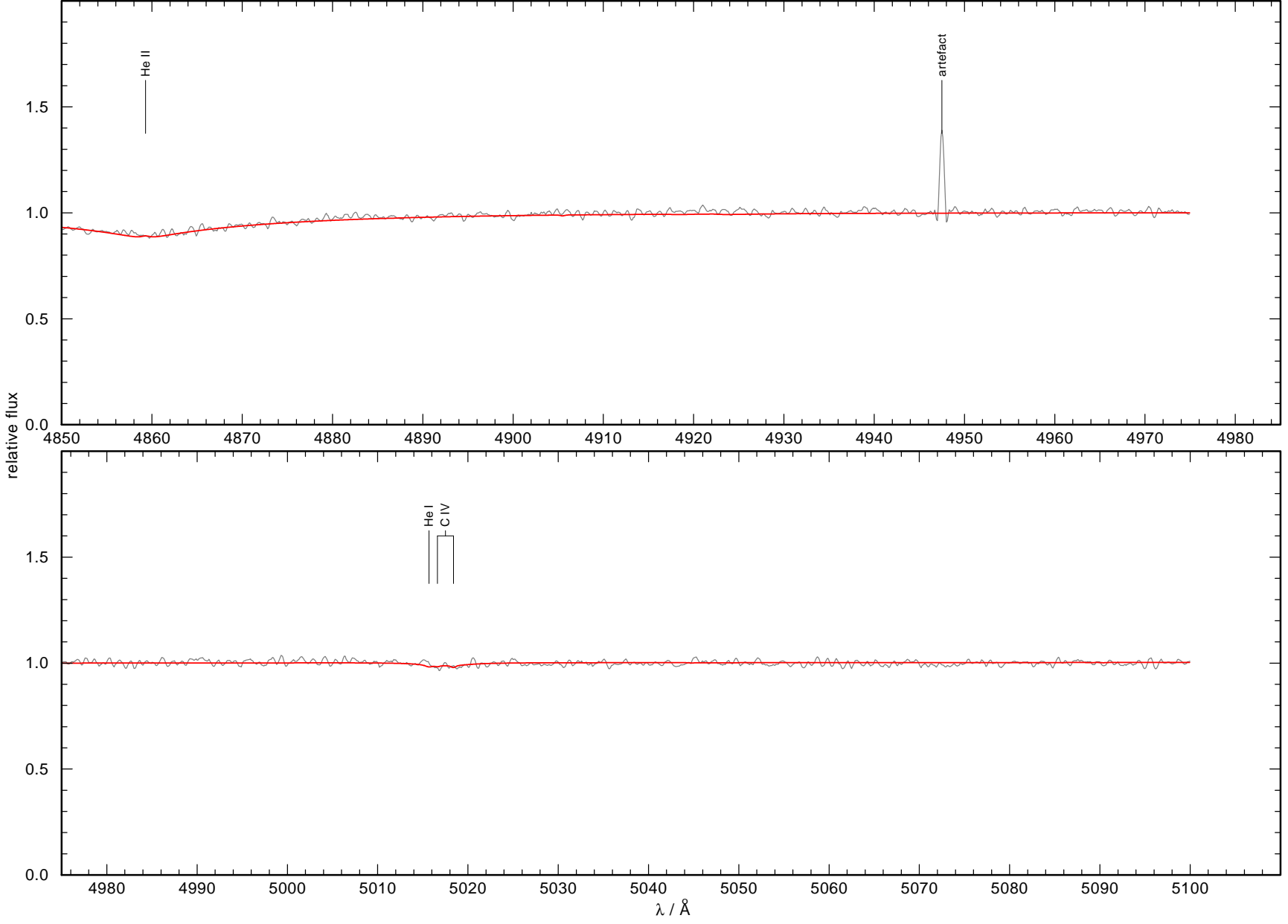


Fig. B.3. Figure B.3 continued.

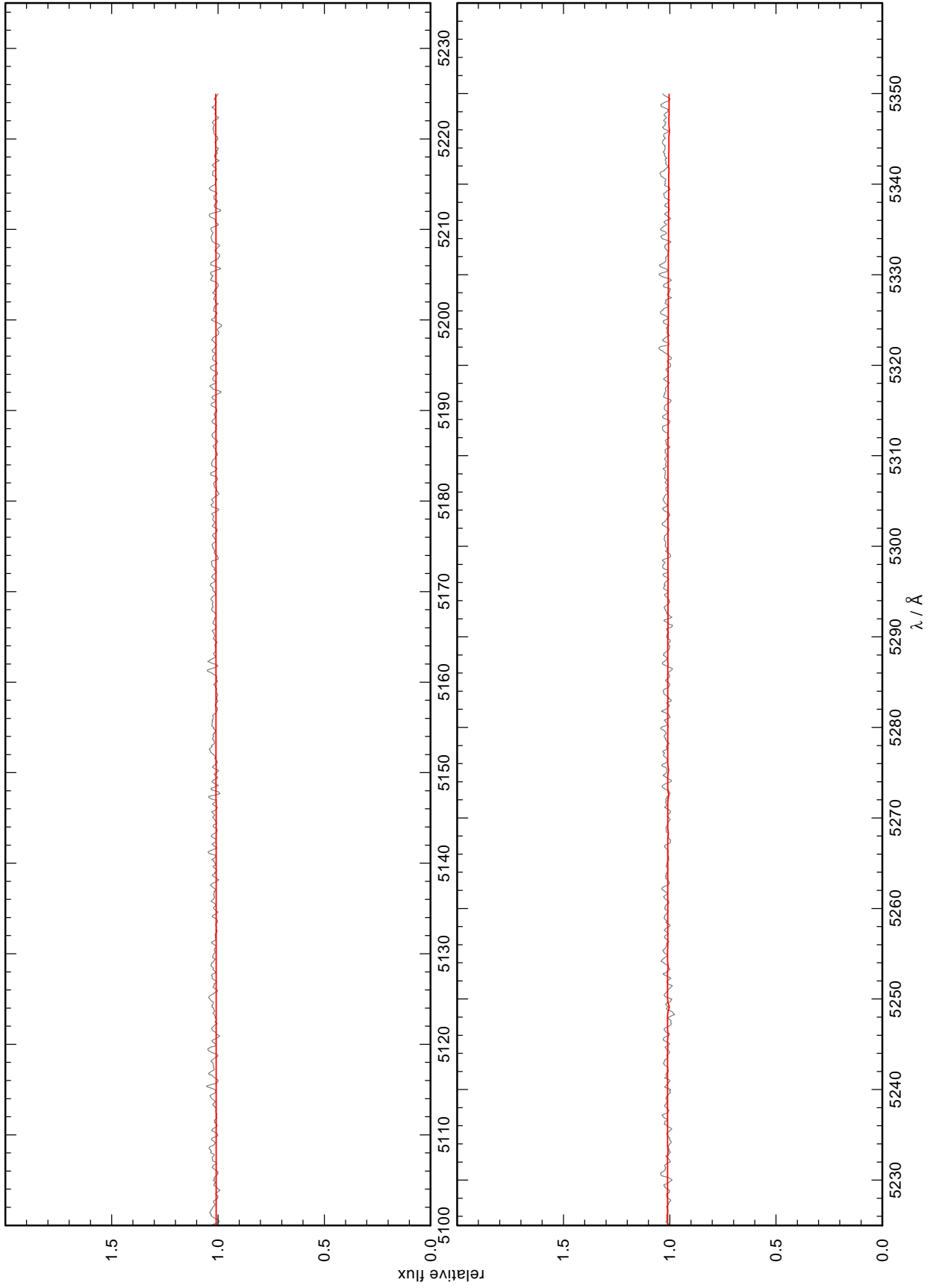


Fig. B.3. Figure B.3 continued.

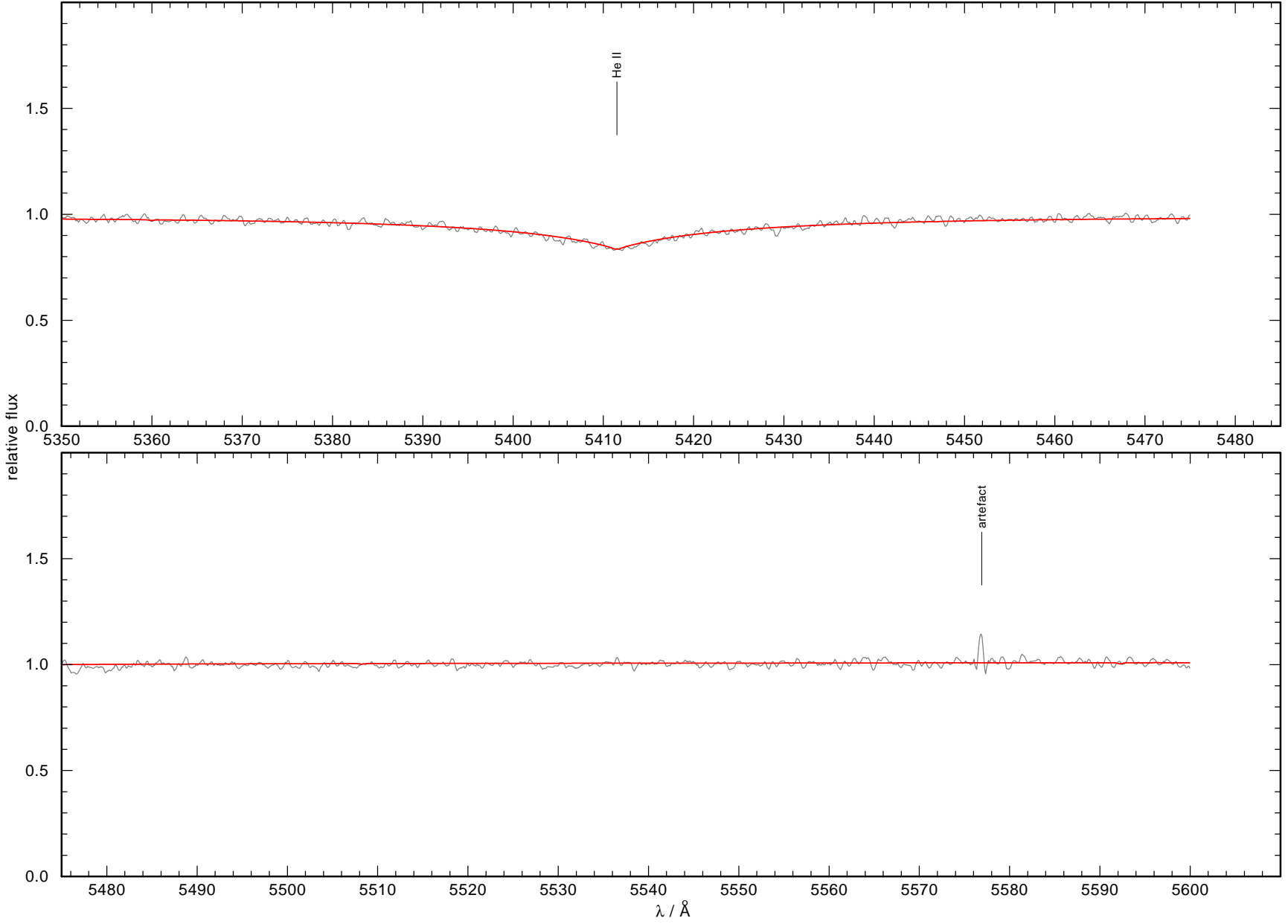


Fig. B.3. Figure B.3 continued.

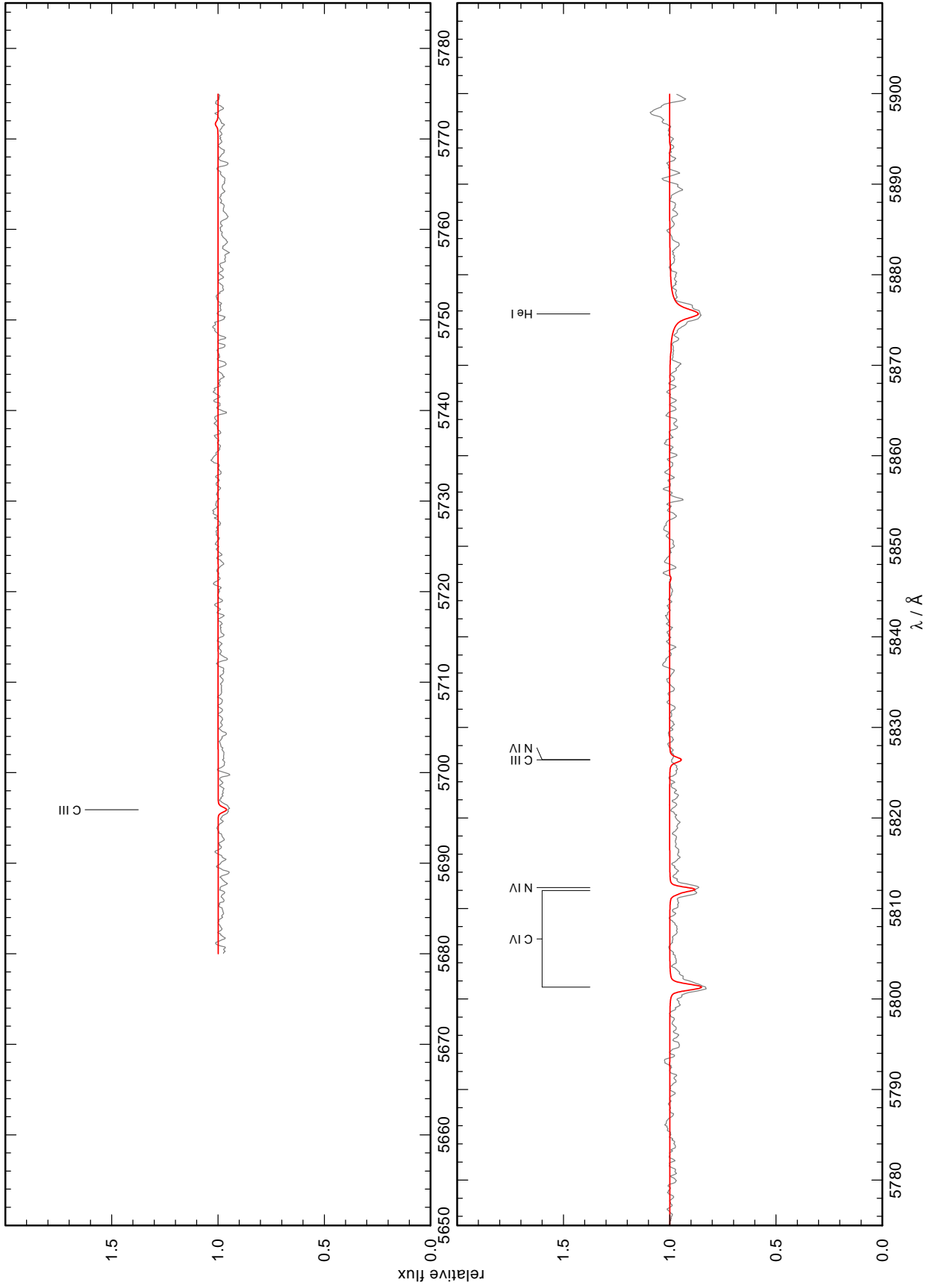


Fig. B.3. Figure B.3 continued.

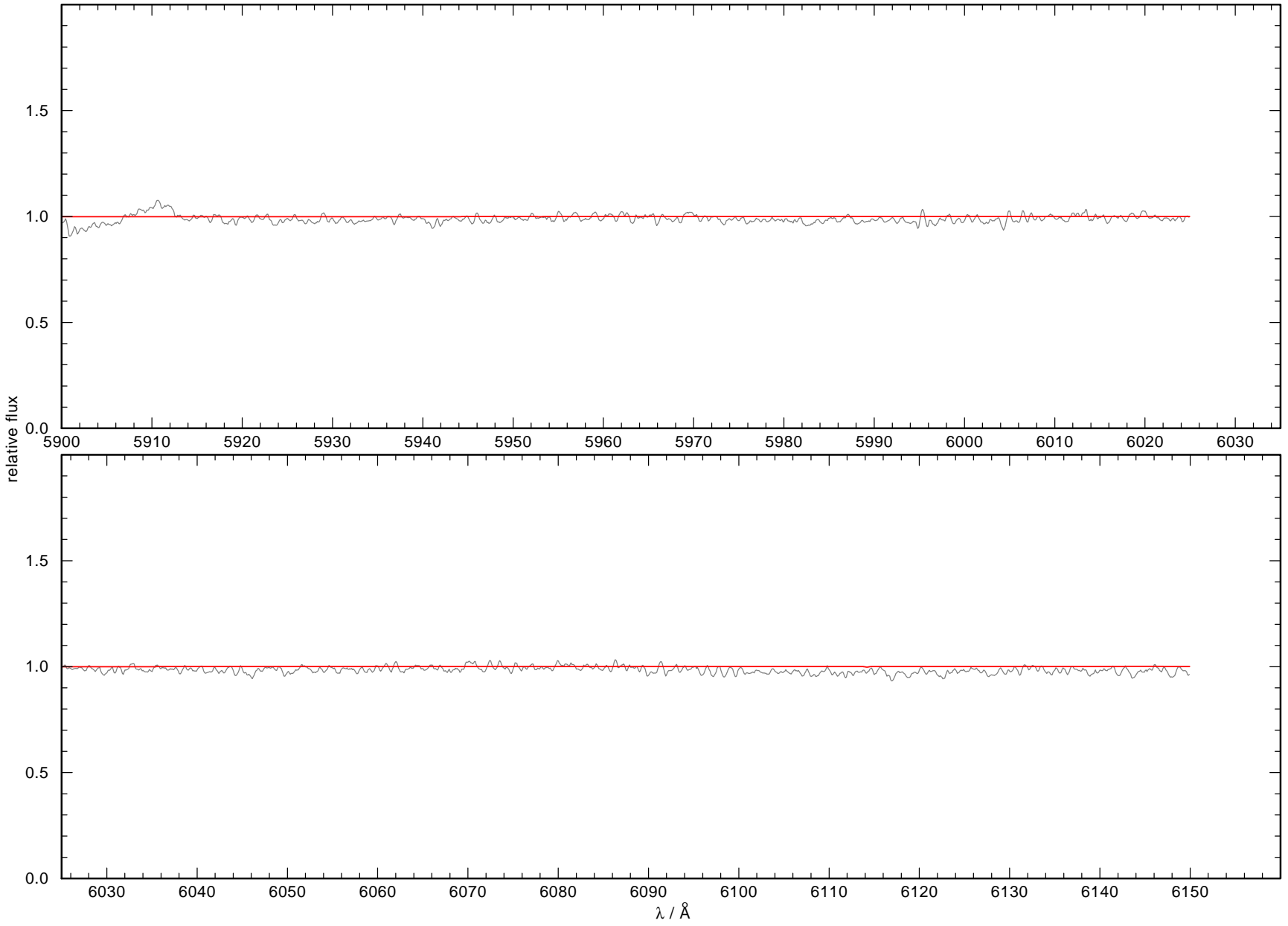


Fig. B.3. Figure B.3 continued.

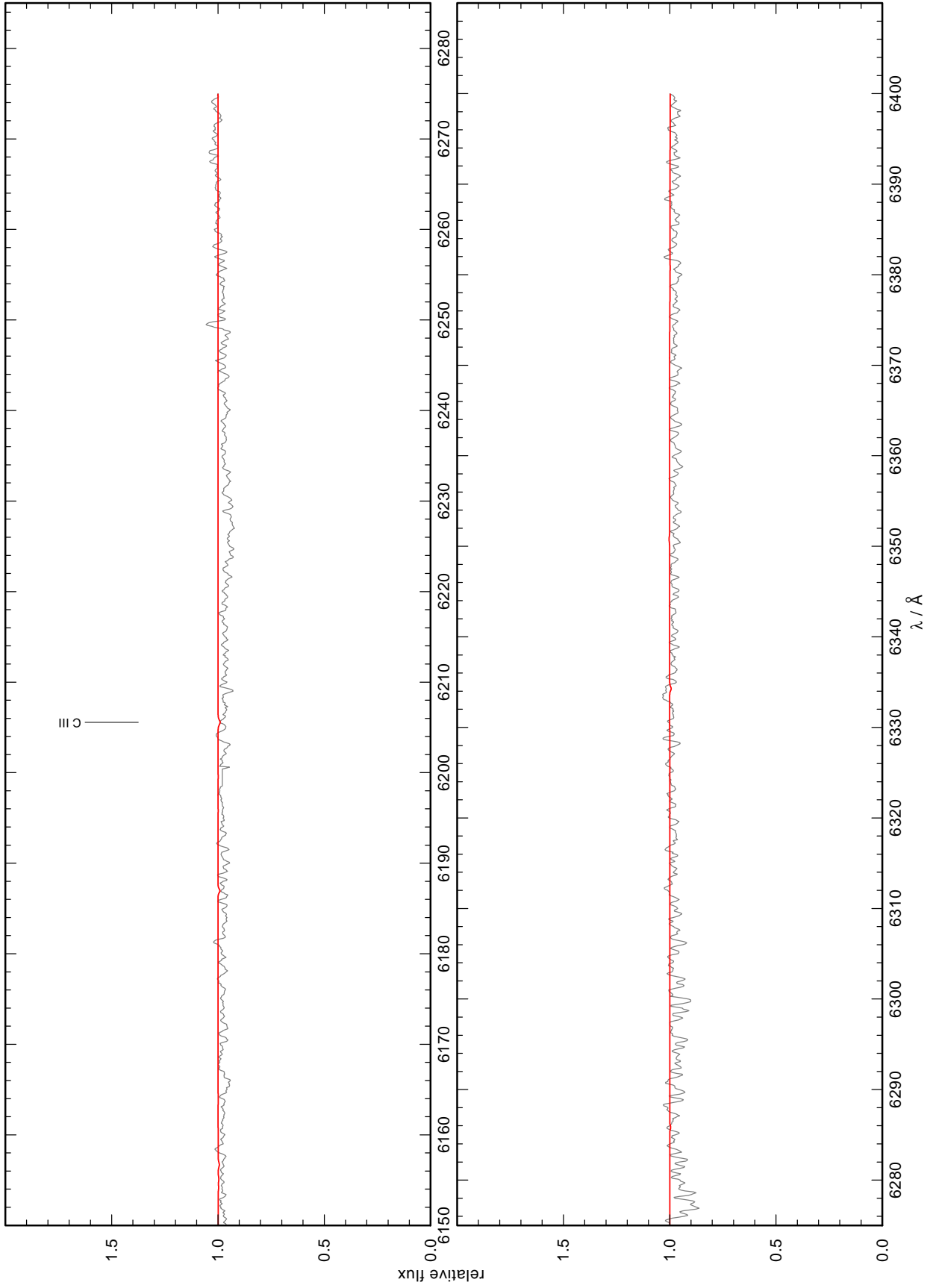


Fig. B.3. Figure B.3 continued.

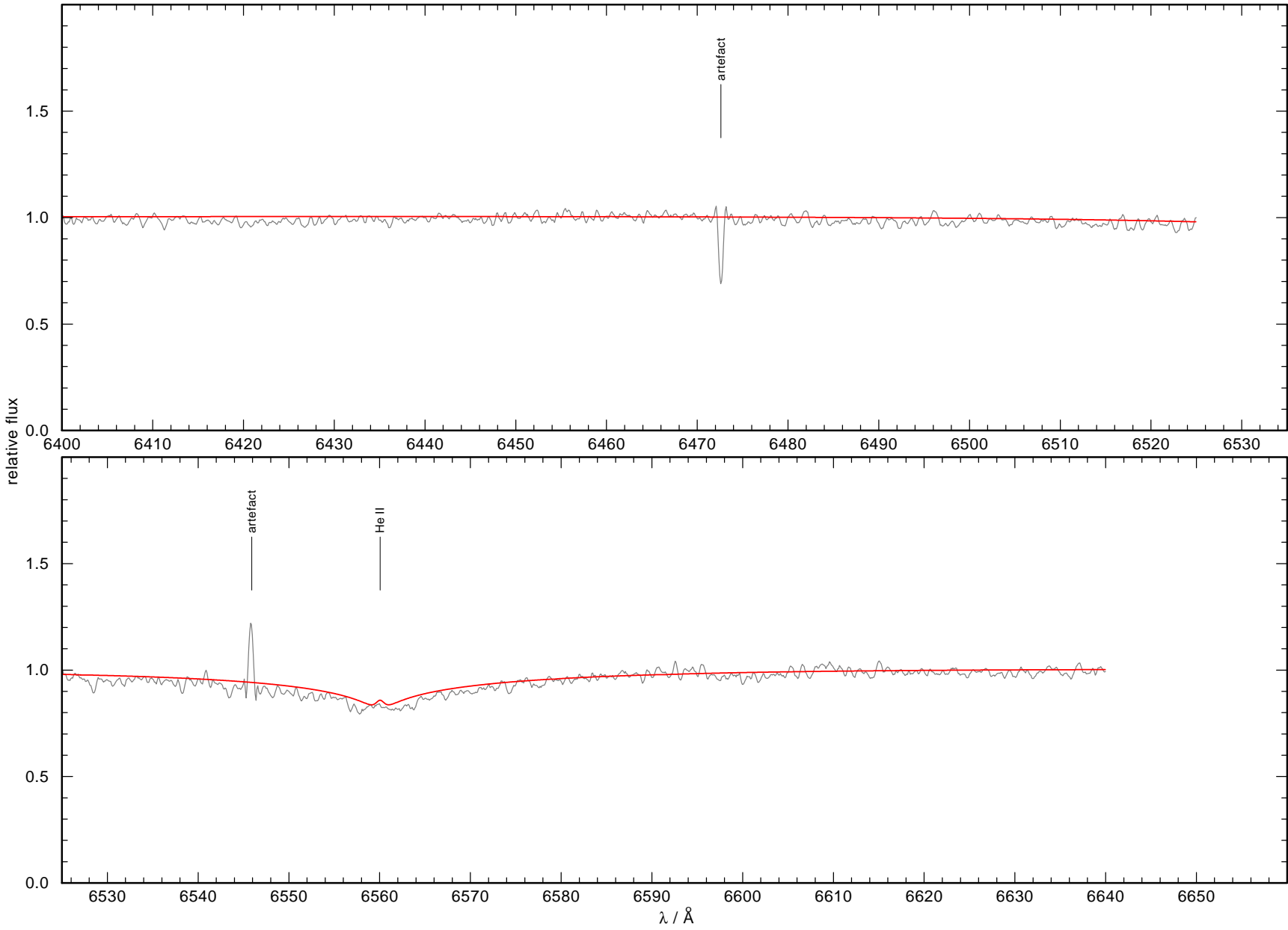


Fig. B.3. Figure B.3 continued.

Appendix C: WWW interfaces of TEUV, TGRED, and TVIS

Fig. C.1. TEUV WWW interface. Not shown on astro-ph, please visit the WWW page.

Fig. C.2. TGRED WWW interface. Not shown on astro-ph, please visit the WWW page.

Fig. C.3. TVIS WWW interface. Not shown on astro-ph, please visit the WWW page.